HYDROGEOLOGICAL AND GEOCHEMICAL CONTROLS ON TRACE METAL CONCENTRATIONS IN LAKE SEDIMENT IN THE HOLYROOD GRANITE

ROBERT MACLEOD

NOTICE

The quality of this microform is heavily dependent upon the quality of the original thesis submitted for microfilming. Every effort has been made to ensure the highest quality of reproduction possible.

If pages are missing, contact the university which granted the degree.

Some pages may have indistinct print especially if the original pages were typed with a poor typewriter ribbon or if the university sent us an inferior photocopy.

Reproduction in full or in part of this microform is governed by the Canadian Copyright Act, R.S.C. 1970, c. C-30, and subsequent amendments.

AVIS

La qualité de cette microforme dépend grandement de la qualité de la thèse soumise au microfilmage. Nous avons tout fait pour assurer une qualité supérieure de reproduction.

S'il manque des pages, veuillez communiquer avec l'université qui a conféré le grade.

La qualité d'impression de certaines pages peut laisser à désirer, surtout si les pages originales ont été dactylographiées à l'aide d'un ruban usé ou si l'université nous a fait parvenir une photocopie de qualité inférieure.

La reproduction, même partielle, de cette microforme est soumise à la Loi canadienne sur le droit d'auteur, SRC 1970, c. C-30, et ses amendements subséquents.

Canada

HYDROGEOLOGICAL AND GEOCHEMICAL CONTROLS ON TRACE METAL CONCENTRATIONS IN LAKE SEDIMENT IN THE HOLYROOD GRANITE

BY

ROBERT MACLEOD

A thesis submitted to the School of Graduate Studies in partial fulfilment of the requirements for the degree of Master of Science

Department of Earth Science
Memorial University of Newfoundland

May 1992

St. John's Newfoundland

ISBN 0-315-78126-2

ABSTRACT

A regional lake/pond sediment survey over the Avalon Peninsula in 1976, by the Nfld. Department of Mines, showed a number of lakes with anomalous concentrations of uranium and other metals in the area of the Holyrood Pluton. These anomalies are not reflected in the average host granite rock geochemistry. The hydrogeological framework, including detailed analysis of the fracture systems as major groundwater conduits, has been studied in an attempt to determine the role of groundwaters in transporting and localizing concentrations of trace metals in lake sediment in four lakes in the area.

Groundwater discharge into the lakes was estimated to range from 20 to 35 percent of their water balances, based on characteristic chemical differences between groundwater and surface waters. Detailed sampling of lake sediment, on a grid pattern, showed a non-uniform areal distribution of metals in these lakes. This sampling also showed that peak concentrations were not restricted to the centres or deepest points in the lakes. The maximum concentration of uranium found in these lakes ranged from 69 to 309 ppm, which is higher than those recorded in the regional survey. In some cases, the elongated shape of the uranium-rich area of sediment is aligned with the orientation of one of the major

fracture sets in the study area. Sampling of vertical sediment profiles showed a considerable variation of metals in the sediment column. However there appeared to be no direct relationship between metal concentration in surface sediment and maximum concentrations at depth. Although concentrations of most metals in the sediment are near levels expected for a detrital granite-source origin, anomalous concentrations of uranium at depth in the cores appear to be associated with a rapid change in organic content. A mechanism is proposed whereby mobile dissolved uranium in oxidizing groundwaters is reduced to its tetravalent state when it encounters organic rich mud as it discharges into a lake. The magnitude of seepage flux values and uranium concentrations found in deep groundwaters in the granite suggest that groundwaters are a possible mechanism for the transport concentration of metals in these post-glacial lake sediments.

ACKNOWLEDGEMENTS

The work carried out in this study was funded by an NSERC Strategic Grant to Professors J. Gale, D. Strong, B. Fryer, and S. Macko of Memorial University. The geochemical analyses of lake sediment samples were provided by the Newfoundland Department of Mines. Fracture data from outcrop scanline mapping was collected under the supervision of Scott Schillereff. Field assistance at various stages of this project was willingly provided by Glenn Bursey, Gerry Whalen and Frank Mooney. Alison Pye and Sandra Halliday provided assistance with the preparation of graphics. Drs. John Gale and John Welhan patiently supervised the project.

I would like to extend a special thanks to John Gale who believed in giving a "local boy" a chance and to John Welhan who somehow managed to teach me something about geochemistry.

Many thanks to my family who continuously supported and encouraged me throughout this project. My deepest gratitude goes to my wife Susan for standing by me through the many missed deadlines.

LIST OF TABLES

LIST OF FIGURES

CONTENTS

Chapter 1 INTRODUCTION

1.1 Statement of Problem

A common preliminary step in the regional assessment of the mineral potential of an area is to conduct a geochemical survey to determine the metal concentrations in lake, pond and stream sediments. Such surveys are useful in identifying gross regional geochemical trends and anomalously high concentrations of trace metals may indicate local mineralization in the surficial materials or bedrock.

Regional lake geochemical surveys in Newfoundland have consisted of collecting one sample from a lake or pond every seven to eight four km^2 (Butler, 1980). This method of sampling assumes that within a given lake there is a systematic distribution of metals in the lake sediment, either areally uniform or related to depth. However, if the areal distribution of metal concentrations in the lake sediment varies non-systematically, it is possible that an anomalous concentration may be missed if it does not coincide with the chosen sampling point in the lake. In addition, samples in most lake sediment survey are collected using a torpedo-shaped sampler which may penetrate up to 1 m into the sediment. Therefore only the upper layers of lake sediment is sampled

and the depth of the sample is variable and unconstrained. Thus the sample provides data only on the most recent accumulations of sediment, which may be biased to identifying surface particulate and dissolved metal inputs, and provides no indication of the distribution of metals in the sediment with depth and possible non-surface metal inputs.

The vertical distribution of trace metals in the sediment column can provide additional data which may identify the processes or mechanisms by which trace metals are transported and concentrated in the sediment (Frape and Patterson, 1981). Metals can be transported to a lake as detrital matter by stream transport or glacial action or as dissolved solids in either surface water or groundwater. Understanding which processes have been responsible for transporting metals to a lake is essential in designing an effective exploration program for the source of metals found in lake sediments.

The processes by which trace metals are transported, as both particulate matter and dissolved constituents, and concentrated in lake and pond sediments, are well documented and have been summarized by Lush (1984). However, the role of groundwater in transporting and localizing concentrations of trace metals in lake sediment is often overlooked. It is known that groundwater can dissolve and transport metal

species as it moves through a rock mass. These dissolved metals could then be concentrated in lake sediment as groundwater discharges into a lake through its sediment (Figure 1.1). Therefore, in order to be able to properly interpret regional lake geochemical surveys, it is important to define the hydrogeological framework of the area surrounding a lake or pond and to identify regional/local recharge and discharge zones when attempting to determine the source(s) of trace metal concentrations in lake and pond sediment.

In Canada, and especially Newfoundland, there are many areas which are covered by only a thin layer of overburden material and are underlain by fractured bedrock. In regions underlain by metamorphic or granitic bedrock, which have low matrix permeability, fractures act as the main conduits for groundwater flow. If groundwater is an important agent for transporting dissolved metals in these areas it is necessary to conduct a detailed analysis of the fracture networks existing in the underlying rock mass. Given the heterogeneity imposed by the dispersed nature of fracture conduits, fracture controlled discharge to a lake may give rise to an uneven distribution of trace metal concentrations in the sediment. Thus, this study focuses on understanding the role of

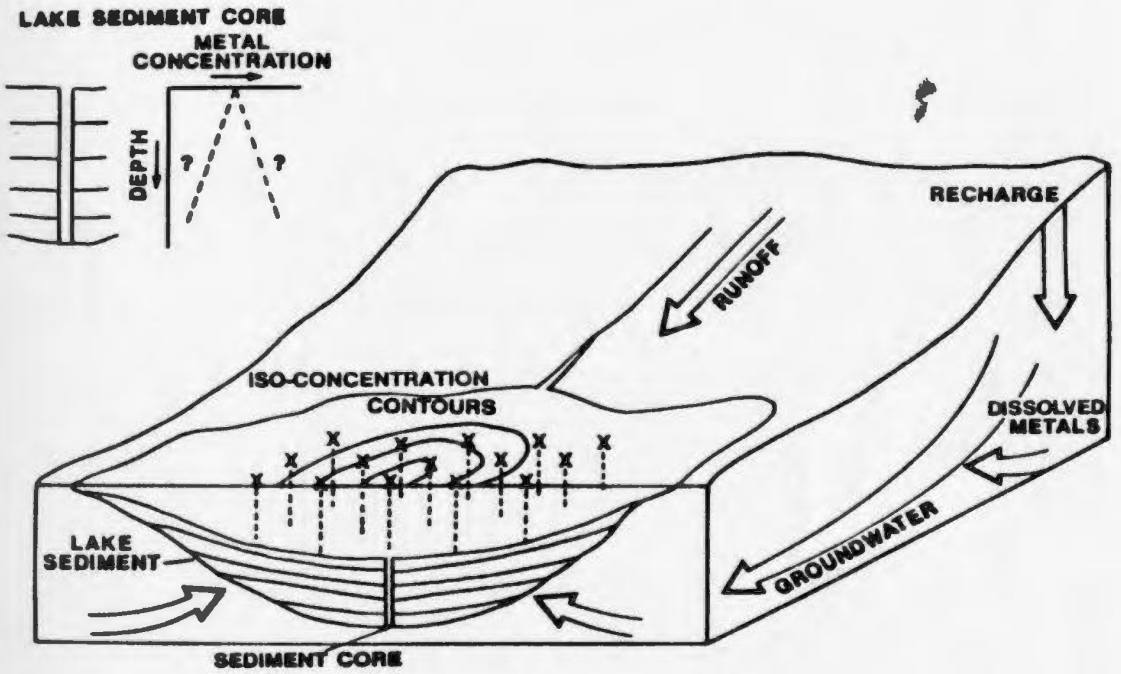

Figure 1.1 Schematic diagram of groundwater discharge into a lake giving rise to metal anomaly in the lake sediment. Sediment sampling points are indicated by X.

groundwater in transporting and localizing trace metals in the sediments of lakes underlain by fractured rock.

1.2 Objectives and Scope

The three main objectives of this field study were: 1) to determine the areal and vertical distribution of trace metal concentrations in the sediments of lakes underlain by fractured rock; 2) to determine the relationship between the concentrations of dissolved metal species found in groundwater and the concentrations observed in lake sediments; and 3) to determine if the hydrogeological framework of the study area is consistent with the distributions and measured concentrations of trace metals in lake sediments.

Four small lakes (locally referred to as ponds) underlain by the Holyrood granite were chosen for this study. Two of the small lakes, Gull Pond and Nut Brook Pond, showed anomalously high concentrations of uranium in a regional lake sediment survey (Davenport and Butler, 1976). The two other adjacent ponds, Pennys Pond and Rocky Pond, were not sampled in the regional survey. In order to establish the distribution of trace metals in the sediment of these lakes a sediment sampling program was undertaken. The first stage of the sampling program, which was carried out during the winter

months, consisted of collecting sediment from each lake on a detailed grid pattern marked on the frozen lake surface. The second stage involved coring and sampling vertical sections of lake sediment, in areas of the lakes known to contain anomalous or background concentrations of trace metals in the sediment.

The groundwater chemistry of the area was determined by evaluating existing regional groundwater chemical data as well as by sampling groundwater which was thought to be discharging into lakes. This was achieved by drilling a shallow borehole at the edge of one of the lakes to intersect discharging groundwater and by drilling through the sediment and into bedrock in another lake to sample groundwater discharging through the lake bottom.

Large scale lineaments and structural features were identified from aerial photographs in an attempt to define the hydrogeological framework of the underlying fractured granite bedrock. Further information on the fracture geometry was provided by an analysis of fracture orientations, trace lengths and spacings from data collected from bedrock outcrops.

Factors controlling the mobilization, transport and subsequent deposition of metal species in lake sediment, such as organic content and oxidation conditions, were also examined to define the relationship between discharging groundwaters and observed sediment anomalies.

1.3 Previous Work

A regional lake sediment survey carried out over the eastern portion of the Avalon Peninsula identified a group of lakes underlain by the Holyrood granite which contained high concentrations of uranium in the sediment, ranging up to 208 ppm (Davenport and Butler, 1976) (Figure 1.2). Some of these lakes also had correspondingly high concentrations of molybdenum and other metals. However, whole rock analyses of the granite, which would be a likely source for the metals, showed no corresponding anomalous concentrations of uranium (Davenport, 1978).

In an attempt to identify a possible source for the uranium, Houle (1985) collected samples of surface waters and shallow sediment from a small lake in the area on a regular grid pattern to determine the distribution of metals in the lake sediments. Results of the sediment sampling showed an uneven distribution of trace metals and localized areas of high

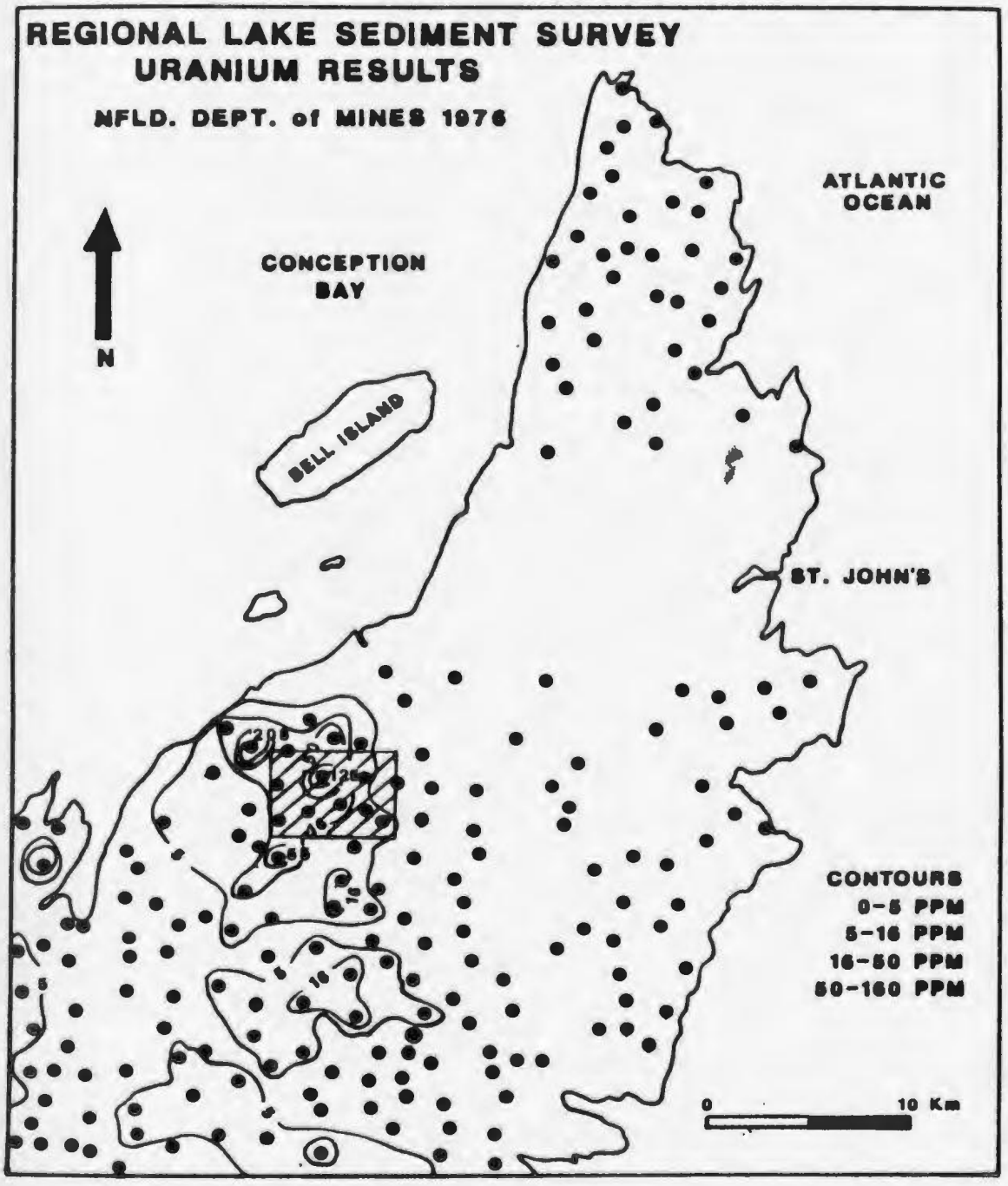

Figure 1.2 Results of uranium analysis from the regional lake sediment survey carried out by Newfoundland Department of Mines (Davenport and Butler, 1976). The cross-hatched rectangle indicates the location of the area described in this study.

concentrations within the lake. The concentrations of metals in the waters were relatively low and did not correlate very well with metal concentrations in the sediment. Since a source of the uranium could not be identified locally in the surrounding bedrock or surface waters it was suggested that groundwaters discharging into the lake may provide a means for transporting trace metals from a distant source.

Until recently, lakes were thought to be isolated from groundwater by the lake bottom sediments. However, detailed research by McBride and Pfannkuch (1975), Winter (1976, 1978) and Lee et al. (1980) which focused on groundwater-lake interactions has shown that lakes form an integral part of dynamic groundwater flow systems. Theoretical and field evidence suggests, that groundwater may discharge into a lake, be recharged from a lake, or both, depending on where the lake is situated relative to local and regional flow systems.

Frape and Patterson (1981) evaluated the distribution of dissolved constituents in groundwaters adjacent to a small lake and in interstitial waters in sediment cores, to define the pattern of groundwater seepage into the lake. The sediment cores, which were also analyzed for trace metals, showed increased concentrations of iron and manganese at particular levels. It was suggested that dissolved iron and

manganese transported by groundwater would precipitate upon encountering an oxygenated zone in the sediment, which could account for the observed metal concentrations in the sediment. A recent study of two lakes in Sweden (Sundblad et al., 1990) was carried out to determine how radionuclides, transported by groundwater, would be distributed in lake sediments. The sediments in these lakes were enriched in uranium in areas where groundwater was discharging into the lake and the uranium enrichment appeared to be associated with organic rich layers of sediment.

Chapter 2 GEOLOGICAL AND HYDROGEOLOGICAL FRAMEWORK

2.1 General Geology

The study area, located on the northeastern Avalon Peninsula, is underlain by granitic rocks of the Holyrood Pluton (Figure 2.1). The Holyrood Pluton intrudes a series of Pre-Cambrian volcanic rocks which make up the Harbour Main Group. The underlying volcanic rocks can be divided into three fault blocks separated by the Topsail - Frenchmens Cove Fault to the east and the South Arm Fault to the west (Hughes and Brueckner, 1971; Gale et al. 1984). The eastern block is dominated by pillow lavas and tuffs. The western block in the Avondale - Harbour Main area is characterized by ash flows mixed with fluvial and lacustrine sediments overlain by basalt flows. The central block, where the lakes in this study are located, consists of mafic and felsic flows, pyroclastics, and minor volcaniclastics which have been intruded by the Holyrood Pluton, a high level granite. The Holyrood Pluton consists mainly of pink, medium grained, biotite granite along with dioritic-gabbroic phases in isolated areas (Strong et al., 1974). The granite is unconformably overlain to the northwest along Conception Bay by shallow dipping marine sediments composed of black shales and green siltstones.

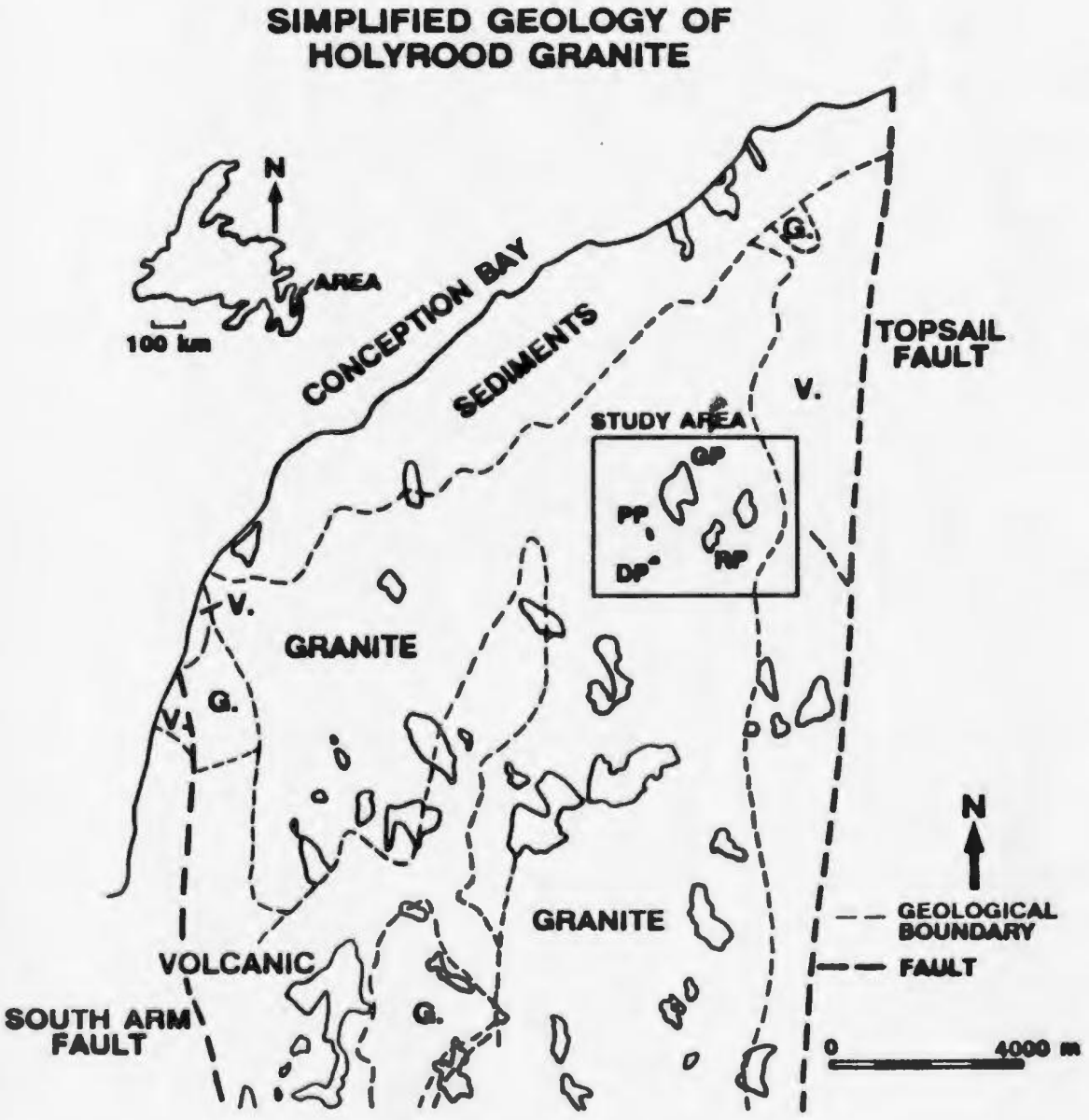

Figure 2.1 Simplified regional geology surrounding the study area (after King, 1984). The lakes sampled in this study are identified as GP = Gull Pond, PP = Pennys Pond, RP = Rocky Pond, and DP = Nut Brook Pond.

The major structural features surrounding the study area are the two north trending regional faults which bound the area. The Topsail fault zone is well exposed along the eastern side of Conception Bay, as evidenced at Topsail Head, and trends south, merging with the Frenchmen's Cove fault in the Formeuse area. The South Arm fault to the west extends southward from the Holyrood area and intersects the Peter's River fault. Several other smaller scale faults and fracture zones as well as numerous joints and fractures have also been observed in the rocks in the study area.

2.2 Fracture Geometry

The bedrock underlying the study area is predominantly granite, which is considered to have characteristically low matrix porosity and permeability. Unlike a porous media system where fluids may easily move through the pore spaces, in a crystalline rock mass, discontinuities such as joints, fractures and shear zones are the major conduits for fluid movement. In a fractured rock system, the orientation, density and interconnectivity of fractures will largely influence the direction and rate of groundwater flow. Therefore, if groundwaters are to be considered a medium for the transport of dissolved metals in this study, it is

necessary to characterize the fracture network in the surrounding granitic rock mass.

On a regional scale, structural features and lineaments were identified from aerial photographs as indicated in Figure 2.2. Most of the lineaments, which were assumed to be sub-vertical features due to their lack of curvature, trend toward the northwest while a smaller group trend toward the northeast (Figure 2.3). The lineaments, that were identified, varied in trace length from 58 m to 1226 m, with a mean trace length of 252 m. Although the ends of some features may be covered by overburden and vegetation, from the aerial photographs the large scale structural features do not appear to be well connected. Hence, the small scale fractures (joints) will be essential to interconnect the large and small scale fracture systems and ensure that a pathway exists for fluids to move through the rock mass. The approach used to characterize the small scale fracture geometry in the study area consisted of collecting and analyzing data on fractures from nine different outcrops (Figure 2.2) surrounding the four lakes using a method of scanline mapping, based on the one used by La Pointe and Hudson (1985). A summary of the mapping approach and procedures along with the fracture data are presented in Appendix A.

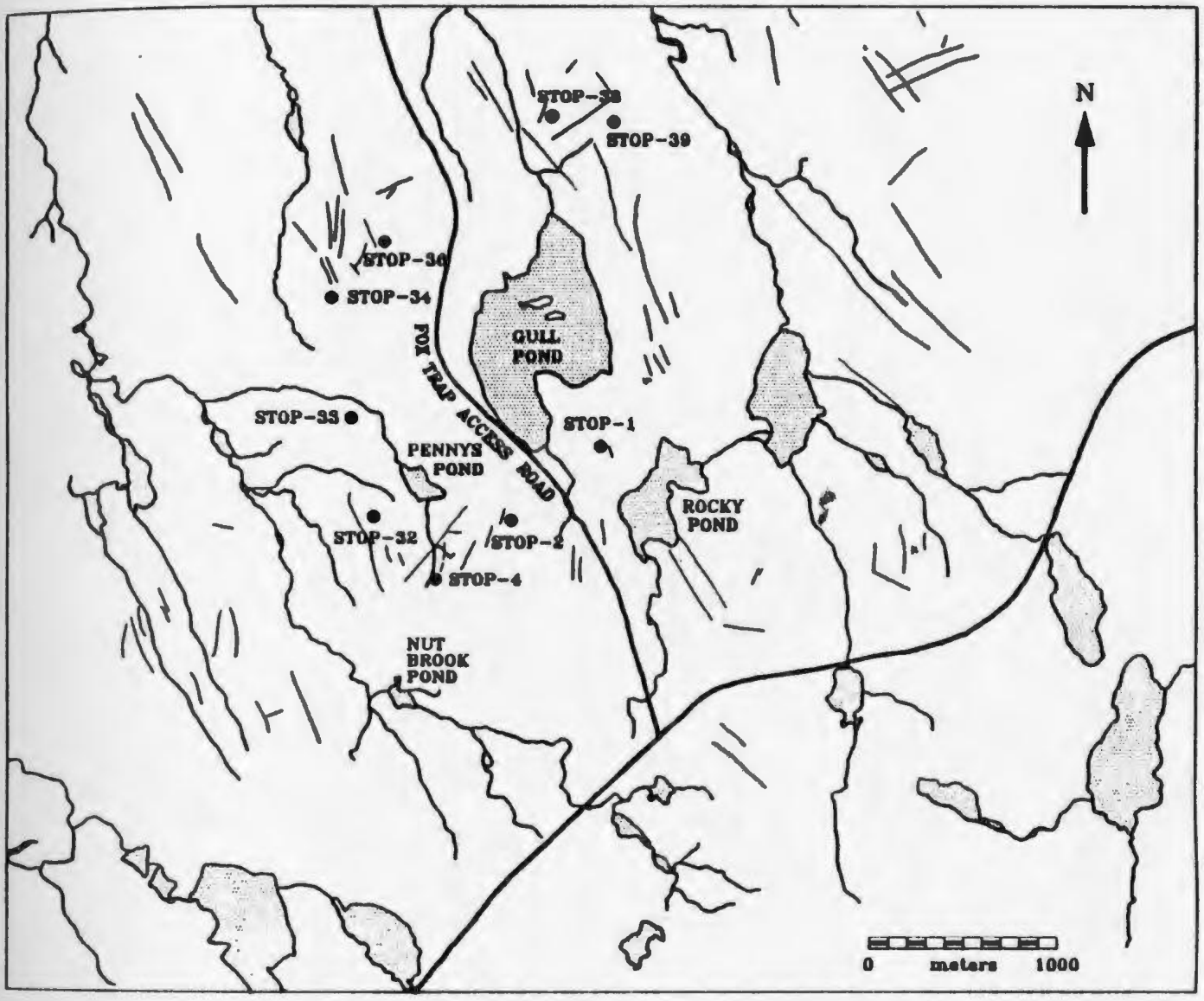

Figure 2.2 Lineaments and structural features observed from aerial photographs. The solid circles indicate the locations of detailed scanline fracture mapping.

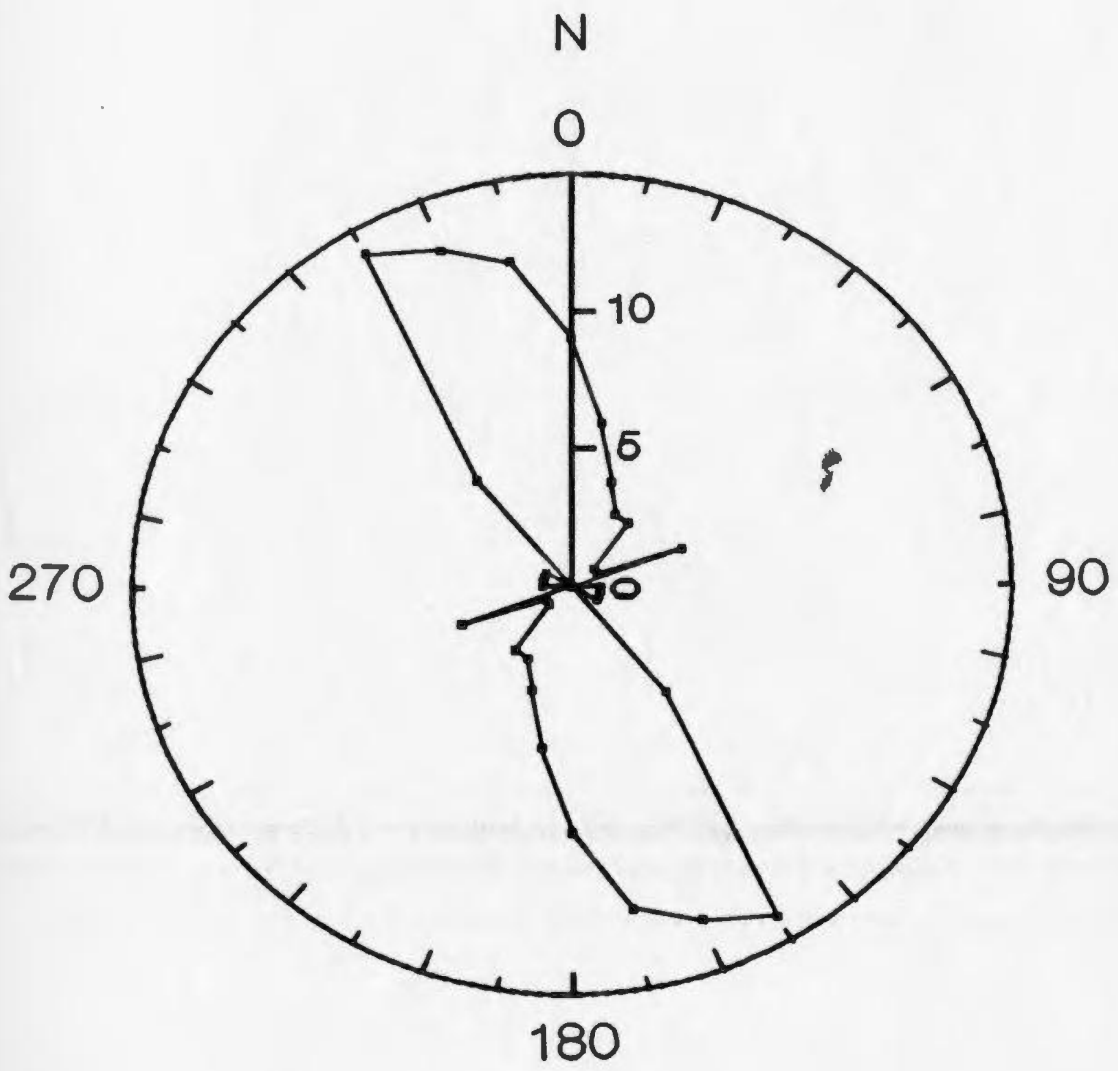

Figure 2.3 Rose diagram of large scale regional structural features and lineaments, showing the frequency of fractures by orientation

The distribution of fracture orientations in the rock mass in the study area was determined by plotting and contouring the poles to fracture planes from all the outcrops mapped on a lower hemisphere stereoplot (Figure 2.4). From Figure 2.4, two dominant sub-vertical sets appear to be present; one oriented northwest-southeast and the other oriented northeast-southwest. Since all the scanlines were laid out on horizontal outcrops, sub-horizontal fractures were less likely to be sampled, which may explain why sub-vertical fractures were dominant in the data set.

To avoid subjective bias introduced by delineating sets solely on the basis of observed peaks on contoured stereoplots, a computer program CLUSTRAN (Gillet, 1987) was used to objectively define clusters and assign individual fractures to a set on a statistical basis. Cluster analysis of the fracture orientations indicated that there were two strong clusters which correlated with the density contours shown in the stereoplot (Figure 2.4). Cluster 1 contains 270 fractures and has a mean orientation of 69.5/82.5 (dip azimuth/dip) while cluster 2 contains 390 fractures and has a mean orientation of 158.4/73.4.

Since the hydraulic interconnectivity of fractures in a rock mass is influenced by the length of individual fractures, the

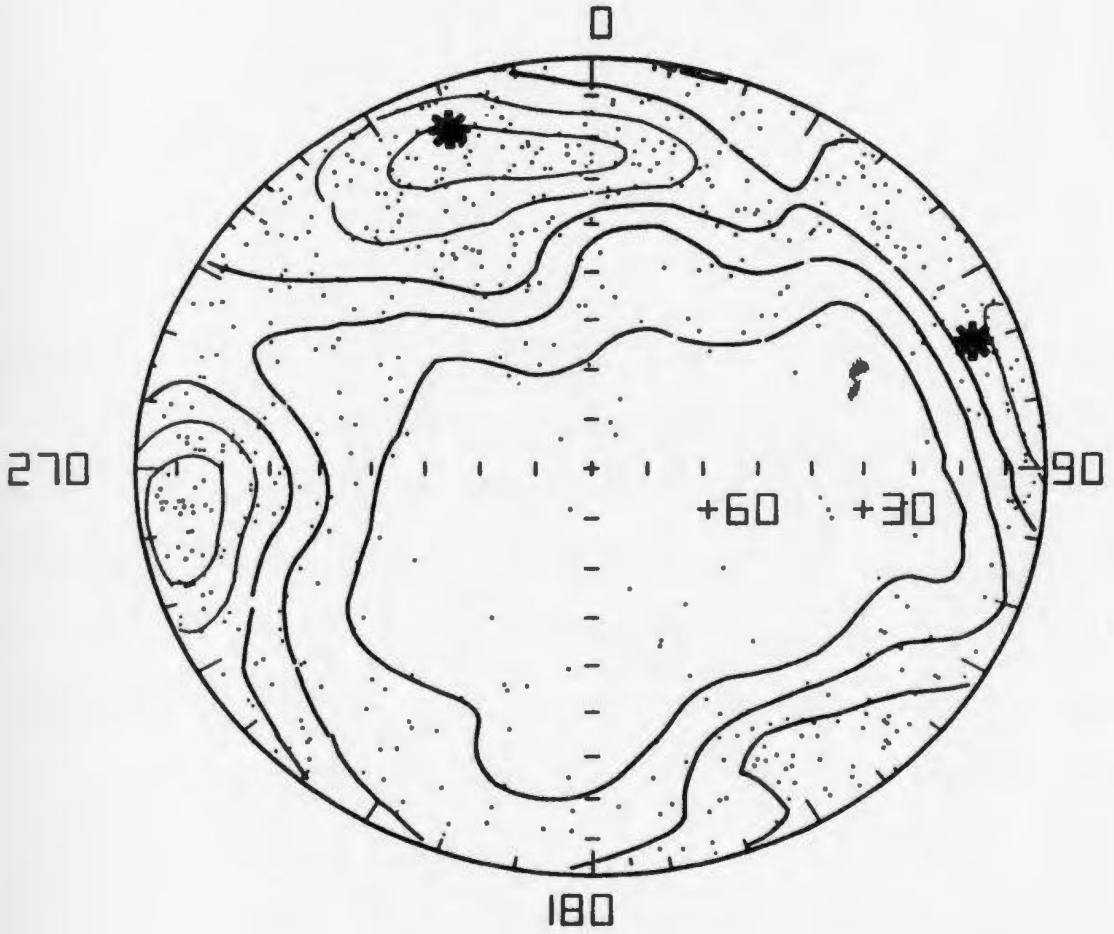

Figure 2.4 Contoured lower hemisphere stereoplots of poles to fracture planes for all fractures mapped in the study area. Mean cluster orientations are shown as solid circles, and individual fracture poles as small dots.

length of fracture traces intersecting the scanlines were measured. The actual length of a fracture trace may be longer than that measured since in the field one or both ends of a fracture trace may be censored, meaning a portion of the total fracture trace is hidden. Figure 2.5 shows the frequency histograms and basic trace length statistics for fractures of each cluster by degree of censoring. Although the distribution of trace lengths is skewed, the focus of this study is on recognizing long fractures which may a have role in forming conduits and accounting for the skewness of the distribution would result in small geometric means. Approximately 55% of fractures in cluster 1, which have a mean trace length of 3.96 m, are censored compared to 36% of fractures in cluster 2 which have a mean trace length of 2.57 m. Since fractures of cluster 1 have a larger mean trace length and are more highly censored than fractures of cluster 2, they are generally considered to be longer, and therefore may have a greater influence on the direction of groundwater movement.

The way in which fractures terminate against each other may also give some indication of ability of the fractures to act as a pathway for fluid movement. A fracture may intersect with another fracture at one end, both ends, or be free at both ends which is important when determining the

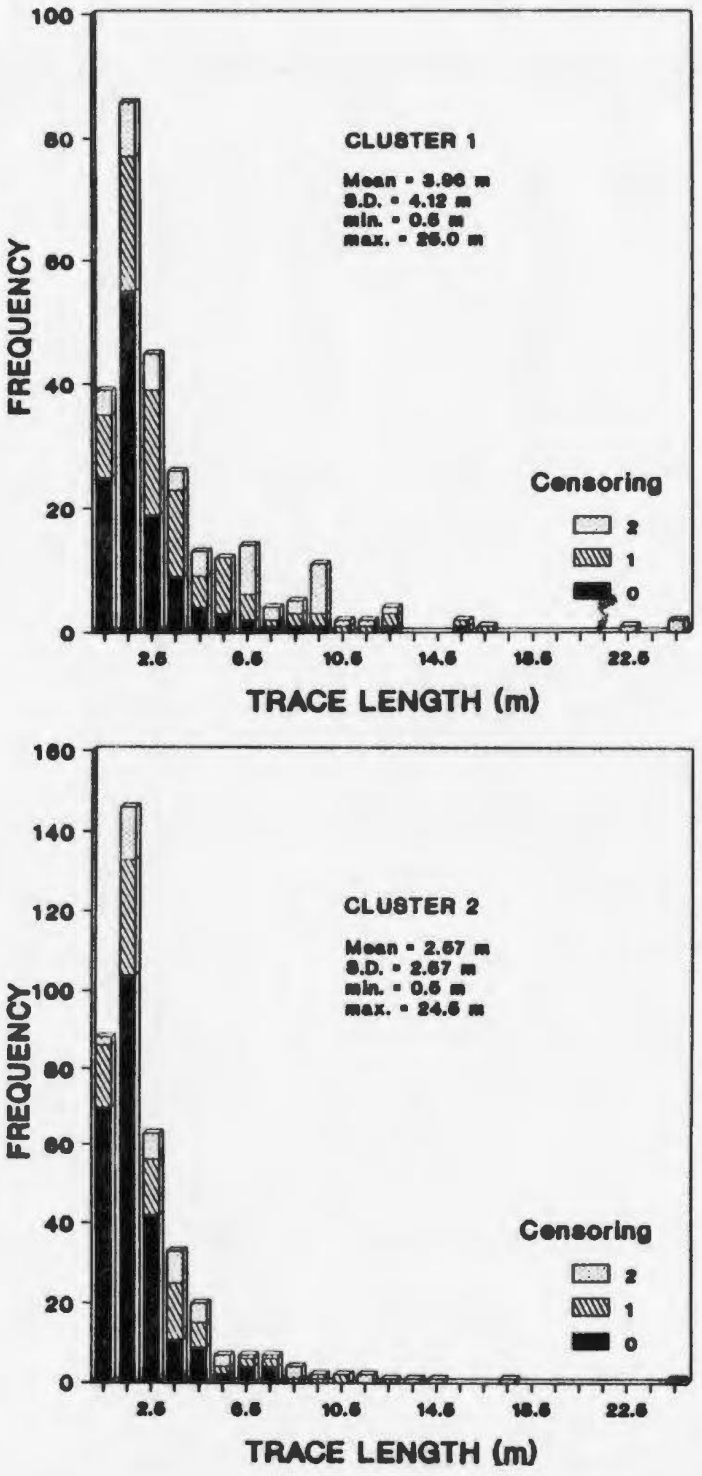

Figure 2.5 Frequency histograms of trace length by censoring (0=both ends exposed, 1=one end covered, 2 = both ends covered) for clusters 1 and 2.

interconnectivity of fractures. Figure 2.6 shows the frequency histograms of trace lengths by termination mode for each cluster. Of the fractures that are uncensored (ones in which the mode of termination can be determined) 55% of fractures in cluster 2 intersect other fractures while 40% of fractures in cluster 1 terminate against other fractures. This indicates a moderate degree of fracture interconnectivity in the rock mass which would allow fluids to easily move in preferred directions through the rock mass along fracture pathways.

The density of fractures in a rock mass can be estimated from fracture spacing which is defined in this study as the perpendicular distance between two fractures of the same set. Fracture spacing is computed from the measured distance between two fractures of the same set intersecting a scanline, and the angle measured between the mean normal of the fracture set and the scanline. Fracture density can then be expressed as the inverse of the fracture spacing.

Frequency histograms and statistics of fracture spacings for cluster 1 and 2 are shown in Figure 2.7. The spacing values vary from near zero to 6.11 m, with cluster 1 having a mean spacing value of 0.77 m compared to cluster 2 which has a mean spacing value of 0.57 m. This indicates that there is a

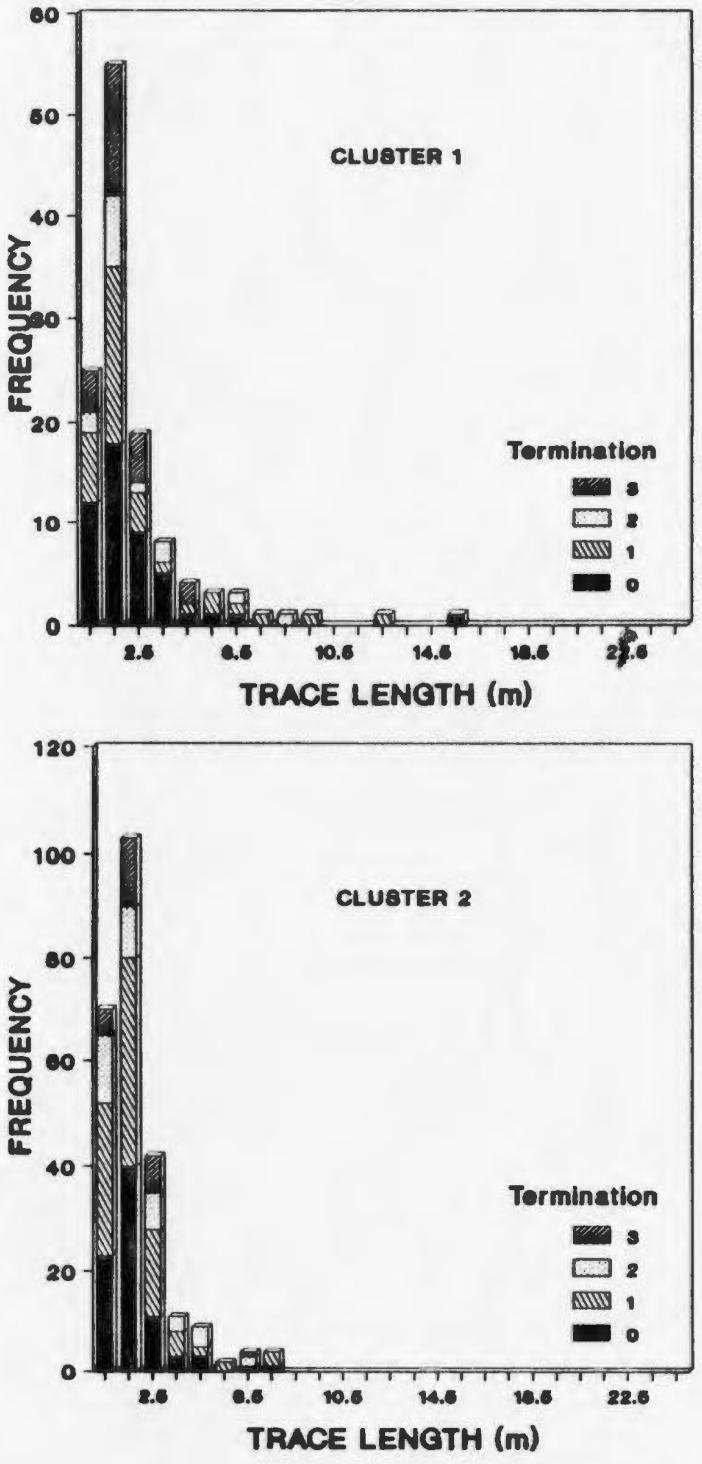

Figure 2.6 Frequency histograms of trace length by termination mode (0=both ends free, 1=one end free, 2=both against another, and 3=splays) for clusters 1 and 2.

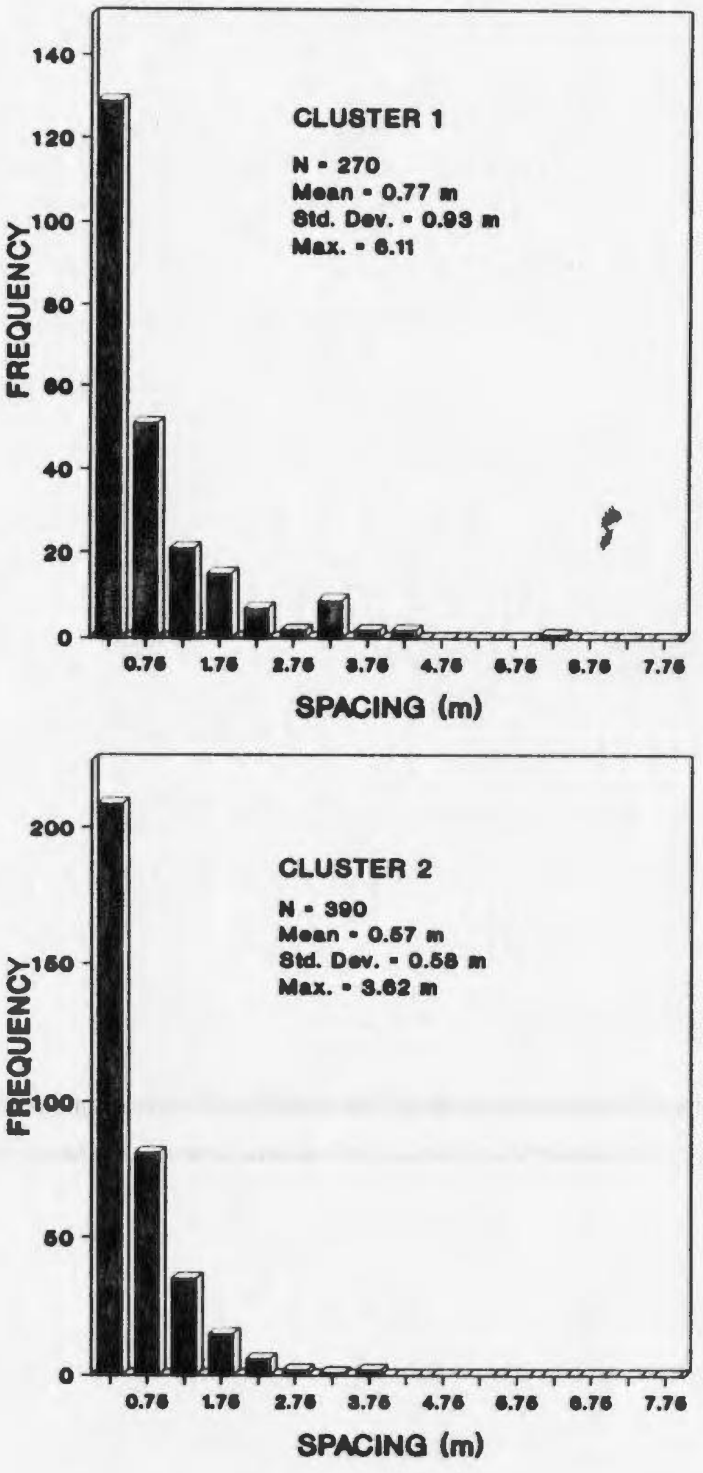

Figure 2.7 Frequency histograms of spacing for clusters 1 and 2.

greater degree of fracturing in the NE-SW direction (cluster 2), 1.75 fractures per metre estimated from the spacing calculation, than in the NW-SE direction (cluster 1), 1.29 fractures per metre. Since only fractures above a given trace length (truncation length equals 0.5 m) are mapped, fracture spacings will increase with increasing truncation bias.

The degree of fracture interconnectivity indicated by the termination mode of individual fractures along with fracture density estimated from fracture spacings indicate that the granitic rock mass is relatively permeable and will allow moderate groundwater movement. The fracture density and trace length calculated for clusters 1 and 2 indicate there is a degree of heterogeneity in the rock mass and that there may be a preferred direction for groundwater movement. On a regional scale the general direction of the hydraulic gradient in the study area is from the southeast towards the northwest. Therefore fractures of cluster 1, which are oriented slightly west of north, sub vertical and have longer traces, are most likely to dominate the direction of groundwater flow. This is consistent with the trend of the regional lineaments observed from the aerial photographs. However, since a greater percentage of fractures belong to cluster 2, which are more closely spaced, on a local scale the dominant flow direction may be towards the northeast depending on the hydraulic

gradients. Although sub-horizontal fractures, such as sheeting fractures, do not appear to be very dominant based on the analysis of the fracture data collected, they do exist in the rock mass and will provide a pathway for sub-horizontal groundwater flow.

2.3 Hydrogeology

The preglacial landscape of the study area is characterized by an upland area typical of the Lawrence Peneplain, (Twenhofel and MacClintock, 1940) with gently rolling relief rising up from the coast toward the southeast to an elevation of about 300 m. The main drainage divide in the region is defined by a northeast trending ridge which directs surface water flow toward the coast of Conception Bay along several narrow, northwest-oriented sub-basins. Regional drainage generally follows preglacial patterns which are largely influenced by bedrock structures and joint features.

Most of the lakes and ponds in the area formed in basins in the granitic bedrock, either excavated by ice or dammed by glacial debris (Henderson, 1972). Sediments in the lakes are comprised of a layer of silty clay, probably deposited from glacial outwash, overlain by up to 400 mm of mineral sediment,

followed by organic sediment accumulations (MacPherson, 1982). These sediments have developed over the past 7000 to 9300 years and organic sediments are estimated to have accumulated at an average rate of approximately 0.6 mm per year, based on dating from pollen analysis.

Hills or topographic highs in the area are characterized by well exposed outcrops while lower areas tend to be filled with thin deposits of glacial material. Glacial drift is relatively thin and discontinuous averaging less than 5 meters in thickness. The lack of overburden material suggests that sub-surface flow in the area is mainly through the granite bedrock where fractures and discontinuities in the rock mass are the major conduits for groundwater movement. Groundwater recharge is expected to occur in topographic highs, although the amount of actual infiltration may be low due to surface run-off over areas of exposed bedrock. Similarly groundwater discharge would occur in topographically low areas. The presence of several small lakes and swamps on aerial photographs and topographic maps of the area suggests that the water table in these areas is close to ground surface and closely reflects the topography of the area. The lakes and ponds in the area are thought to be points of local and/or regional discharge, and have an important role in controlling the groundwater flow system (Gale et al., 1984).

All of the four lakes in this study are contained in individual sub-basins and each lake has only one stream flowing into it which derives its head waters from within close proximity of each lake (Figure 2.8). Although the lakes are not connected by streams, due to differences in lake elevations (Figure 2.8), there may be some sub-surface flow between local drainage basins, particularly through fracture channels.

The four lakes are located in the mid to upper portion of the regional flow system and therefore groundwater discharging into these lakes would be mainly from local flow systems in their vicinity. For example, Pennys Pond at an elevation of 154 m, is located at the base of Pennys Hill which rises to an elevation of 210 m. The lake has very little stream inflow but has a sizeable outflow, and has a marshy area surrounding the lake which suggests that Pennys Pond is being fed by local groundwater.

Although pole plots of fractures recorded from outcrops surrounding the lake indicate that the dominant orientation of fracturing is toward the northeast (Figure 2.9.), there is also another set of fractures present which are oriented slightly west of north. Given the hydraulic gradient toward the lake imposed by Pennys Hill, along with the abundance of

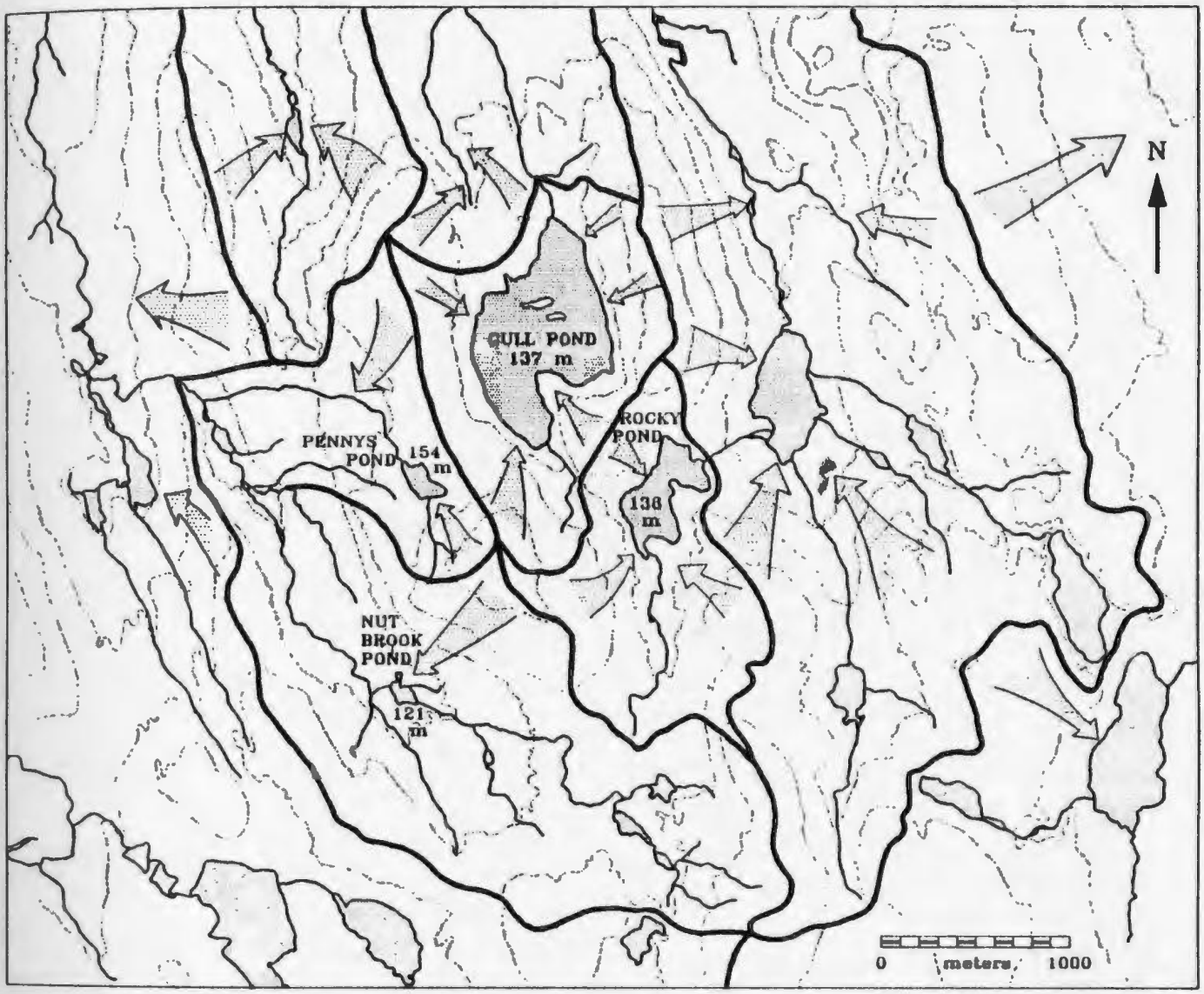

Figure 2.8 Map showing drainage and lake outlines, topographic contours (faint lines), drainage basin divides (thick lines), and inferred direction of groundwater movement (arrows) in the study area. The water level elevation for each lake in the study is given in meters.

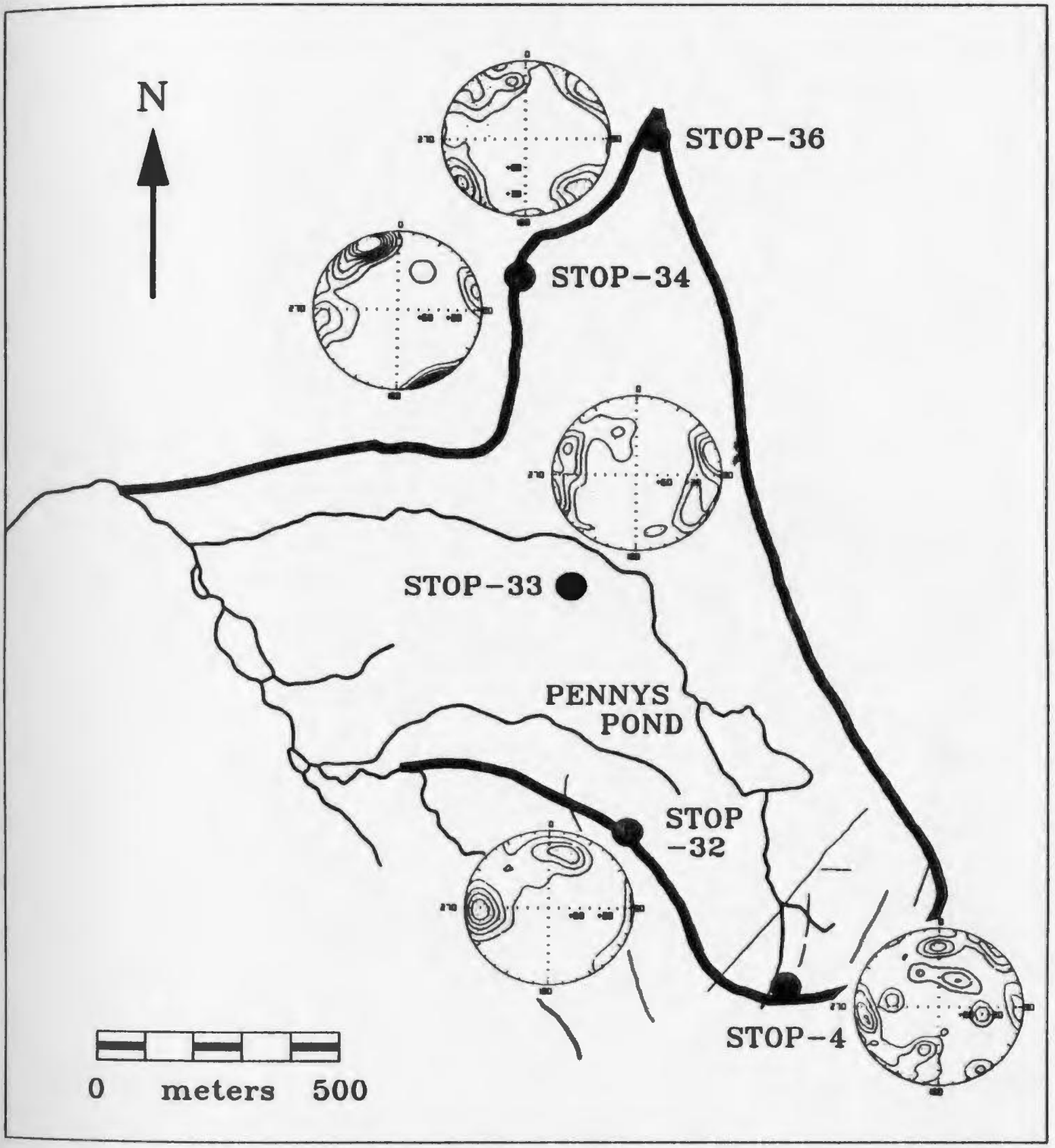

Figure 2.9 Map showing large scale structural features and contoured lower hemisphere stereoplots of fractures identified from scanline mapping of outcrops in the vicinity of Pennys Pond.

large scale features in the area oriented toward the northwest it is likely that groundwater would be directed toward the lake along northwest trending features.

Figures 2.10 and 2.11 show the pattern of fracturing surrounding Gull Pond and Rocky Pond. As in the case with Pennys Pond, the direction of groundwater movement into these lakes will be influenced by local gradients and the orientation of the two major fracture sets that are present. Gull Pond is surrounded by a ridge on three sides which funnels groundwater into the lake. Gull Pond and Rocky Pond are at approximately the same elevation, 137 m and 138 m respectively, but are separated by a ridge which acts as a basin divide between the two lakes. Although Rocky Pond has a common point of recharge with Gull Pond it also derives waters from an area to the southwest.

Nut Brook Pond to the southwest is the smallest lake included in this study and is at the lowest elevation, 121 m. Pennys Hill is to the northeast of Nut Brook Pond which serves as a substantial driving force for the local groundwater recharge toward the lake. The area surrounding the lake is extremely wet and boggy indicating that the water table is quite high and that groundwater is discharging in the area.

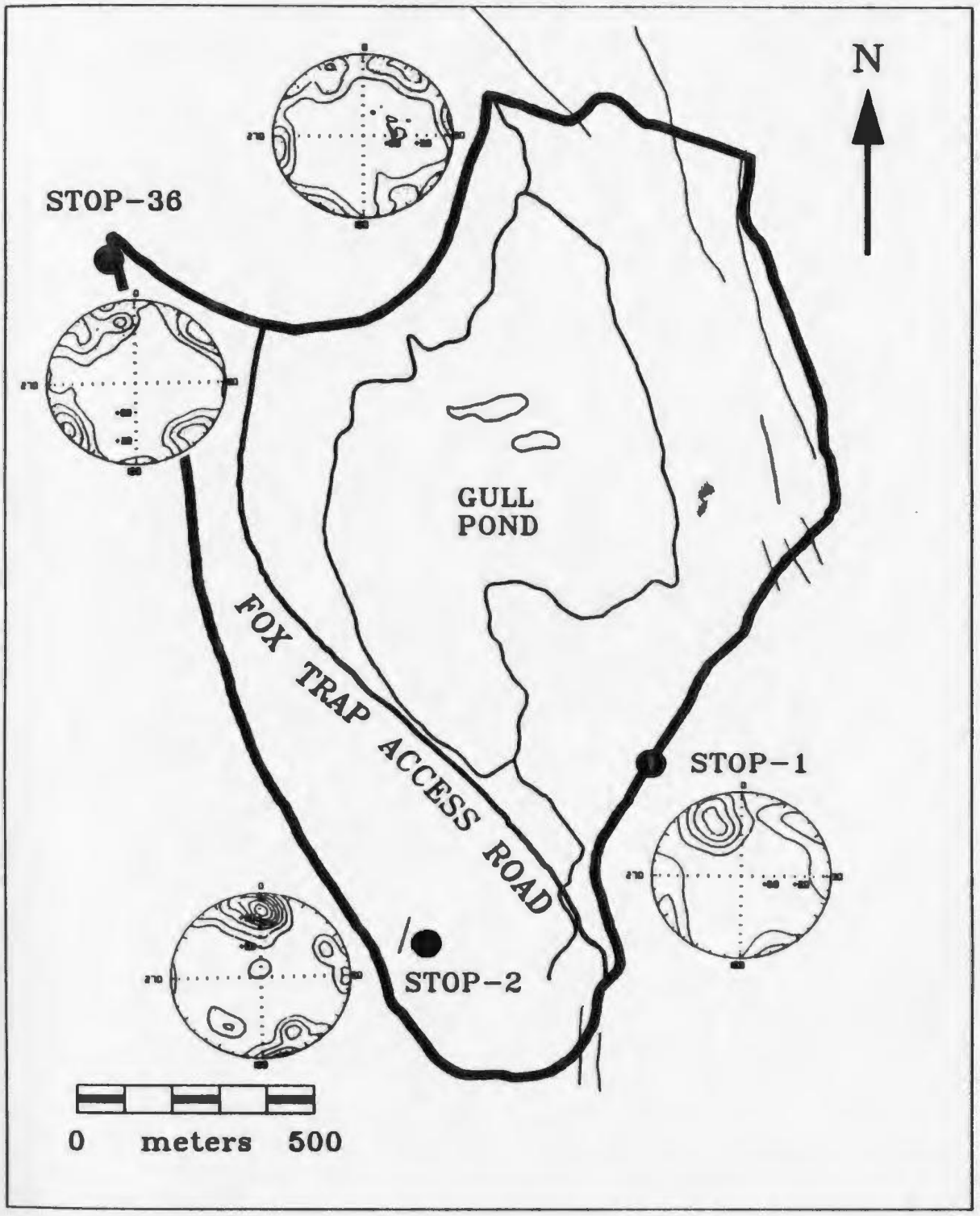

Figure 2.10 Map showing large scale structural features and contoured lower hemisphere stereoplots of fractures identified from scanline mapping of outcrops in the vicinity of Gull Pond.

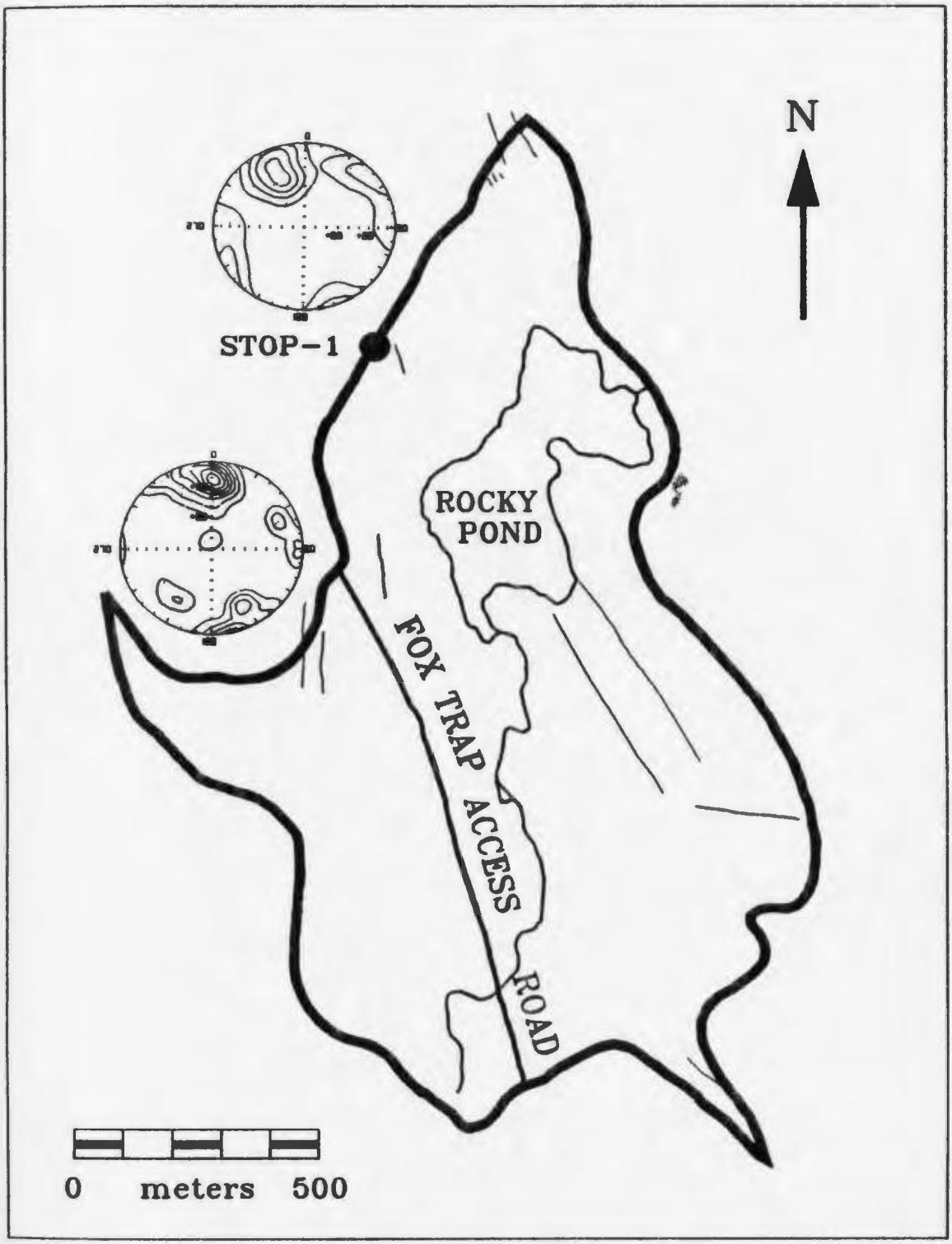

Figure 2.11 Map showing large scale structural features and contoured lower hemisphere stereoplots of fractures identified from scanline mapping of outcrops in the vicinity of Rocky Pond.

Chapter 3 LAKE SEDIMENT AND GROUNDWATER SAMPLING PROCEDURES

3.1 Lake Sediment Sampling and Analysis

The spatial distribution of metal concentrations within the sediments of the four lakes in this study were determined by collecting samples of sediment on a grid pattern marked on the ice surface of each lake. In the first phase of sampling, carried out during the winter of 1986, lake sediment samples were collected from Gull Pond (8980 m^2) and Rocky Pond (2320 m^2) using a 100 m grid pattern, while Nut Brook Pond (280 m^2) which was smaller in size, was sampled at 25 metre intervals. Pennys Pond (490 m^2) was sampled in 1985 using a 25 metre grid (Houle, 1985). A second phase of sampling was carried out over parts of Gull Pond and Rocky Pond during the winter of 1987, using a 50 metre grid, to more completely define the metal anomalies identified by the 1986 sampling.

Sediment samples were collected from the lake bottom using a weighted pipe torpedo-type sampler similar to the one described by Hornbrook et al. (1975). Holes were augured through the ice at the grid points and the sampler dropped through the hole allowing it to penetrate up to 1 metre into the lake sediment. After a sample was retrieved it was described in terms of colour, texture, and content and the

water depth at the grid location recorded. Each sample was then dried and crushed, and the crushed material sieved through 180 μm mesh screens to remove large bits of organic matter. One gram of each sample was digested in a 6 ml solution of 4M HNO_3 - 1M HCl at 90° C for two hours. The solution was then made up to 20 ml and analyzed by atomic absorbtion spectrophotometry for Cu, Pb, Zn, Fe, Mn, Cd and Mo. Neutron activation was used to determine uranium concentrations. An estimate of organic content was determined by measuring the percent weight of sample lost by ignition of 0.5 grams of sample at 500° C for four hours.

In addition to the samples of surface sediment collected from the lake bottom a total of eleven sediment cores were taken from Gull Pond, Rocky Pond, and Nut Brook Pond during the winter of 1987, in areas of anomalous and background metal concentrations as identified by the grid sampling, to define the vertical distribution of trace metals in the lake sediment. Continuous core samples were taken using a 0.5 m long half core sampler in water up to 16 m in depth. The core sampler was lowered on steel pipe through a 100 mm diameter ABS guide pipe which extended from the water surface to the lake sediment, allowing re-entry into the same hole each time to maintain a continuous sampling sequence. The cored sections of sediment ranged from 0.5 to over 3.0 metres. The

Nut Brook Pond cores were split into 50 mm sections for analysis. However, this did not always provide enough sample for a complete analysis. Hence, the cores from Gull Pond and Rocky Pond were divided into 100 mm sections. Analysis of the sediment core samples followed the same techniques as described above.

3.2 Groundwater Sampling and Analysis

The groundwater chemistry and hydraulic gradients beneath and adjacent to two of the study lakes were determined in order to establish the relationship between metal concentrations in lake sediment and groundwaters. A shallow 44 mm diameter borehole was drilled on an exposed outcrop at the edge of Pennys Pond to a depth of 12 m to intercept and sample discharging groundwaters (Figure 3.1). Permeable zones in the borehole were identified by performing fixed interval falling head permeability tests over the entire length of the borehole. After the borehole testing was completed, a multilevel piezometer modelled after those designed by Cherry and Johnson (1984), using chemical sealant packers, was installed in the borehole. Double packer assemblies were used to increase the length of the seal between sampling intervals to 600 mm and to minimize the possibility of short-circuiting

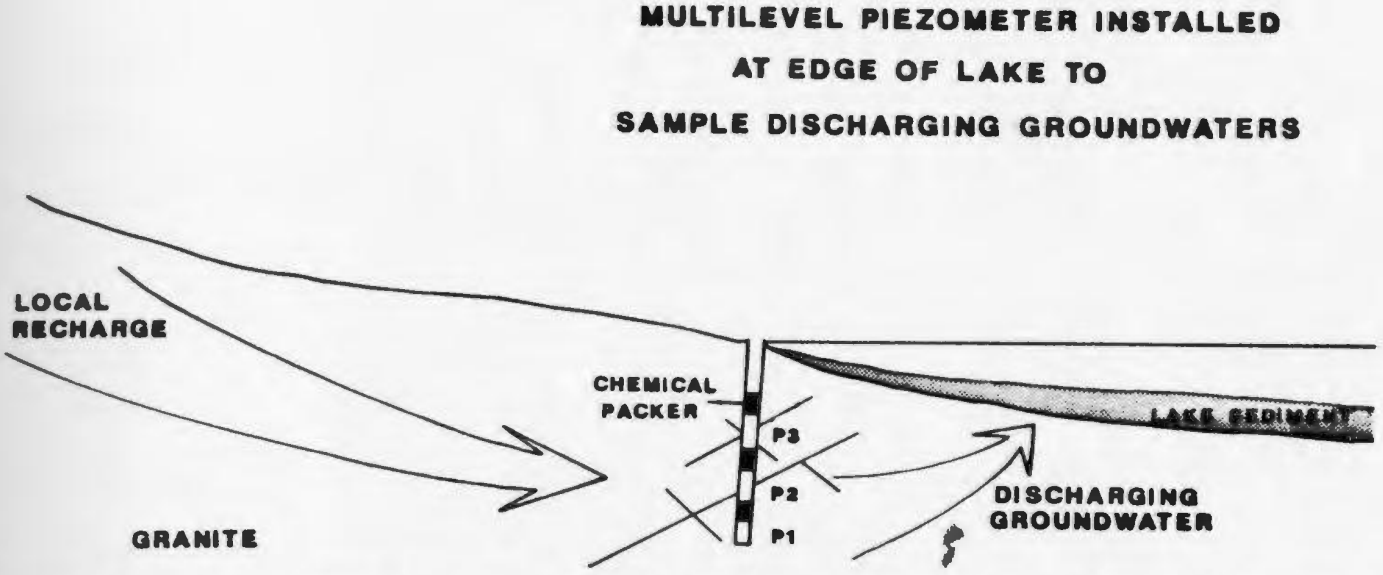

Figure 3.1 Schematic of multilevel piezometer installed on the shore of Pennys Pond.

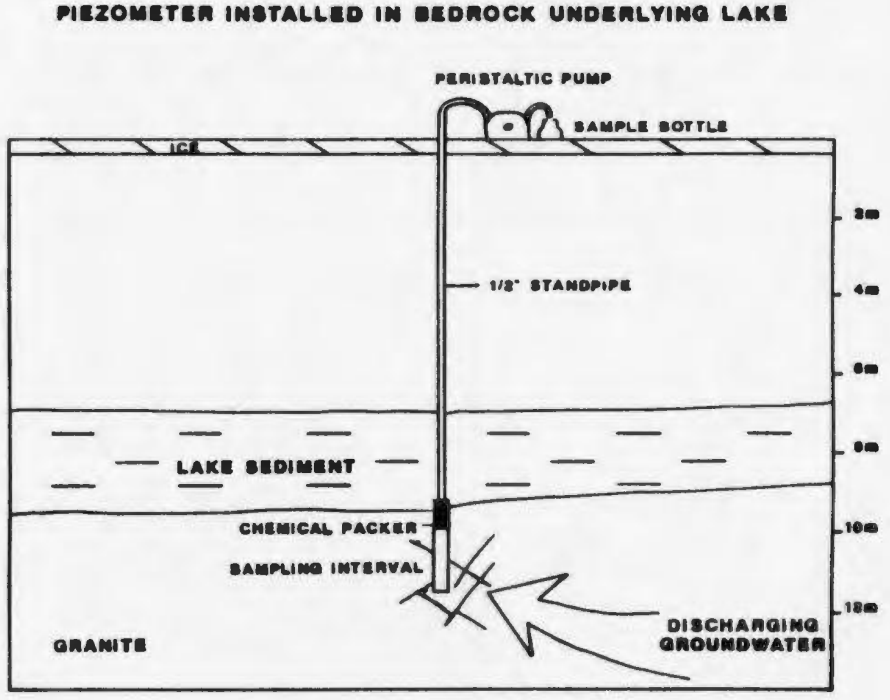

Figure 3.2 Schematic of piezometer installed through the lake sediment and into bedrock in Gull Pond.

between sampling intervals by connected fractures. This multilevel piezometer configuration provided three ports for the measurement of hydraulic gradients in the borehole and water sampling.

A second borehole was drilled from the ice surface, during the winter of 1988, in an area of Gull Pond which was identified as having anomalously high concentrations of uranium in the sediment in the previous grid sampling. The borehole penetrated the lake sediments and continued approximately two metres into granite bedrock. The bottom of the borehole provided a sampling interval which was sealed with a chemical packer (Figure 3.2). A 1/2 inch diameter polyethylene tube attached to the chemical packer was brought to the surface through the ice cover which allowed the hydraulic head in the isolated interval to be measured and groundwater samples to be collected directly at the bedrock/sediment interface.

Groundwater samples were extracted from all of the sampling intervals using a peristaltic pump. Measurements of pH and total conductivity were taken in the field at regular intervals during pumping. After stable readings were observed, two 125 ml polyethylene bottles of groundwater were collected. Two 125 ml bottles of lake water were also collected at the same time. Within four hours, each sample

was passed through a 0.45 μm filter and half the sample acidified with 1 ml of 16M nitric acid. Alkalinity was determined by acid titration of a portion of unacidified, unfiltered sample and reported as mg/l of equivalent bicarbonate. Analysis of major cations was done by atomic absorption spectrophotometry and trace metal concentrations were determined by inductively coupled plasma mass spectrometry (ICP/MS). Since bicarbonate was the dominant anion only semi-quantitative measurements of chloride and total sulphur were done by ICP/MS which gave values with a precision of ± 15%.

Chapter 4 GEOCHEMICAL AND ISOTOPIC FRAMEWORK

4.1 Regional Water Geochemistry

A hydrogeochemical data base for the Foxtrap - Holyrood area has been compiled as part of a regional groundwater flow system study (Gale et al., 1987). A survey of thirty one lakes and ponds in the area was carried out during May and June, 1985, to collect lake water samples for chemical analysis. The basic environmental parameters of pH, Eh, electrical conductivity and dissolved oxygen were measured at the time the water samples were collected. The water samples were analyzed for major anions and cations as well as trace metals. Groundwater samples were collected throughout the area from domestic water wells as well as from a series of research boreholes. Analytical results of the water samples collected are presented in Appendix B.

Results of the major ion analysis of samples collected from wells and lakes located in granitic bedrock have been plotted on a Piper diagram (Figure 4.1) to compare the chemical composition of groundwaters and surface waters. Surface waters (plotted as *) fall mainly in the Na-Cl field of the plot while groundwaters (plotted as x) range from Ca-HCO_3 to Ca-Na-HCO_3 or Ca-Na-Cl. All groundwaters have a greater

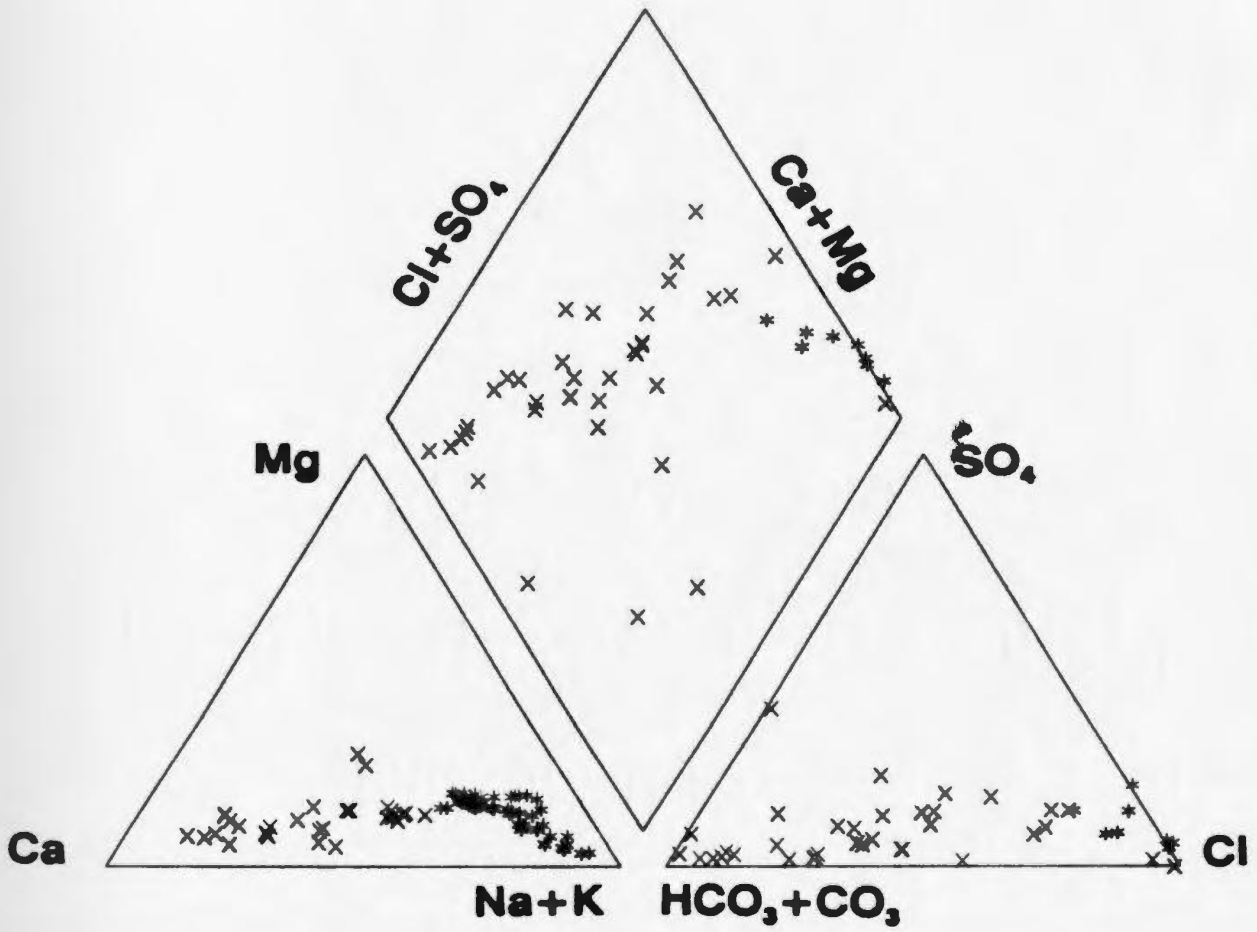

Figure 4.1 Piper plot for groundwater (x) and surface water (*) samples collected in Holyrood - Foxtrap area, May-June 1985, March 1987, and March 1989.

proportion of calcium than surface waters, and most have a higher proportion of bicarbonate, which is consistent for waters evolving in carbonate or plagioclase rich terrains. In general, surface waters have a Na/Ca ratio greater than 1.5 to 1, while groundwaters have Na/Ca ratios less than 1.5 to 1. This difference in sodium and calcium content can be used to differentiate between surface waters and shallow groundwaters.

Waters from most of the lakes in the study area have relatively low pH (less than 7) with several having pH values as low as 4.5. The Na-Cl character of surface waters is most likely related to the close proximity of the lakes to the coast and, in a few cases, road salt contamination introduced from the main highway and secondary roads which run through the head waters of the study area. Generally, the surface waters tend to be low in total dissolved solids compared to groundwater as approximately 80% of the lakes sampled had less than 10 ppm Na and less than 2 ppm Ca, while about 80% of the groundwater sampled contained greater than 10 ppm Ca. Concentrations of trace metals, with the exception of iron, also tend to be higher in groundwaters than in lake waters. The ratio of metal concentrations in groundwater to metals found in surface waters is in the range of 3 to 1, to 20 to 1, with the exception of uranium which is almost 1000 times greater in groundwater than in surface waters (Table 4.1).

Table 4.1 Comparison of the average trace metal concentrations found in groundwaters with the average concentrations found in surface waters.

	Cu ppb	Pb ppb	Zn ppb	Mn ppb	Fe ppm	Mo ppb	U ppb
Average Surface Water	9.7	2.0	22.8	31.5	140.7	0.1	0.1
Average Groundwater	35.9	10.2	70.9	408.3	43.9	1.7	89.4
Ratio GW/SW	3.7	5.1	3.1	12.9	0.3	17.0	894.0

Groundwater samples from deeper research boreholes (25 to 60 metres) along the Seal Cove River Valley to the west of the study area indicate that pH and dissolved solids generally increase with depth. The groundwaters from these boreholes are characteristically Ca-HCO_3 with slightly higher relative Na content in shallower intervals. Although dissolved solids in groundwater generally increase with depth, the groundwaters show no systematic increase of trace metal concentrations with depth. The exception to this is uranium which was found in concentrations up to 350 ppb in the deepest intervals sampled. This is consistent with relatively high Eh values observed in these intervals, which indicate that uranium should exist in its hexavelant state and would therefore be soluble at these depths. Domestic wells sampled in the lower part of the regional flow system and completed in the Holyrood granite

have similar water chemistry but generally lower pH, total dissolved solids, and uranium content. This may be due to dilution and mixing with shallow groundwaters, induced by long term pumping.

A number of samples collected from the research boreholes over a period of several days, as the boreholes were being pumped, were analyzed for stable isotopes. The $\delta^{18}O$ values determined for these boreholes ranged from -8.5 to -9.0 per mil vs SMOW (Standard Mean Ocean Water) and as high as -8.3 in the deepest borehole. Analysis of precipitation in 1985/86 indicated $\delta^{18}O$ mean annual values of -8.0 to -10.0 per mil for meteoric waters in the area (Welhan, pers. comm., 1987). Therefore it is difficult to differentiate between shallow and deep groundwaters using oxygen isotopes due to the similarity in ranges of $\delta^{18}O$ values.

An attempt was made to use differences in water chemistry from the regional lake survey as an indicator of lakes which are fed by groundwater. Lakes located in the lower portion of the regional groundwater flow system, and therefore likely to have a large component of groundwater discharging into them showed no apparent difference in water chemistry compared to other lakes in the area. The only lakes sampled which showed an enrichment in calcium and other dissolved solids were part of

the Kelligrews River system. These lakes were located downstream from a local dump which is a likely source for the observed increase in dissolved solids (Griffen, 1988). Oxygen isotopes proved to be inconclusive in distinguishing the component of groundwater discharge into a lake due to the lack of contrast in the isotopic composition of groundwaters and lake waters.

Samples of lake water taken in Gull Pond, Pennys Pond, Rocky Pond and Nut Brook Pond through the ice in the winter had higher concentrations of Ca than in samples collected in the spring (Table 4.2). Although there were corresponding increases in concentrations of Na in three of the four lakes they were not as significant as the increases in the concentrations of Ca indicating a possible enrichment by Ca - rich groundwater.

An estimate was made of the proportion of groundwater that would be necessary to enter each lake to produce the observed increase in calcium concentrations. It was assumed that the concentrations of Na and Ca observed in the samples of lake water taken in the spring were representative of normal surface waters conditions. It was also assumed that the concentrations of Na and Ca observed in lake water samples taken in the winter were indicative of surface water mixed

Table 4.2 Comparison of Ca and Na concentrations (ppm) in lake waters in Spring and Winter

		Spring	Winter	% change	Proportion of Groundwater
Gull Pond	Ca	1.5	2.2	46	23%
	Na	9.2	11.4	24	
Rocky Pond	Ca	2.7	4.6	70	29%
	Na	31.9	40.8	28	
Pennys Pond	Ca	0.7	0.9	28	20%
	Na	5.0	5.3	6	
Nut Brook Pond	Ca	11.1	15.2	37	35%
	Na	173.6	163.2	-6	
Average Groundwater	Ca	22.4			
	Na	13.2			

with a higher proportion of shallow groundwater during a period of no evaporation and little surface water input. The proportion of groundwater required to produce the concentrations observed in the mixed waters were calculated based on the minimum ratio of Na to Ca for shallow groundwater in the area of 1.5 to 1, determined from Figure 4.1.

These calculations indicate that groundwater contribute in the range of 20 to 35 percent of the total water recharging the lakes over the winter period. These estimates are probably low since during the winter period there is minimal surface run-off to the lakes and the greater percentage of water discharging into the lakes should be derived from groundwater.

In addition, the maximum Na/Ca ratio for groundwater was used in the calculations which maximizes the estimate of the proportion of groundwater entering each lake. These estimates are very approximate since Ca balance depends on the size, volume and flushing rate of the lake as well as the actual proportion of the lake's water balance that is comprised of groundwater. However, they do suggest that groundwater is discharging into these lakes.

4.2 Local Groundwater Geochemistry

Analytical results for water samples taken from Pennys Pond and Gull Pond and from boreholes drilled at both lakes are given in Table 4.3 while analytical results from other selected boreholes, are given in Table 4.4 for comparison. Samples PP-1, PP-2 and PP-3 were taken from three intervals of the multilevel piezometer installed in a 12 m borehole at the edge of Pennys Pond. Sample GPGW is from a borehole drilled through the bottom of Gull Pond. Sample NS7 is from a water well adjacent to Nut Brook Pond and H285B6 and H3851 are from two research boreholes located in the Seal Cove River Valley adjacent to the study area. The samples taken from the boreholes are typical of the groundwaters in the area since the dominant ions in these samples are calcium and bicarbonate.

Table 4.3 Analytical results of water samples collected from Pennys Pond and Gull Pond and from boreholes drilled at both lakes.

sample		PPLAKE	PP-P1	PP-P2	PP-P3	GPGW	GPLAKE
depth	(m)	NA	7.92	6.10	3.35	NA	NA
pH		4.64	7.21	7.44	7.20	6.66	6.04
cond		39	195	375	200	190	105
Ca^{2+}	mg/l	0.9	43.2	46.4	41.5	11.8	3.0
Mg2+	mg/l	1.1	2.7	3.0	2.6	2.9	1.4
K^{+}	mg/l	0.2	0.2	3.3	0.5	1.0	0.4
Na^{+}	mg/l	5.3	7.0	40.2	9.1	16.2	14.5
Fe^{2+}	mg/l	0.0	0.5	0.6	0.6	14.4	0.0
SiO_2	mg/l	0.8	4.8	4.4	4.0	6.4	0.9
HCO_3^-	mg/l	3.9	123.4	138.9	123.4	46.3	7.8
Cl^-	ppm	0.5*	0.4*	0.7*	0.4*	1.5*	1.3*
SO_4^{2-}	ppm	2.4*	4.1*	73.1*	9.4*	1.2*	2.6*
Cu	ppb	2.7	1.7	5.8	2.7	1.7	2.8
Pb	ppb	1.7	0.8	16.0	1.6	0.7	1.6
Zn	ppb	15.0	11.0	18.0	8.5	13.0	11.0
Co	ppb	0.1	0.1	1.2	0.0	0.1	0.1
Ni	ppb	2.6	0.4	8.0	1.4	0.1	0.3
Mn	ppb	15.9	469.6	539.0	392.6	566.9	4.7
Fe	ppb	181.4	590.8	609.1	716.4	18813.0	9.8
Mo	ppb	0.1	14.6	31.2	9.6	1.4	0.1
U	ppb	0.1	81.6	133.8	61.5	0.6	0.1
Charge balance	%	±48.8	±11.9	±7.0	±9.5	130.8	161.5
$\delta^{18}O$		-8.35	-7.69	NA	NA	-7.7	-6.06

* = ICP/MS analysis ± 15%
NA - not available

The multilevel piezometer installed in the Pennys Pond borehole sampled three distinct intervals. The interval depths were P3, from 2.85 m to 4.85 m, P2, from 5.65 m to 7.65 m, and P1, from 8.50 m to the bottom of the hole which was

Table 4.4 Analytical results of water samples taken from selected boreholes in the study area.

sample		H285B6	H3851	NS7
depth	(m)	62.80	24.86	90.0
pH		NA	NA	7.26
cond		NA	NA	470
Ca^{2+}	mg/l	17.9	32.5	54.6
$Mg2+$	mg/l	1.4	3.7	4.7
K^{+}	mg/l	1.0	0.7	5.9
Na^{+}	mg/l	8.1	8.3	43.6
Fe^{2+}	mg/l	0.4	0.0	NA
SiO_2	mg/l	NA	6.0	NA
HCO_3	mg/l	NA	127.5	152.5
Cl	ppm	4.4	8.0	67.3*
SO_4^{2-}	ppm	2.6	3.8	15.8*
Cu	ppb	8.8	4.6	8.6
Pb	ppb	1.1	1.5	134.9
Zn	ppb	6.0	78.7	230.0
Co	ppb	0.9	0.1	NA
Ni	ppb	13.7	5.2	3.0
Mn	ppb	972.3	78.5	1030.5
Fe	ppb	41.5	21.2	77.6
Mo	ppb	0.4	0.5	1.5
U	ppb	213.3	357.5	99.0
Charge balance	%	NA	$\pm$1.7	$\pm$4.5
$\delta^{18}O$		-6.06	-8.45	-8.00

* - ICP/MS analysis $\pm$ 15%
NA - not available

approximately 11.25 m. Based on the fracture frequency observed in the drill core and from permeabilities calculated from falling head tests, the size and location of the intervals were chosen to include zones which had the

highest rate of flow into the borehole. Hydraulic heads measured in the three piezometers were approximately 10 mm above the water level of the lake. There was a 2 to 3 mm increase in the interval heads with depth interval indicating that an upward gradient existed over the length of the borehole and that groundwater was discharging into the lake at that point.

Water samples taken from the three intervals had characteristically higher pH, conductivity, alkalinity and trace metal concentrations than the lake waters. Like other groundwater samples in the area, samples from the Pennys Pond borehole were found to have high concentrations of uranium ranging from 61 to 134 ppb uranium which were significantly higher than the lake waters. No other trace metals showed significant differences between lake water and groundwaters. The ratio of Na to Ca for groundwaters extracted from these three intervals were 0.14, 0.75 and 0.19 for P1, P2, and P3 respectively which, along with the relatively high measured concentrations of bicarbonate, indicates that the groundwaters are from part of the local flow system around the lake. Although the three samples were similar in composition, the middle interval (P2) was found to have higher concentrations of most dissolved constituents. This suggests that the groundwater extracted from this interval has possibly

travelled more slowly, and has been in contact with the rock mass for a longer period of time. This is consistent with the permeability calculated for the P2 interval which was approximately an order of magnitude lower than the other two intervals.

The borehole drilled through the lake bottom and into bedrock in Gull Pond was drilled approximately two metres into granite bedrock through a bouldery rubble zone below the organic sediments. The frequency of fractures in the interval was relatively low with only a few fractures being observed in the core that was recovered. A chemical packer was placed at the first contact with intact bedrock to provide a distinct sampling interval in the bottom section of the borehole. The hydraulic head measured in this interval was approximately 10 mm above the water level in the lake indicating a positive upward gradient suggesting that groundwater was discharging into the lake through the lake sediments. Also, when water was being pumped from the interval during sampling, there was very little drawdown of the water level in the piezometer suggesting that water was recharging into the interval.

It is important to note that when this borehole was first sampled the pH and specific conductivity were 7.27 and 395 uS/cm respectively, but after a minute of pumping these

readings had changed to approximately 6.50 and 190 µS/cm. One possible explanation for the rapid change in pH and conductivity is that the initial values represented groundwater, but as the interval was pumped, lake water was drawn down into the sampling interval and mixed with discharging groundwater. The concentrations of both major ions and trace metals in the water sample (Table 4.3) suggest that it is neither a typical groundwater nor surface water compared with others waters in the study area. For example, values of alkalinity and calcium measured for the water sample are not as high as those found in most groundwaters but are higher than values found in surface waters. The ratio of Na to Ca for the sample is approximately 1.2 : 1 which suggests that the sample is composed of shallow groundwater that has been mixed with surface water. The lack of uranium in the water suggests that it is more typical of surface water.

Chapter 5 RESULTS AND DISCUSSION OF SEDIMENT GEOCHEMISTRY

5.1 Results of Surface Sediment Sampling

A total of 143 surface sediment samples were collected, using a regularly spaced grid, from the four lakes; 63 from Gull Pond, 36 from Rocky Pond, 28 from Pennys Pond and 16 from Nat Brook Pond. Sample coverage was fairly complete except in some near-shore or shallow areas where there was insufficient sediment to collect a sample. The surface sediment samples consisted mainly of black brown silty organic ooze. A summary of the sediment analyses for the lakes sampled in this study are given in Table 5.1, while a complete list of analyses is given in Appendix C.

Frequency histograms and statistics of metal concentrations found in the sediment of each lake sampled (Figure 5.1) show that trace metals are not evenly distributed throughout the sediment in these lakes. Most of the concentration values for each element are close to or slightly less than the mean, but values range up to several standard deviations above the mean value. For example, Gull Pond has an average concentration of 31.2 ppm uranium in surface sediment but a localized area of the lake has a much higher concentration of 159 ppm uranium. Peak concentrations in the sediment vary from lake to lake,

Table 5.1 Summary of trace metal analyses of surface sediment samples (avg.= mean, std.= standard deviation).

		Cu ppm	Pb ppm	Zn ppm	Mn ppm	Fe %	Mo ppm	U ppm	LOI %
Gull Pond	avg.	18.4	18.7	107.3	2680.7	3.2	10.7	31.2	32.0
	std.	7.4	6.1	28.7	5066.8	1.9	4.4	25.5	9.8
	min.	7.0	12.0	45.0	159.0	0.5	3.0	13.4	2.8
	max.	52.0	54.0	185.0	28600.0	7.1	30.0	159.0	44.2
	#	63	63	63	63	63	63	63	63
Rocky Pond	avg.	12.1	13.8	46.7	4127.9	3.8	9.3	14.2	29.8
	std.	2.8	4.8	18.1	9284.4	2.8	10.3	12.2	8.6
	min.	8.0	8.0	23.0	355.0	1.1	3.0	6.2	10.8
	max.	24.0	29.0	98.0	50600.0	11.7	68.0	69.0	40.3
	#	36	36	36	36	36	36	36	36
Pennys Pond	avg.	6.0	17.5	9.6	50.3	0.8	4.5	46.3	15.8
	std.	4.9	7.6	7.1	41.6	0.5	1.5	59.2	5.8
	min.	3.0	10.0	4.0	2.0	0.2	3.0	15.9	1.1
	max.	29.0	47.0	33.0	194.0	2.5	10.0	309.0	37.1
	#	28	28	28	28	28	28	28	28
Nut Brook Pond	avg.	13.9	38.9	26.4	190.6	0.7	7.6	92.0	28.9
	std.	3.4	10.9	29.6	140.5	0.4	3.1	66.5	6.4
	min.	9.0	23.0	3.0	34.0	0.3	3.0	30.8	15.0
	max.	21.0	60.0	124.0	536.0	1.5	13.0	250.0	40.6
	#	16	16	16	16	16	16	16	16
All Ponds	avg.	13.9	19.5	63.9	2251.4	2.6	8.8	36.7	27.9
	std.	7.3	9.9	46.8	5950.2	2.3	6.5	44.8	10.4
	min.	3.0	8.0	3.0	2.0	0.2	3.0	6.2	1.1
	max.	52.0	60.0	185.0	50600.0	11.7	68.0	309.0	44.2
	#	143	143	143	143	143	143	143	143

Table 5.2 Results of regional survey for Gull Pond and Nut Brook Pond (Davenport and Butler, 1976), based on a single sediment sample from each lake.

	Cu ppm	Pb ppm	Zn ppm	Mn ppm	Fe %	Mo ppm	U ppm	LOI %
Gull Pond	42	15	108	923	2.9	23	125	26.8
Nut Brook Pond	7	37	32	448	1.1	10	189	33.6

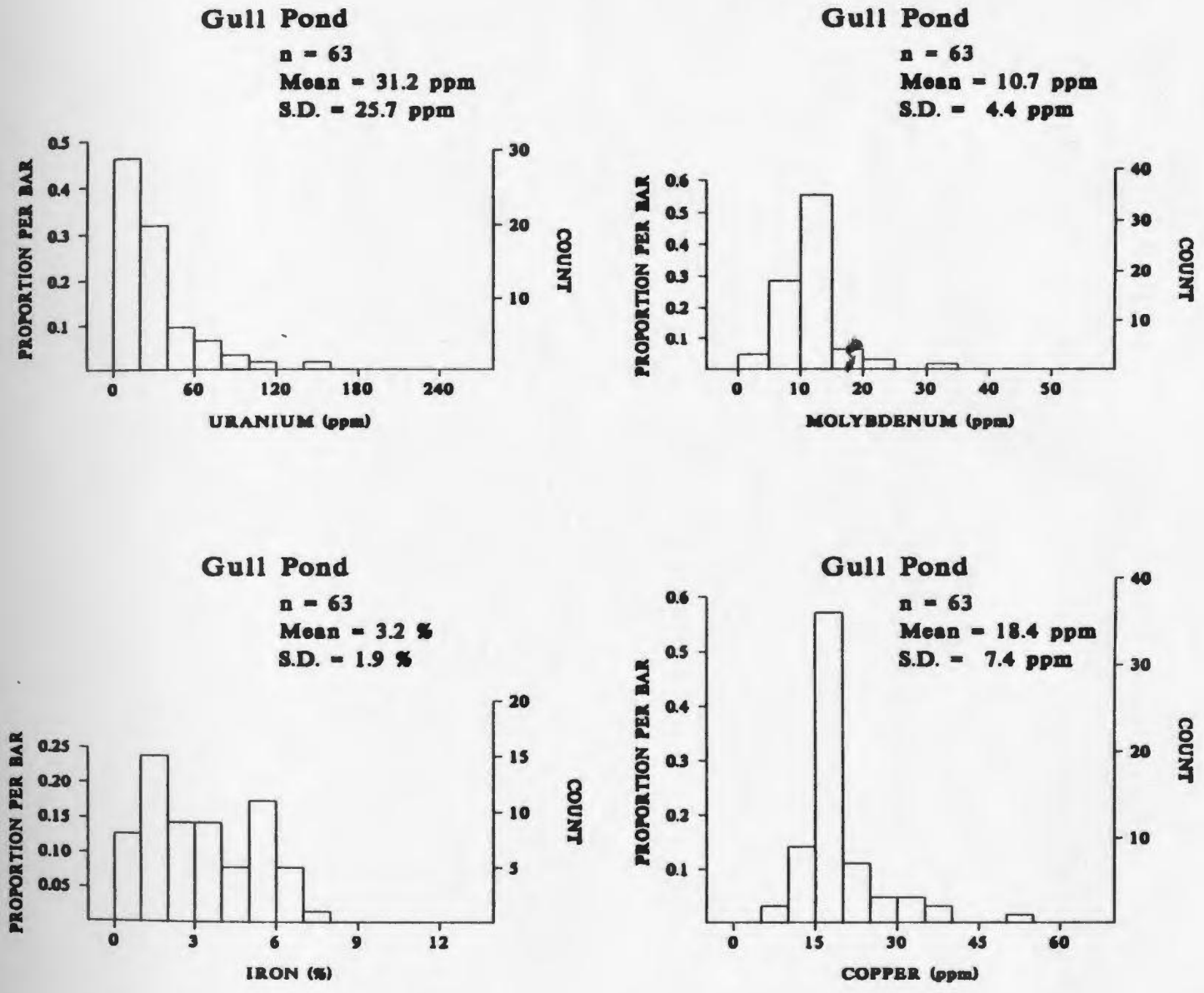

Figure 5.1 Frequency histograms showing the distribution of selected metals in the sediment in a) Gull Pond, b) Rocky Pond, c) Pennys Pond and d) Nut Brook Pond.

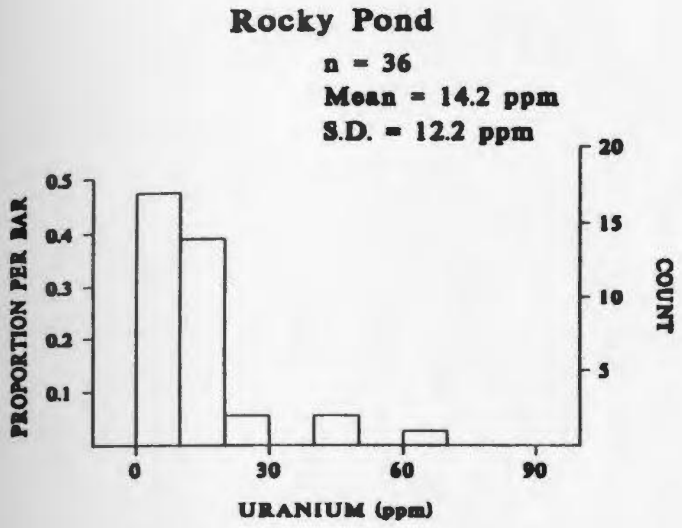

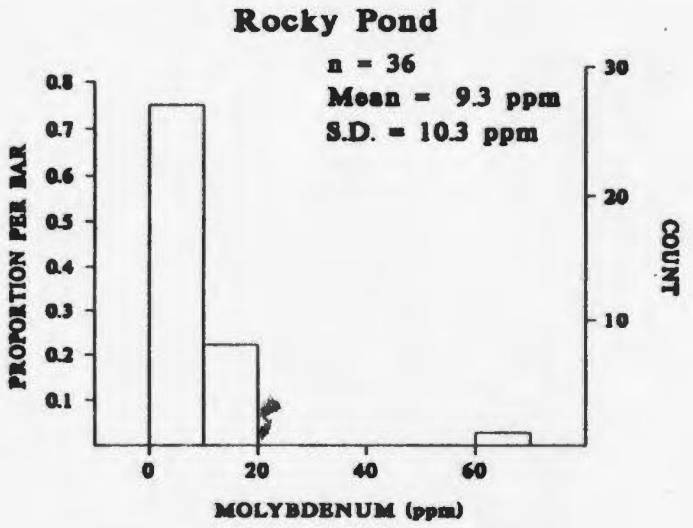

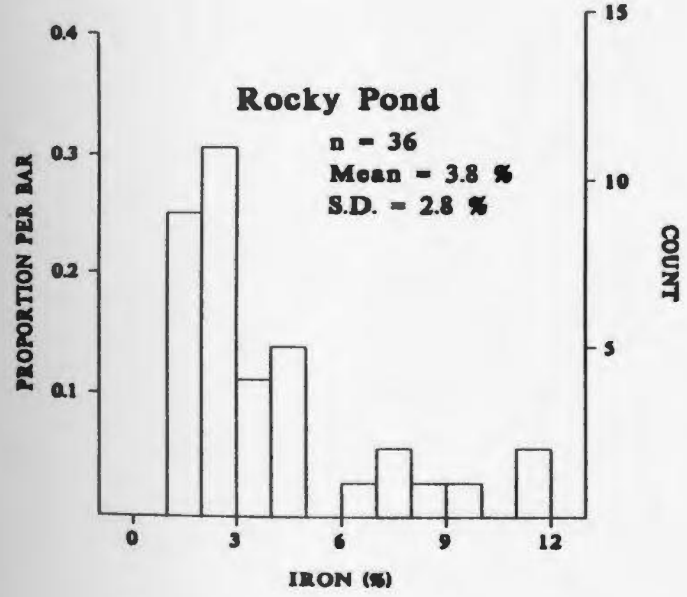

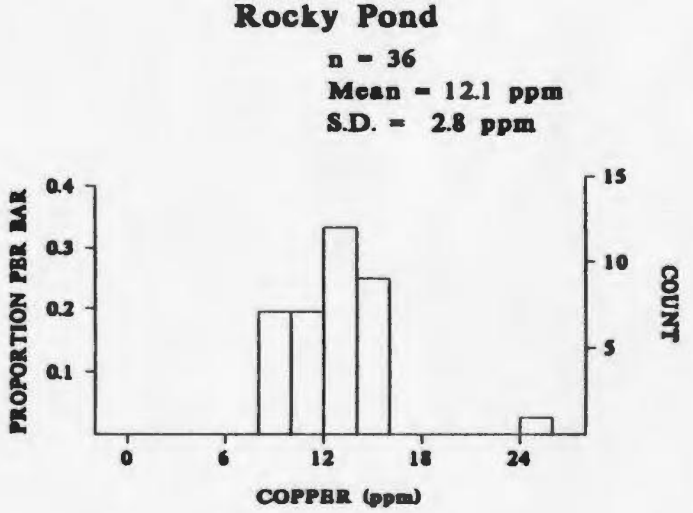

Figure 5.1 (cont'd)

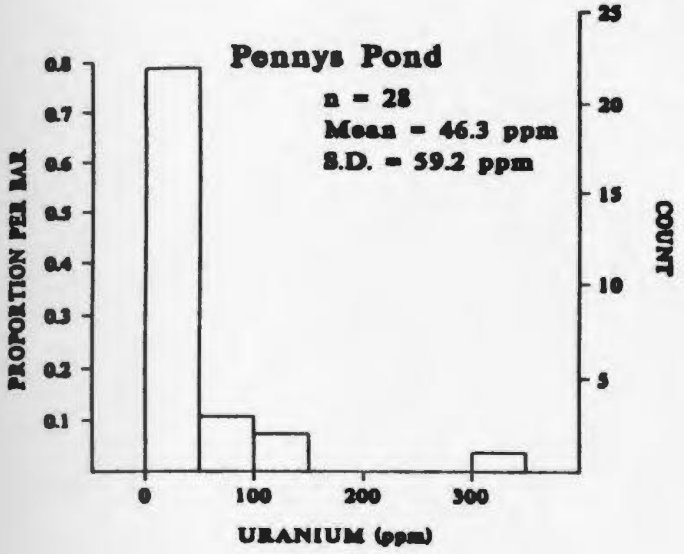

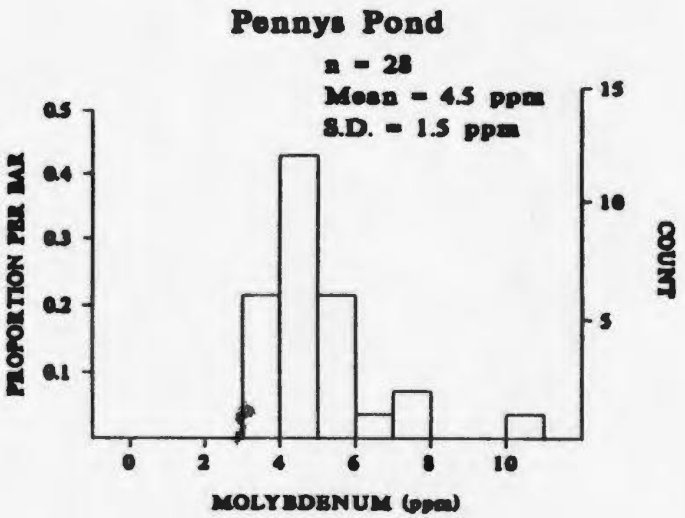

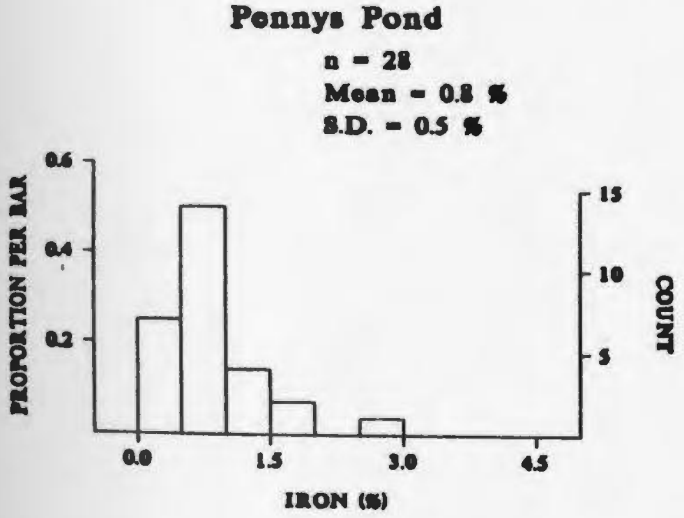

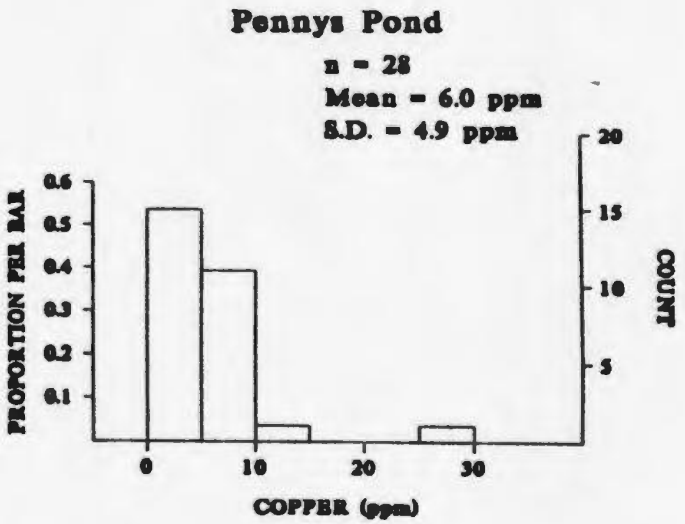

Figure 5.1 (cont'd)

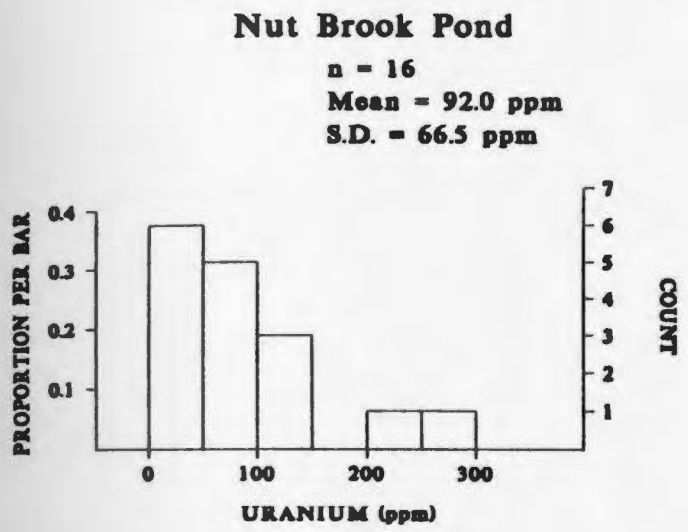

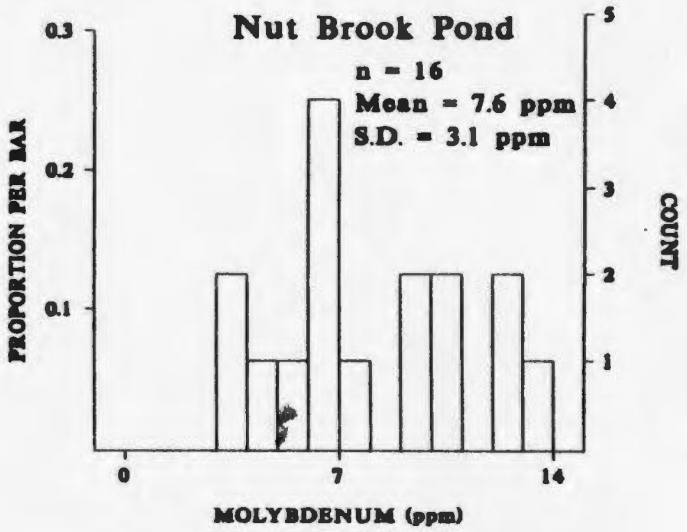

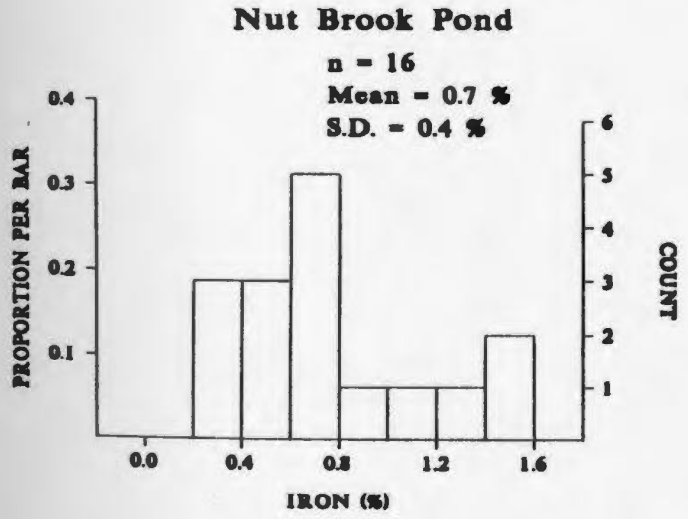

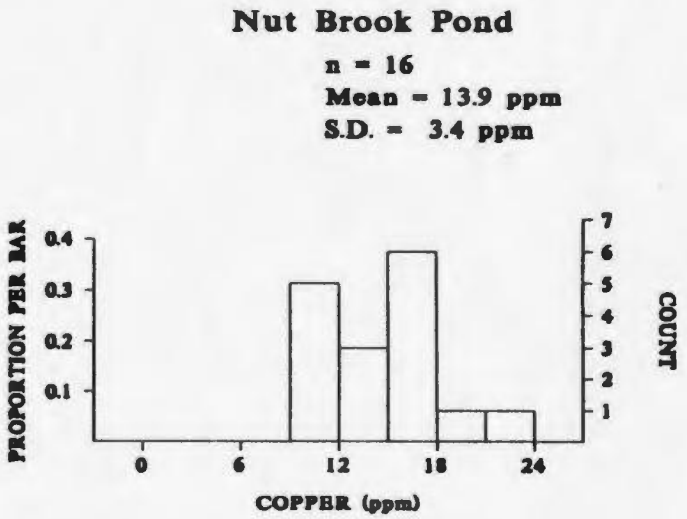

Figure 5.1 (cont'd)

but are generally 2 to 3 times the average value for that lake. In each lake there is a location within the lake which had an anomalously high concentration for a particular metal in the sediment. However, the peak concentrations for different metals were not always found at the same location within a lake.

The results of the detailed sampling showed that there were locations sampled in Gull Pond and Nut Brook Pond that contained metal concentrations that exceeded the values recorded in the regional survey (Table 5.2). The regional survey reported values of 125 ppm and 189 ppm U versus maximum values of 159 ppm and 250 ppm in the detailed sampling for Gull Pond and Nut Brook Pond, respectively. Pennys Pond which reported the highest concentration of uranium, 309 ppm U, in the detailed sampling was not sampled in the regional survey.

The contoured plots of uranium concentration for each lake (Figure 5.2) show that the anomalous areas are not found at any particular location in each lake, with respect to the lake morphology or inflow and outflow streams. The uranium anomaly in Nut Brook Pond is near a source of surface water input but is in a relatively central area in Pennys Pond and Gull Pond, and near a stream outflow in Rocky Pond. The extent and shape of the uranium anomalies were also different in each lake.

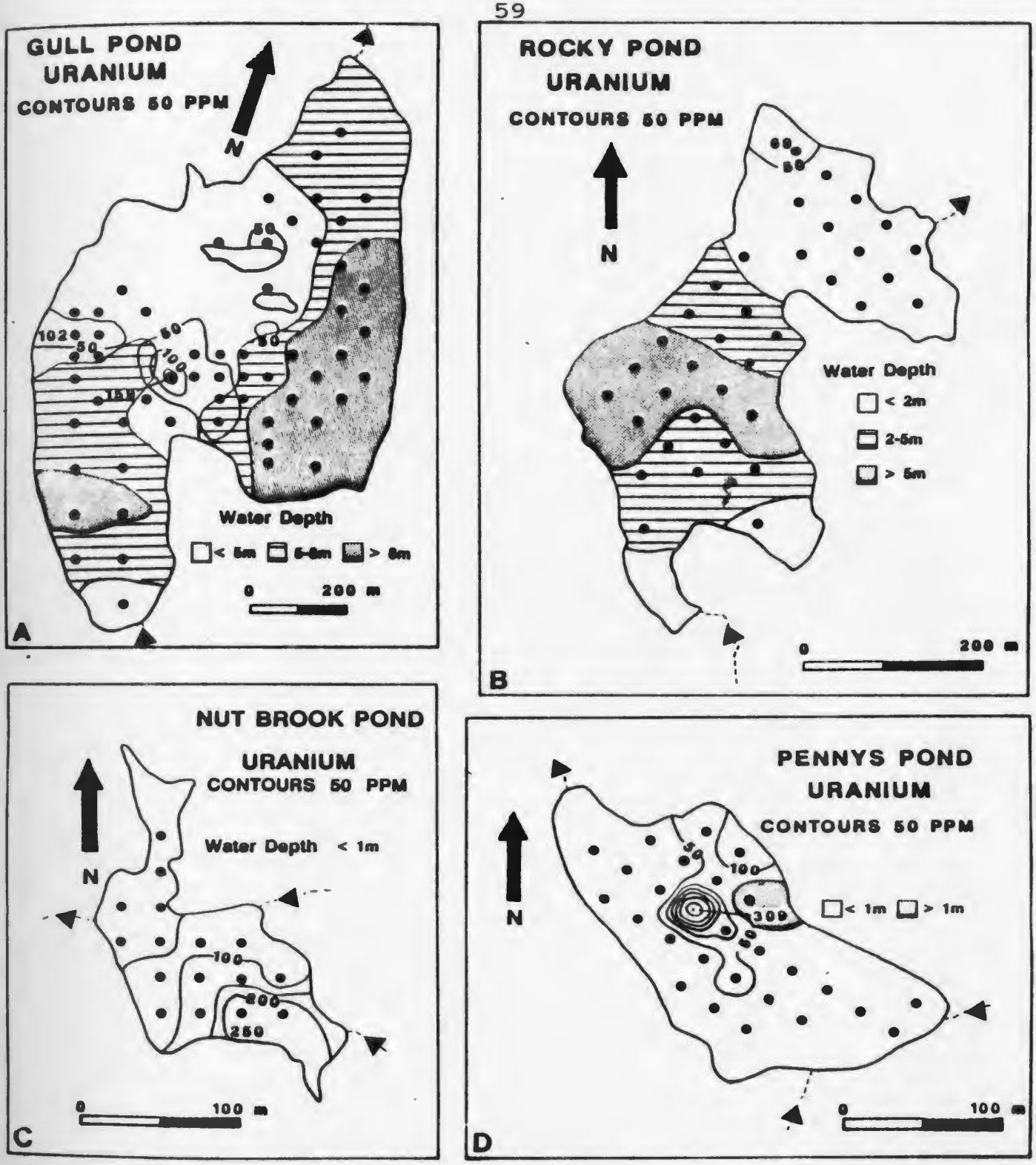

Figure 5.2 Contour plots showing the distribution of uranium concentrations in lake sediment as well as the distribution of water depth in a) Gull Pond, b) Rocky Pond, c) Nut Brook Pond and d) Pennys Pond. Arrows indicate direction of streamflow.

For example, in Pennys Pond the anomaly was somewhat elongated, peaking in a circular "bulls eye" type of pattern located in the centre of the lake. The uranium anomaly in Gull Pond showed a similar pattern to Pennys Pond, with the peak of the anomaly located in the middle portion of the lake, where the water depth at that point was only 2 to 3 metres. In Nut Brook Pond the uranium anomaly formed a frontal pattern which decreased outward into the lake away from its peak point near a stream inlet. Finally in Rocky Pond, which had the lowest concentrations of uranium relative to the other lakes, only one sampling point showed concentrations above 50 ppm.

5.2 Discussion of Surface Sediment Sampling

The detailed sediment sampling carried out in this study has shown that there is variability in the intensity of metal concentrations in lake sediments and that anomalous areas are not always located in the centre or deepest part of a lake (Figure 5.2). Lake centres are normally sampled in regional geochemical lake sediment surveys because they are thought to be the most likely location to find concentrations of metals in the sediment and for consistency between lakes (Hornbrook et al. 1975a). The centre or deepest part of a lake is usually sampled because this is where the fine size particles are most likely to be found. The finer particles have a

greater exposed surface area and are therefore better able to absorb and retain metal species as they settle in the water column. However, there are many factors which can influence where metals will be concentrated in the lake sediment, such as the size, depth and morphology of the lake and particulate size. The circulation patterns and the degree of mixing of waters within a lake will also affect where metals are concentrated in the lake sediment. Therefore, in a regional survey, a representative sample of metal concentrations may not always be obtained by only sampling sediment from the deepest or most central part of a lake.

A comparison was made between the concentrations of metals found in the sediment and those found in the granitic bedrock to determine if the concentration of metals found in the sediment was a result of detrital input into the lake from the granitic bedrock or other processes. Samples of the granitic bedrock from the northeastern portion of the Holyrood Granite near alteration zones were collected and analyzed for trace metals as part of a study by Hayes (1989). Data from the freshest and least altered samples were used to determine the average concentrations for Cu, Pb, Zn, Fe, Mn and Mo in the granite. The average uranium concentration was calculated by Davenport (1978) from samples collected by Strong et al. (1974). Average concentrations of metals in lake sediment

were determined from lake sediment samples collected in the regional sediment survey (Davenport and Butler, 1976); only those lakes located in granite catchment basins were averaged. The average concentrations for each metal in both the rock and lake sediment, as well as the ratio of concentrations in the sediment to the concentrations in the rock are given in Table 5.3.

The ratios of Cu, Pb, Zn and Fe concentrations in sediment to rock were close to 1:1, which would suggest that trace metals in the sediment were transported as detrital material with only minor secondary enrichment. The sediment to rock ratio for molybdenum is slightly higher at 2.8, while the ratios for uranium and manganese are approximately an order of magnitude higher than the others. The high manganese ratio can possibly be accounted for by the way in which Mn in a mineral phase in the granite would be liberated as Mn^{2+}, and would later oxidize and precipitate as it is transported by surface drainage to the sediment. Manganese may exist in the mobile Mn^{2+} state longer than iron, since the phase boundary between Fe^{2+} and oxidized iron occurs at a lower oxidation potential than for Mn.

Davenport (1978) suggests that the difference in the average concentration factor of uranium in lake sediment relative to

Table 5.3 Comparison of average trace metal concentrations found in Holyrood Granite and in lake sediments found in the granite catchment basins (Davenport, 1978 and Hayes, 1989).

		Cu ppm	Pb ppm	Zn ppm	Mn ppm	Fe %	Mo ppm	U ppm
Granite	Mean	13.5	24.9	40.3	539	2.5	5.2	2.4
	S.D.	11.4	26.2	22.2	308	1.5	6.3	0.8
	#	15	15	15	15	15	15	15
Sediment	Mean	11.4	39.5	71.4	10150	5.0	14.4	28.7
	S.D.	9.1	36.2	45.3	18178	2.8	14.1	44.4
	#	21	21	21	21	21	21	21
Sed/Rock		0.9	1.6	1.8	18.8	2.0	2.8	12.1

bedrock is a result of either the under sampling of late phase aplites and pegmatites in the granite where uranium may be enriched, or the depletion of uranium in the granite by weathering of minerals such as uraninite. The comparison of metal concentrations in the sediment with bedrock concentrations indicates that most metals in the sediment represent detrital concentrations. However, the elevated levels of uranium in the sediment compared to concentrations found in the underlying granitic bedrock suggest that uranium is being concentrated in the lake sediments.

The variability in the intensity and location of peak metal concentrations found in the surface layer of the lake sediment and the enrichment of uranium suggest that processes other

than detrital deposition and the adsorption of metals on particulate matter as it settles in the water column may be responsible for concentrating metals in the sediment. The elongated uranium anomalies identified in both Pennys Pond and Gull Pond are oriented slightly west of north which coincides with the orientation of fractures of cluster 1, identified from the mapping of outcrops in the area (Figure 2.4), and the orientation of most of the linear features identified from aerial photographs (Figure 2.2). The shape and location of the anomalies in the sediment of these lakes suggest that the uranium anomalies could be related to fracture zones or structural features in the underlying granitic rock mass.

5.3 Results of Sediment Core Sampling

Vertical sections of sediment were sampled from three of the four lakes in this study to determine the vertical distribution of metals in the sediment. Sediment cores were taken in anomalous areas defined by surface sediment sampling as well as background areas from five locations in Gull Pond and three locations in each of Rocky Pond and Nut Brook Pond. The location of the cores within the individual lakes are shown in Figure 5.3. Most of the sediment in the retrieved cores consisted of dark brown organic silt and generally with the deepest sediment consisting mainly of grey silty sand.

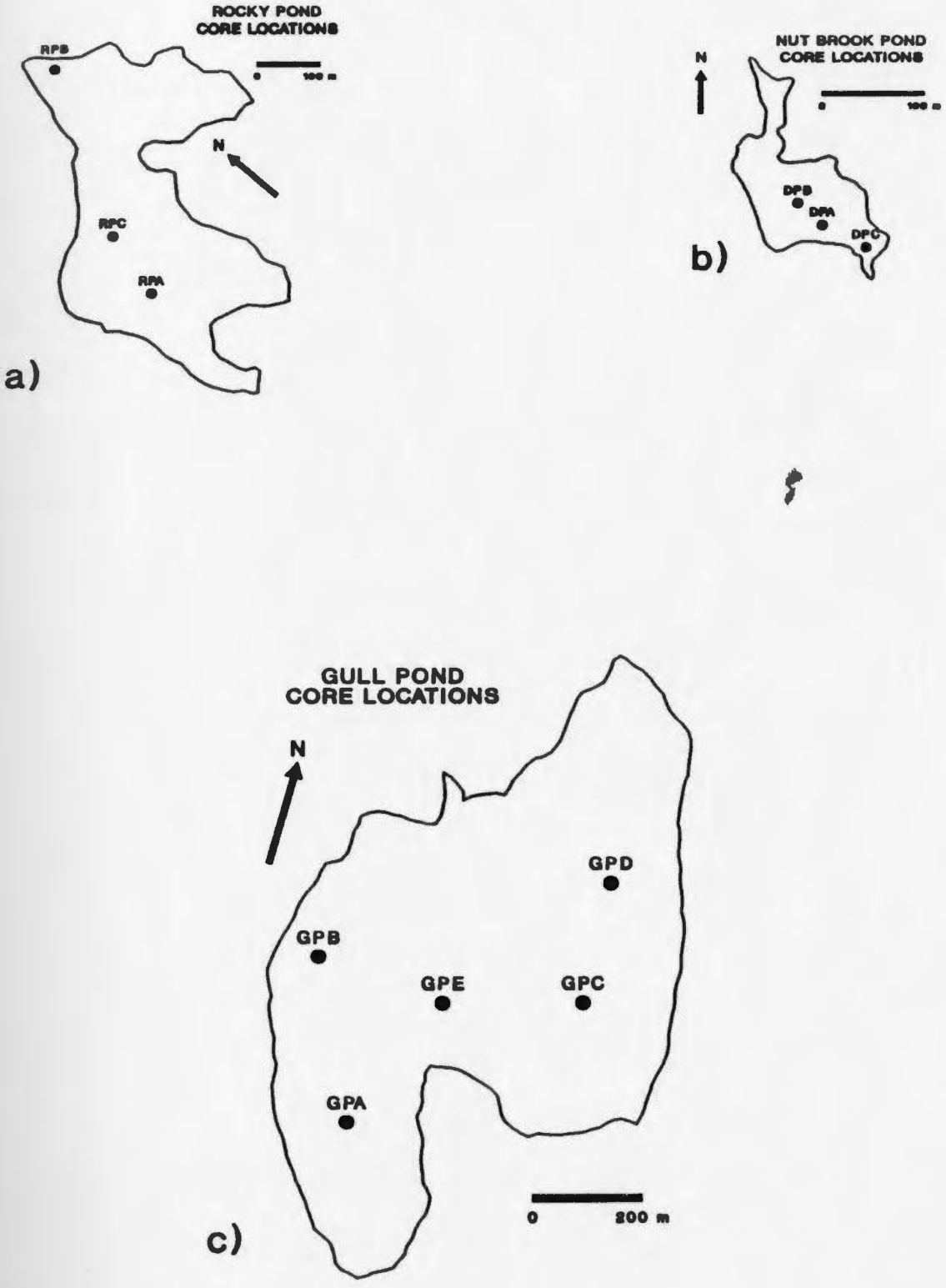

Figure 5.3 Locations at which sediment cores were collected in a) Rocky Pond, b) Nut Brook Pond and c) Gull Pond.

Sediment cores taken from other lakes on the Avalon Peninsula by MacPherson (1982) also contain sediments which consist of organic rich "gyttja" in the top sections grading to grey silty clay (indicative of accumulations of mineral sediments) in the bottom sections of the cores.

The cores ranged from 0.5 to 3.0 m in length depending on where in a particular lake the core was taken (near-shore or lake centre). Since the coring device could only penetrate as far as it could be manually pushed through the sediment it is not certain if the bottom of the cores represents the true thickness of the sediments. This uncertainty was due to the high resistance of the dense clay or sandy layers which, if encountered, could not be penetrated by the corer. Therefore it was difficult to correlate core depths and as a result there was little or no stratigraphic control between cores. Metal analyses on the core sections are tabulated in Appendix D.

The sediment cores from each lake show that metal concentrations vary vertically in the sediment column (Figure 5.4). In general, the maximum trace metal concentrations are found in the deeper part of the cores and usually exceed the concentrations found in the surface sediment sampled at those locations. However, there was no apparent correlation between

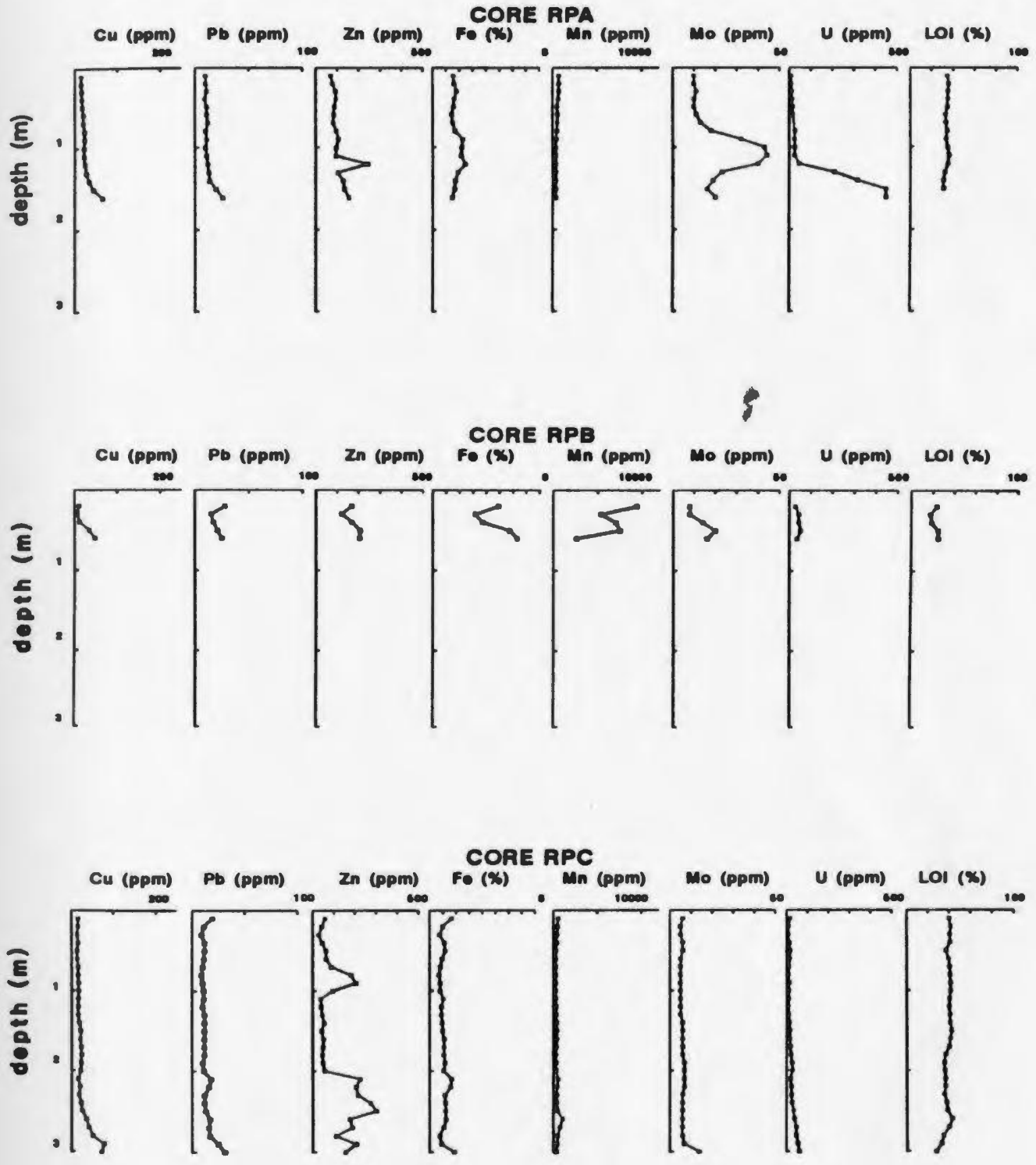

Figure 5.4 Trace metal analyses of sediment core sections from a) Rocky Pond, b) Nut Brook Pond, and c) Gull Pond.

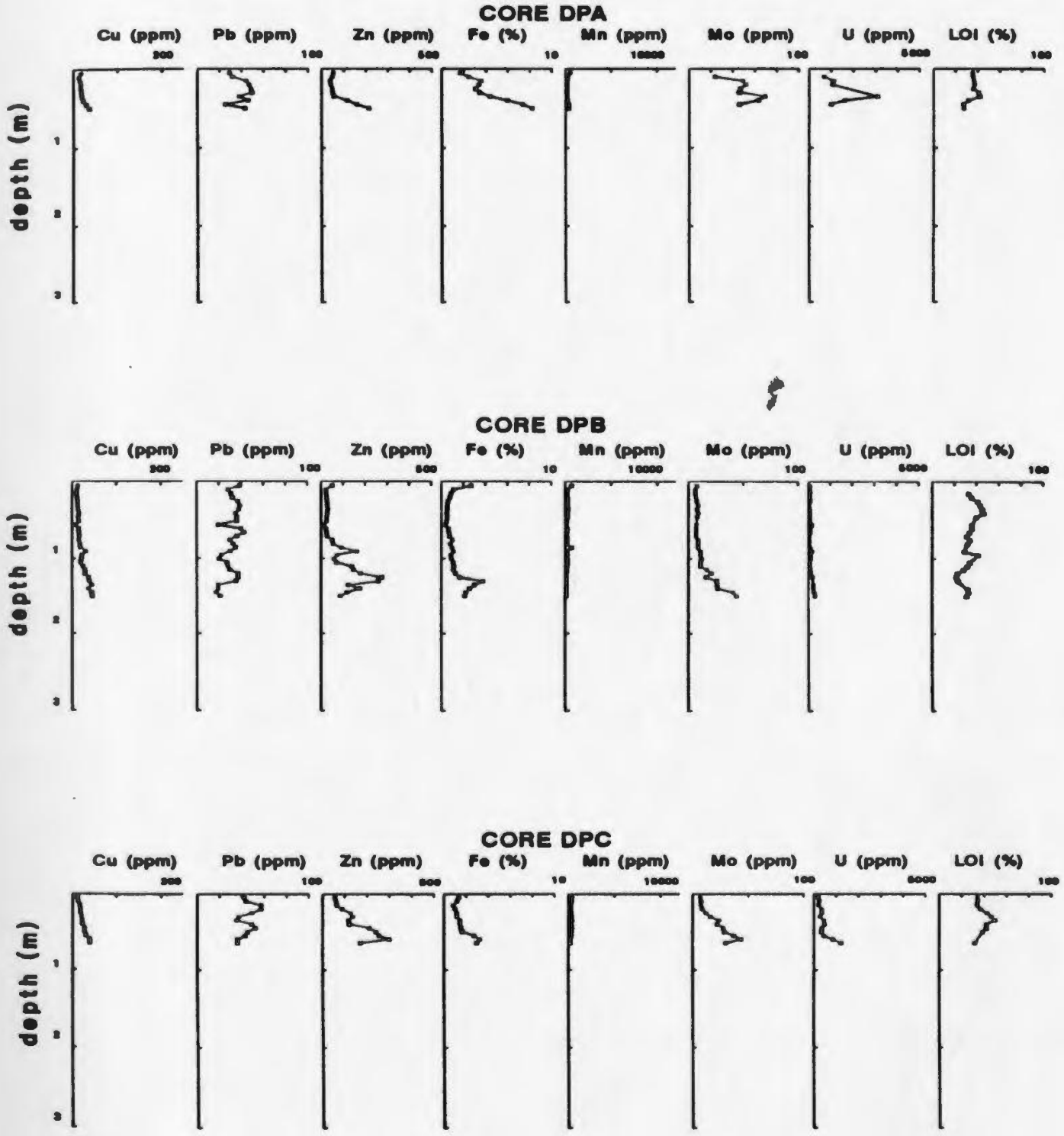

Figure 5.4 (cont'd)

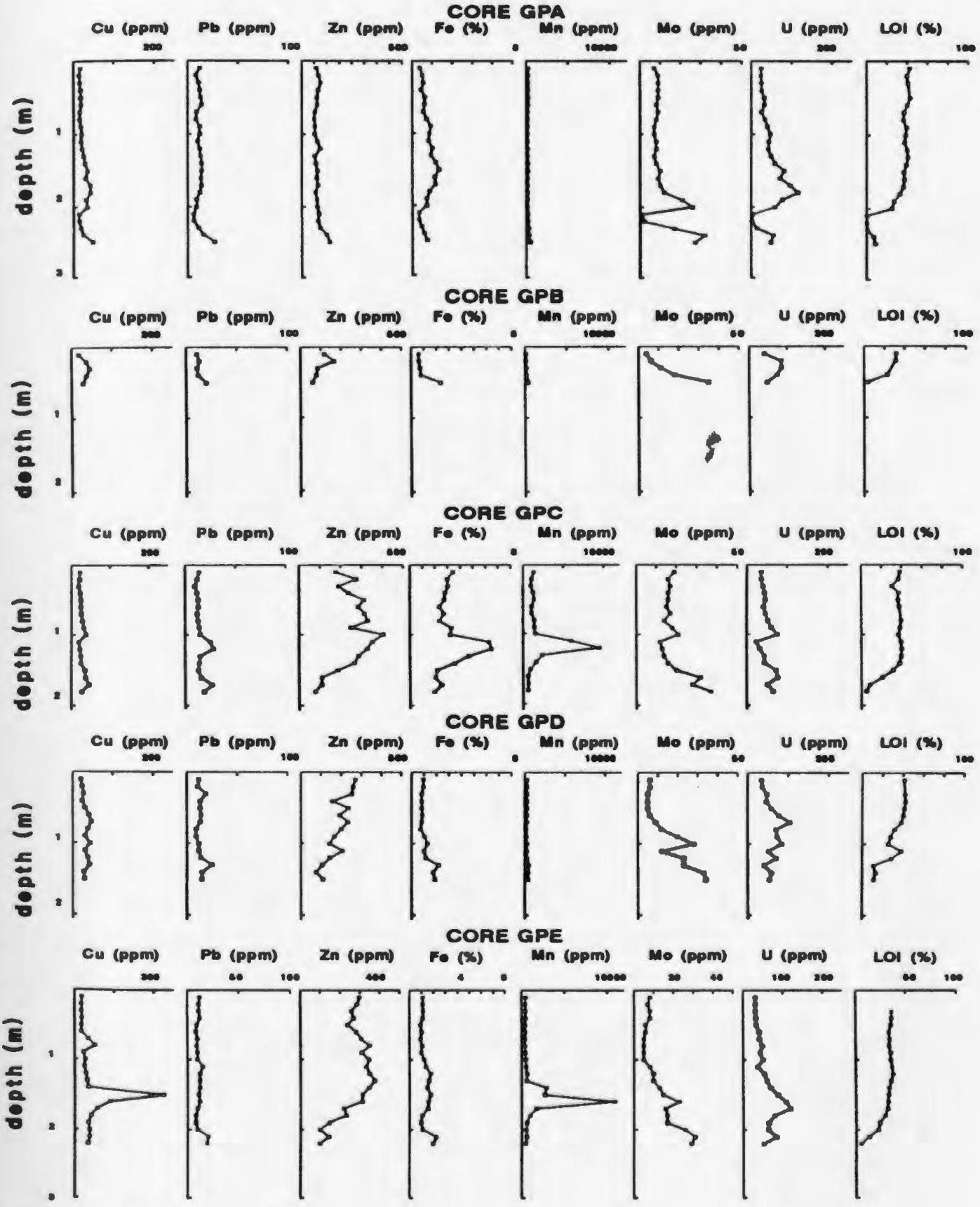

Figure 5.4 (cont'd)

the peak metal concentrations found in the sediment cores and concentrations found at the surface of the sediments. Although there did not appear to be any overall trend of increasing or decreasing trace metal concentrations in the sediment with depth for any particular element, in some cases concentrations of a particular metal would peak over a short interval of the sediment core.

5.4 Discussion of Sediment Core Samples

Since the sediment samples in the cores contain varying amounts of organic material, the results of the sediment analysis were normalized by dividing the total weight of metal in the sample by the total weight of inorganic material. The normalized results for core GPE, taken in Gull Pond near an area anomalously high in uranium, are shown in Figure 5.5. The normalized metal concentrations are indicated by X, the raw concentrations by solid squares, and the average concentrations for the granitic bedrock are drawn as solid straight lines. Normalizing the data in this manner emphasizes peak concentrations at particular depths and indicates that the peaks are not simply a function of the amount of organic content in the sediment.

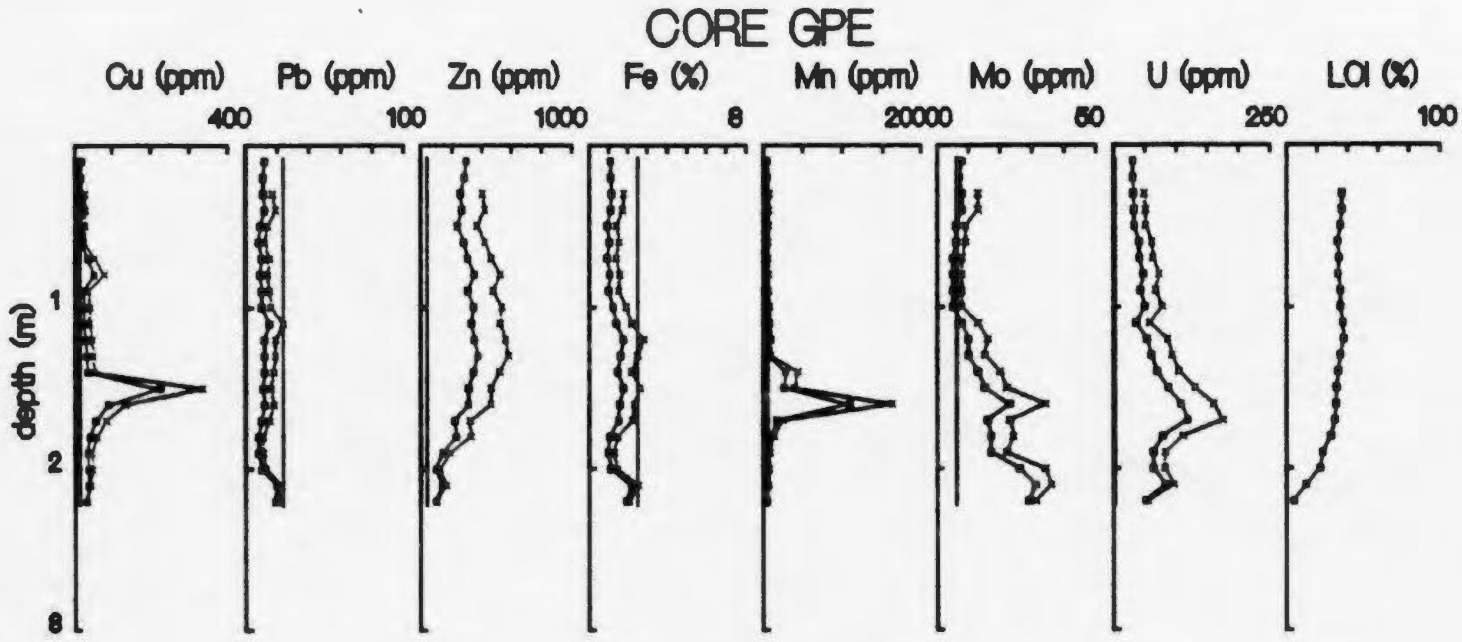

Figure 5.5 Trace metal analyses of sediment core section GPE. Raw data are indicated by solid squares, normalized data are indicated by X, and average granite rock concentrations are indicated by a straight solid line.

In most cores, the concentrations of the elements iron, manganese and lead are generally equal to, or slightly less than detrital levels, while concentrations of zinc, molybdenum and uranium appear to be enriched in the sediment. Increased concentrations of Fe and Mn would not be expected in the sediment since they are both soluble over the range of Eh-pH conditions that would exist during weathering processes, and solid phases only occur under higher oxidizing conditions. Based on published Eh-pH diagrams (Brookins, 1988), lead is soluble only at very low pH (less than 1) and therefore would tend not to be mobilized from the granite by groundwater. On the other hand Cu, Zn, Mo and U are all soluble over a wide range of Eh-pH conditions suggesting that groundwater could be a transport agent for these elements.

In general, the concentrations of metals in core GPE can be explained to some degree by direct input of rock detritus, together with input of dissolved metals on organic matter. However, like core GPE, most of the sediment cores collected in this study show metal concentrations which peak at depth, and whose peaks are not directly correlated with organic content. Therefore, there appear to be other processes that can enrich the sediment in selected metals at certain depths.

Biological processes could possibly have caused trace metal enrichment in the lake sediment at selected levels. Periods of high algal or diatom growth at a particular time in the sediment history of the lake could have concentrated certain elements from lake waters. MacPherson (pers. comm., 1990) has reported the frequent occurrence of an algae named Pediastrum in basal inorganic lake sediments on the Avalon Peninsula, but since most of the peak concentrations in this study were located in sediments above the basal inorganic sediments, it is not known whether this organism may be a factor in controlling the metal concentrations measured in this study.

In cores which have a localized, high uranium concentration, the uranium peak coincides with the point at which there is an abrupt decrease in the organic content (indicated by LOI) in the bottom section of the core. Peak uranium concentrations ranged from twice background levels as in Gull Pond cores up to a peak of over 3000 ppm in one of the cores from Nut Brook Pond. In some cases other metals show peak concentrations over the same depth interval, but this pattern is not consistent. The relationship between increased uranium concentrations at the point where organic content suddenly drops off does not appear to be related to the core length or location of core within the lake. The same trend was seen in

both shorter cores taken near-shore and in long cores taken in the middle of the lake.

It appears that the peaks in uranium concentrations are mainly associated with an abrupt change in organic content in the sediment. It is hypothesised that the peak concentrations are a result of the change in oxidation potential experienced when oxidized metal species interact with the reduced organic rich sediment. If uranium were present in an oxidizing groundwater it would exist in its hexavalent state; when it encountered sediments with increased organic content the uranium would tend to be reduced to its tetravalent state and be adsorbed or precipitated within the sediment.

Core GPC shows coincident peaks of iron and manganese and possibly lead which correlate with a sharp decline in the concentrations of Cu, Zn, Mo, and U (Figure 5.6). The high concentrations of the iron and manganese oxides suggest that oxidizing conditions may exist at this depth, supported by the presence of insoluble oxides of Fe^{III} and Mn^{IV}. Therefore, dissolved metals carried by groundwater, which otherwise would precipitate at this depth in the sediment, would tend to remain oxidized and be mobilized out of the sediment leaving them relatively depleted at this particular depth. In addition, any metals initially deposited with detrital

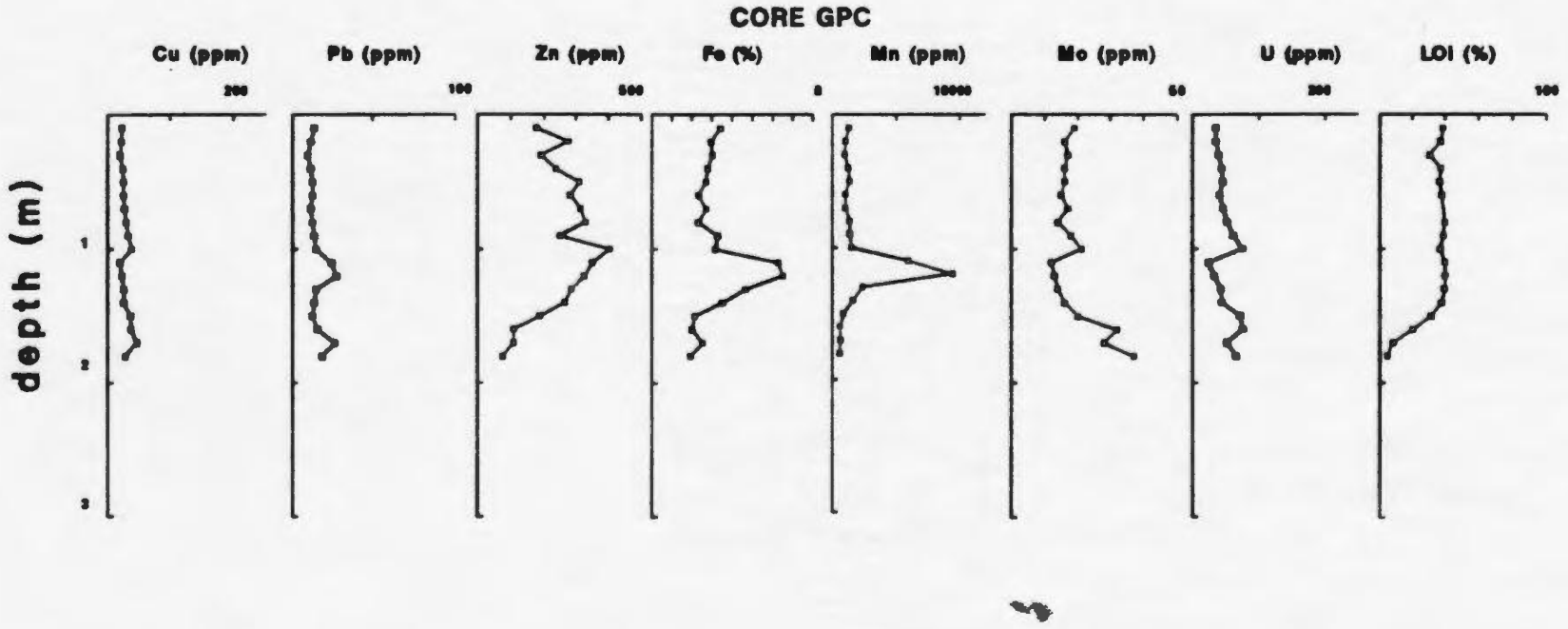

Figure 5.6 Trace metal analyses of sediment core section GPC.

sediment would tend to be oxidized by the Fe and Mn oxides and also be mobilized out of the sediment with time. The high concentrations of uranium observed in groundwater compared to surface water in the study area suggests that groundwater may be a source from which uranium (and other metals) may be concentrated in the sediment. To test this hypothesis, the amount of uranium precipitated in sediments through which groundwater discharges was calculated. Assuming 100% of the uranium in the groundwater would precipitate in the sediment, approximately 2 million litres of groundwater with an average uranium concentration of 90 ppb would be needed to precipitate an amount of 100 g of uranium in 1 m^3 of sediment. This is equivalent to a seepage flux of 0.00113 m^3/day over 5000 years, which is in the range of seepage fluxes observed in lake sediments near the study area with similar hydraulic gradients (Schillereff, pers. comm., 1988).

Following the same assumptions, the amount of other metals that could be precipitated in the sediment from the same volume of groundwater was calculated. The calculated concentrations that could be deposited from the groundwater are in the range of typical concentrations found in the sediment (Table 5.4). With the exception of Fe, Mn, and Mo the calculated average metal concentrations in the hypothetical lake sediment are within a factor of 3 of the

Table 5.4 Comparison of average trace metal concentrations found in groundwaters, with computed and actual concentrations found in the sediment.

	Cu ppm	Pb ppm	Zn ppm	Mn ppm	Fe %	Mo ppm	U ppm
Average Groundwater	0.0359	0.0102	0.7090	0.4080	0.0044	0.0017	0.0900
Calculated Sediment	40	11	80	456	6.1	2	100
Actual Sediment (Core GPE)	57	10	220	1730	1.2	16	119

observed average metal concentrations in Gull Pond sediment core E. Therefore it appears that there is a sufficient amount of dissolved metals in groundwater to account for the amount of metals found in the sediment, in addition to the possibility of being transported as detrital material, providing that the geochemical conditions are present for the metals to precipitate.

In order to determine the ionic state in which various metals would exist as they moved through the rock mass, an Eh-pH stability diagram was constructed with the aid of PHREEQE (Parkhurst et al., 1980). PHREEQE is a fortran computer program designed to model geochemical reactions and has the capability to calculate the composition of solutions in equilibrium with multiple phases. Chemical data typical of

groundwater in the Pennys Pond area were used as input to the model. The metal concentrations used to construct the Eh-pH diagram are given in Table 5.5. Consecutive model runs were performed allowing the modelled groundwater composition to equilibrate at different oxidation conditions by adjusting the Eh level, thus simulating the effects of reduction by organic carbon reduction. Several runs were also made with different amounts of dissolved inorganic carbon present to determine the phase changes associated with increased inorganic carbon concentrations.

Results from this equilibrium modelling exercise along with data from Brookins (1988), Garrels and Christ (1965) and Krauskopf (1967), were then used to plot the phase boundaries that would exist for the various elements on an Eh-pH diagram (Figure 5.7). The results indicate that, given high Eh and low pH conditions, most of the trace metals would be soluble in groundwater, and could thus be transported by groundwater.

Table 5.5 Concentrations of total inorganic species used to construct Eh-pH diagram.

Ca ppm	Mg ppm	Na ppm	K ppm	SiO_4 ppm	Cl ppm	HCO_3 ppm	S ppm	Cu ppb	Pb ppb	Zn ppb	Mn ppb	Fe ppb	U ppb
46.4	3.0	40.2	3.3	4.4	0.6	139	73	6	16	18	539	600	133

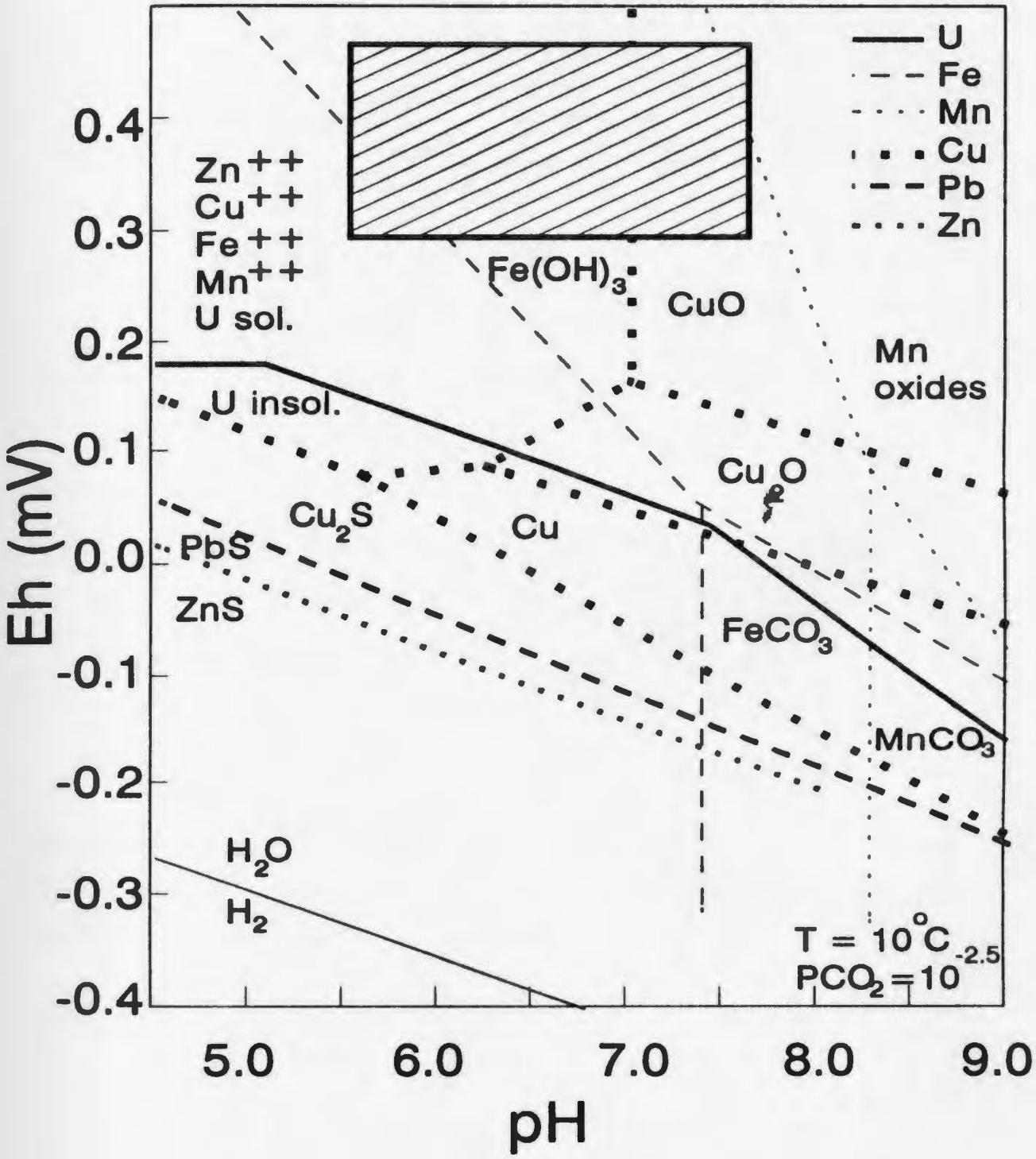

Figure 5.7 Eh-pH diagram showing stability fields for various solid phases with respect to dissolved metals. The cross hatched area indicates the range of Eh-pH values measured in groundwaters in the area.

Groundwaters sampled from granitic rock in the Foxtrap - Holyrood area have a range of pH (5 to 8) and relatively high Eh (approximately +300 to +500 millivolts) which indicates that the groundwaters are oxidizing. If these groundwaters discharge into a lake bottom they will interact with organic rich sediments in which a lower oxidation potential may exist. From Figure 5.7 it can be seen that it would only take a small decrease in Eh for soluble uranium in an oxidizing groundwater to be reduced to an insoluble uranium oxide. The uranium phase boundary is the first to be encountered as oxidation potential is lowered, which may explain why increased uranium concentrations show the strongest correlation with a rapid change in LOI. It would take a much greater reduction in Eh to reach a phase boundary for other elements such as copper or zinc. Since insoluble iron and manganese oxides are stable at higher oxidation potentials than observed in these groundwaters, they might be expected to be deposited as particulate material together with detrital sediments.

The phase boundaries indicated in the Eh-pH diagram may also help to explain concentrations of other metals observed in the sediment, when compared to the granite host rock (Table 5.3). Groundwaters fall into the $Fe(OH)_3$, CuO, and $PbSO_4$ fields (Figure 5.7; Brookins, 1988) for the observed Eh and pH conditions. Therefore metals such as iron, copper, and lead

would tend not to be transported as dissolved species but rather as detrital material. This is consistent with the ratios of these trace metal concentrations in lake sediment relative to original rock. In contrast, the precipitation of dissolved uranium in the sediment from oxidizing groundwaters by reduction with organic sediment could account for the observed enrichment of uranium in lake sediments relative to bedrock concentrations.

Chapter 6. SUMMARY, CONCLUSIONS, AND RECOMMENDATIONS

Detailed sampling of lake sediment from the four lakes in this study over a regular grid pattern has shown that trace metal concentrations are not evenly distributed in the lake sediment and that peak concentrations of metals in the sediment are not restricted to a common location in each lake. Therefore, sampling the sediment from only the deepest or most central area of a lake, where trace metals are thought to be concentrated (Hornbrook and Garrett, 1975; Lush, 1984), may not always provide a sample which represents the distribution of trace metals in the sediment of that lake. A comparison between the concentrations of metals found in the sediment and those found in the granitic bedrock suggests that the metals in the sediment may be derived from detrital material. However, elevated values of some elements, such as uranium, suggest that metals are being enriched in the sediment relative to bedrock concentrations.

Vertical profiles of sediments provide additional information on the processes or mechanisms by which trace metals are transported and concentrated in the sediment. It was found that metal concentrations also varied in the sediment column, and in some cases very high concentrations of a particular metal occurred over a short section of the core. In cores

which had a uranium concentration peak, the peak often coincided with the point at which there was a rapid change in the organic content in the sediment near the bottom of the core. It is proposed that the peak uranium concentrations are a result of the change in oxidation potential produced when oxidizing groundwater interacts with reducing, organic-rich sediment. It would thus be possible for uranium, which would be soluble in an oxidizing groundwater which was discharging in to a lake bottom, to be reduced and absorbed or precipitated in the sediment when it encountered sediments with increased organic content. While the source of metals found in lake sediment is generally thought to be from detrital inputs it is proposed that oxidizing groundwaters discharging into a lake may provide an alternative source of dissolved metal species which may become concentrated in the lake sediment.

An interpretation of the hydrogeological framework of the area surrounding the four lakes in this study included an analysis of the fracture networks that exist in the underlying fractured granitic bedrock. Analysis of the fracture geometry in the area has indicated that on a regional scale, fractures orientated slightly west of north are likely to dominate the direction of groundwater flow. Elongated zones of anomalous uranium concentrations in both Pennys Pond and Gull Pond,

identified from grid sampling of lake sediment, are aligned approximately in the same orientation as the major lineaments and fractures in the area. This suggests that fracture controlled groundwater input to the lake could be contributing to the formation these anomalies. In this respect, fracture intersections may provide a vertical pathway for groundwater discharge, which could result in the localized distribution of metals in lake sediment, as observed in Gull Pond and Pennys Pond.

Given the possibility that dissolved metals transported in groundwater may be concentrated in lake sediment, an estimate was made of the time required to produce a trace metal anomaly of the observed magnitude under present conditions. Assuming a constant seepage rate, constant groundwater metal concentrations and 100% efficiency in removal of metals in solution, it can be shown that groundwater with a uranium concentration of 90 ppb seeping into a lake at a rate of 0.00113 m^3/day (measured seepage for lake bottom sediment in adjacent area, Schillereff, pers. comm., 1988) would take approximately 5000 years to produce an anomaly of 100 ppm uranium in 1 m^3 of sediment (Appendix E). Radiocarbon and pollen analysis of core samples collected from lakes on the Avalon Peninsula indicate that ice from the last glaciation retreated about 9300 years ago (MacPherson 1982). Therefore,

it is possible that groundwaters are responsible for the observed lake sediment metal anomalies, which have developed since the end of the last glacial period.

Seepage rates may be quite variable throughout a lake. The rate at which groundwater discharges through lake bottom sediment will affect the amount of time required for anomalous concentrations of metals to accumulate in the sediment. In future studies, the location and amount of groundwater seeping through lake bottom sediments should be more clearly defined. This could be achieved quite simply in a small lake, such as Pennys Pond, using a series of seepage meters such as the one described by Lee (1977). For a larger lake a three dimensional numerical model may be useful, both for defining the area of local discharge as well as regional flow paths in and around the lake.

It has been shown that it is possible for groundwaters to contribute to the formation of trace metal anomalies in lake sediments. Understanding the relationship between the concentrations of trace metals in groundwater and lake sediments may prove to be a useful tool in mineral exploration. Determining the composition of groundwater, at points along the flowpath up-gradient of an area having known anomalous concentrations of trace metals in lake sediment may

provide information on the source of metals. In the case of this study, it is possible that the source of uranium may be traced back to Pennys Hill, which is a common point of recharge for all four lakes in this study which all showed some enrichment of uranium in their sediment.

Lake bottom sediments comprise a very complex environment where there are many possible physical, chemical and biological processes taking place. It is difficult to identify the contribution of any single one of these processes to the concentration of metals in the sediment. However, a mechanism has been suggested by which fracture-controlled groundwaters can transport dissolved metal species and concentrate these metals in lake sediment by inorganic chemical processes described above. Although more than one mechanism may be responsible for the concentration of metals in the lake sediment, the role of groundwater cannot be ignored, especially in lakes located in known areas of groundwater discharge.

REFERENCES

Brookins, D.G, 1988, Eh-pH Diagrams for geochemistry. Springer-Verlag, Berlin Heidelberg, 176 p.

Butler, A.J., 1980, Lake sediment geology of Lloyd's River area, southwest Newfoundland. In Current Research. Newfoundland Department of Mines and Energy, Report 80-1, 230-239.

Cherry, J.A. and Johnson, P.E., 1984, A multilevel device for monitoring in fractured rock. Groundwater Monitoring Review, 2, no. 3, 41-44.

Davenport, P.H., 1978, Uranium distribution in the granitoid rocks of eastern Newfoundland, Newfoundland Department of Mines and Energy, Mineral Development Division, Open File NFLD. 946.

Davenport, P.H. and Butler, A.J., 1976, Uranium distribution lake sediment western Newfoundland and on the Avalon and Burlington Peninsulas, Newfoundland Department of Mines and Energy, Mineral Development Division, Open File NFLD. 904.

Frape, S.K. and Patterson, R.J., 1981, Chemistry of interstitial water and bottom sediments as indicators of seepage patterns in Perch Lake, Chalk River, Ontario, Limnology and Oceanography, 26(3), 500-517.

Garrels, R.M, and Christ, C.L., 1965, Minerals, solutions and equilibria. Harper and Rowely, New York, 453 p.

Gale, J.E., Andrews, J.A., Fryer, B.J, Macko, S.A, Strong, D.F, Calon, T.J., Welhan, J.A., and Davenport, P.H, 1987, Groundwater flow system in fractured crystalline rocks - application to mineral exploration and toxic waste disposal. Final Report - NSERC strategic grant.

Gale, J.E., Francis, R.M., King, A.F. and Rogerson, R.J., 1984, Hydrogeology of the Eastern Avalon, Water Resources Report 2-6, Groundwater Series, Newfoundland Department of the Environment, 142 p.

Gillot, S.L., 1987, Extract clusters from axial data sets using the algorithm of Shanley and Mattab, Unpublished IBM-PC computer program.

Griffin, C.A., 1988, A geochemical comparison between two rivers in the Conception Bay Area, Newfoundland. BSc. Thesis, Memorial University of Newfoundland, St. John's, Newfoundland, 102 p.

Hayes, J.P., 1989, Trace metal analysis of granitic rocks of the Holyrood Pluton, unpublished data.

Henderson, E.P., 1972, Surficial geology of the Avalon Peninsula, Newfoundland, GSC Memoir, 368, 121 p.

Hughes, C.J. and Brueckner, W.D. 1971, Late PreCambrian rocks of the Avalon Peninsula, Newfoundland - a volcanic island complex. Can. Journal of Earth Science, 8, 899-915.

Hornbrook, E.H.W. and Garrett, R.G., 1975, Regional and geochemical lake sediment survey, east-central Saskatchewan. GSC paper 75-41.

Hornbrook, E.H.W., Davenport, P.H. and Grant D.R., 1975a, Regional and detailed geochemical exploration studies in glaciated terrain in Newfoundland. Newfoundland Department of Mines and Energy, Report 75-2, 116 p.

Houle, L.M., 1985, Chemical character of surface waters and lake sediments of Pennys Pond. BSc. Thesis, Memorial University of Newfoundland, St. John's, Newfoundland, 100 p.

King, A.F, 1984, Bedrock geology of the Avalon Peninsula area. 1:250,000 scale map.

Krauskopf, K.B., 1967, Introduction to geochemistry, McGraw-Hill Book Company, New York, 617 p.

La Pointe, P.R. and Hudson, J.A., 1985, Characterization and interpretation of rock mass joint patterns, Geological Society of America Special Paper 199, 37 p.

Lee, D.R., 1977, A device for measuring seepage flux in lakes and estuaries. Limnology and Oceanography, 22, 140-147.

Lee, D.R., Cherry, J.A., and Pickens, J.F., 1980, Groundwater transport of a salt tracer through a sandy lake bed. Limnology And Oceanography, 25(1), 45-61.

Lush, D.L., 1984, Regional geochemical surveys. in Mineral Association of Canada, Short Course in Environmental Geochemistry, Editor M.E. Fleet. London Ontario, 1984, 197-216.

MacPherson, J.B., 1982, Postglacial vegetational history of the eastern Avalon Peninsula, Newfoundland, and Holocene climatic change along the eastern Canadian Seaboard. Geographie Physique et Quaternaire, vol 36, no. 1-2, 175-196.

McBride, M.S. and Pfannkuch, H.O., 1975, The distribution of seepage within lakes. U.S. Geol. Surv. Journal of Research, 3, 505-512.

Parkhurst, D.L., Thorsten, D.C., and Plummer, L.N., 1980, PHREEQE - A computer program for geochemical calculations. U.S.G.S., Water resources Investigations, 80-96.

Strong, D.F., Dickson, W.L., O'Driscoll, C.F. and Kean, B.F., 1974, Geochemistry of eastern Newfoundland granitoid rocks, Newfoundland Department of Mines and Energy, Mineral Development Division, Report 74-3, 140 p.

Sundblad, B., Puigdomenech, I., and Mathiasson, L., 1990, Interaction between geosphere and biosphere in lake sediments. SKB technical report, 91-40, 74 p.

Twenhofel, W.H., and MacClintock, P., 1940, Surface of Newfoundland, Bull. Geol. Soc. Am., 51, 1665-1728.

Winter, T.C., 1976. Numerical simulation analysis of the interaction of lakes and groundwater. U.S. Geol. Surv. Prof Paper 1001, 45 p.

Winter, T.C., 1978. Numerical simulation of steady-state, three dimensional groundwater flow near lake. Water Resources Research, 14, 245-254.

APPENDICES

Appendix A Description of Scanline Mapping Procedures and Fracture Data File

A.1 Data Collection

Fracture data were collected from rock outcrops using detailed aerial photographs, taken from a helicopter, as base maps. Scanlines, varying in length, were laid out in perpendicular directions on each outcrop and fractures that intersected the scanlines were numbered and traced on mylar overlays. The number of scanlines used per outcrop ranged from two to ten depending on the number needed to adequately sample each outcrop area. Data were collected for each fracture including the location of the fracture intersection with the scanline, dip, dip direction, trace length, degree of censoring, termination style and other descriptive fracture characteristics. Due to time constraints when collecting fracture data over a large area and the fact that fractures shorter than the mean fracture spacing are thought to have a minimal contribution to the total flux through a fracture system, only fracture traces longer than 0.5 metres were sampled.

A.2 Analysis

Contoured lower hemisphere stereoplots of the poles to fracture planes for each of the outcrops mapped were created to determine the distribution of fracture orientations in the rock mass in the study area (Figure A.1). Although density of fractures are biased by the orientation of the scanlines, since fractures perpendicular to the scanline are more likely to sampled, in most cases two distinct sub-vertical sets can be identified and in some cases a third, weaker set appears to be present. Since all the outcrops were in the same vicinity and there appeared to be little spatial variability between outcrops, to simplify the analysis of the fracture geometry in the area, all the data were combined to define clusters for the region. Table A.1 gives a summary of the parameters that characterize the fracture geometry that exists in the rock mass in the area surrounding the study lakes.

Aopendix A

Table A.1. Summary of fracture characterization parameters.

	Cluster 1	Cluster 2
# of fractures	270	390
ORIENTATION		
mean dip azimuth	69.5	158.4
std. dev.	23.1	
mean dip	82.5	73.4
std. dev.	18.9	
general trend	NW-SE	NE-SW
TRACE LENGTH		
mean (m)	3.96	2.57
std. dev.	4.12	2.57
min.	0.50	0.50
max.	25.00	24.50
SPACING		
mean (m)	0.77	0.57
std. dev.	0.93	0.58
max.	6.11	3.62

Appendix A

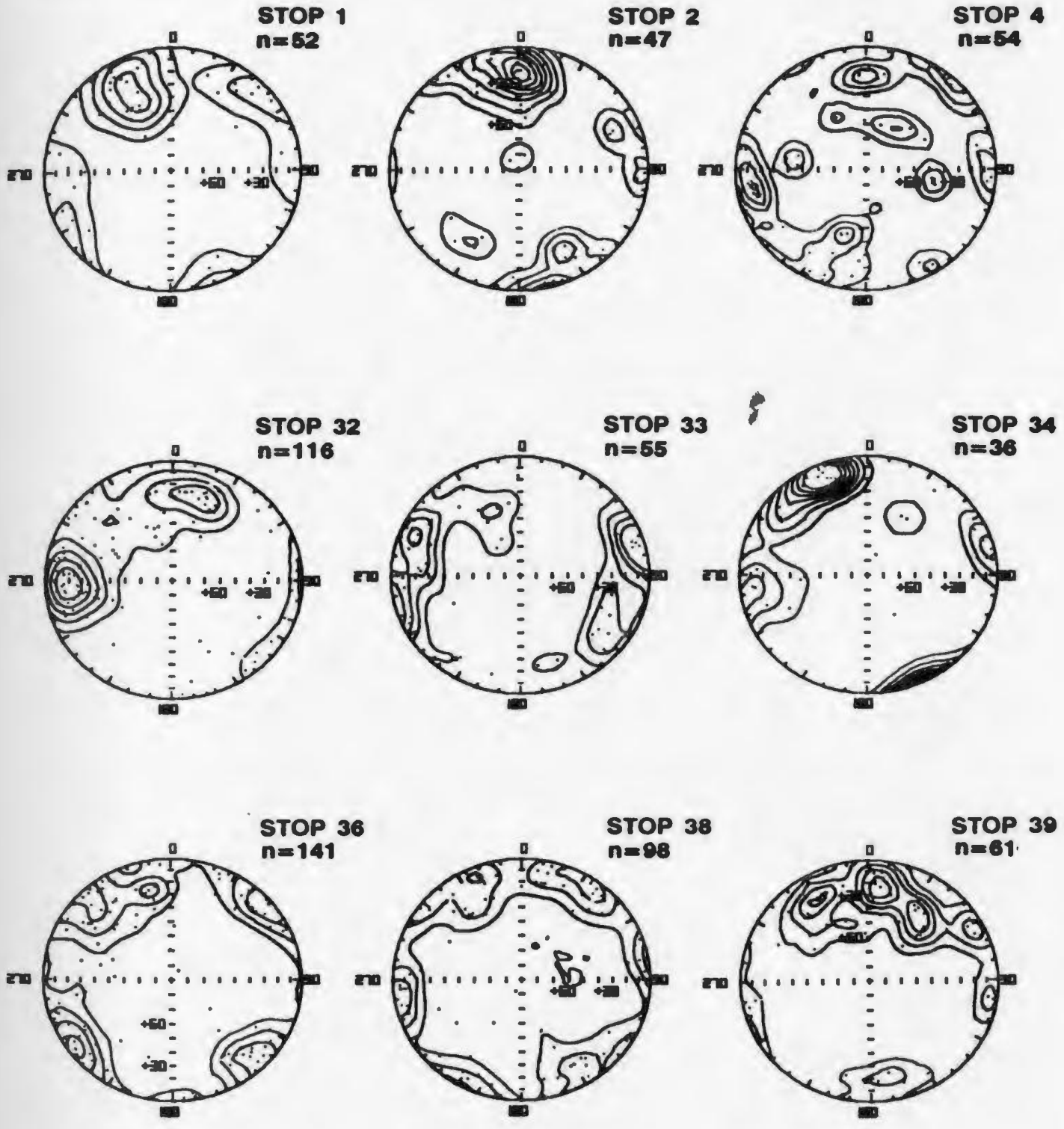

Figure A.1 Contoured lower hemisphere stereoplots of poles to fracture planes for each mapping location indicated in Figure 2.2.

Appendix A

A.3 Structure and Codes for Fracture Data File

Columns 1-2	Flag 11 - Fracture Data	33 - Comments
Columns 3-7	Photo number	
Columns 8-10	Scanline trend (0 - 360 degrees)	
Columns 11-12	Scanline plunge (0 - 90 degress)	
Columns 13-16	Sequential fracture number	
Columns 17-22	Scanline intersection in metres	
Columns 23-24	Fracture Type JT - joint CN - rock contact	FZ - fracture zone VN - vein
Columns 25-28	Dip direction (0 - 360 degrees)	
Columns 29-30	Dip (0 - 90 degrees)	
Columns 31-35	Trace length in metres	
Columns 36-37	Type of censoring 0 = both ends exposed 2 = both ends covered	1 = one end covered
Columns 38-41	Mineral infilling Q = quartz E = epidote	H = hematite R = rock rubble
Column 42	Large scale roughness P = planar U = undulating	C = Curved S = Stepped
Column 43	Small scale roughness S = smooth	R = rough
Column 44	Rock Type	G = granite
Column 45	Termination mode 0 = both ends free 2 = both against another	1 = one end free 3 = splays
46 - 80	Comments	

Appendix A

A.4 Fracture Data File

STOP 1

```
33 PHOTO S1-02 LINE A
110102A07900   1  0.60JT 26985  1.5 0    PRG0
110102A07900   2  1.65JT 26980  2.0 0  R SSG0
110102A07900   3  2.60JT 18051  1.0 0    CSG1 ENDS AT 2
110102A07900   4  3.70FZ 23290 17.0 1  R URG
110102A07900   5  4.50FZ 23290 25.0 2  R URG
110102A07900   6  4.95JT 22585  4.5 0    CSG3 JOINS FZ 5
110102A07900   7  5.55JT 23485  5.0 0    PSG0 SLIGHT FOLIATION;STR:054
33                                                      DIP:SUBVERT
110102A07900   8  5.95JT 10078  2.8 0    PSG1 ENDS AT 7
110102A07900   9 10.65JT 29084  3.0 0  R SSG0
110102A07900  10 12.20JT  8166  2.5 1  R SRG  SPLAYS TO N
110102A07900  11 12.65JT  7073  1.0 1    PSG
110102A07900  12 13.65FZ 22577 25.0 2 RQ --G
110102A07900  13 15.40FZ 13062  8.0 1  R SRG  ENDS AT 12
110102A07900  14 17.05JT 26175  8.0 1  R URG  ENDS AT 12
33 LINE A CONTINUES ON PHOTO S1-03
33
110103A07900  15 20.60FZ  7080 10.0 2  R --G
110103A07900  16 22.50JT 14590  4.0 0  R URG1 ENDS AT 15
110103A07900  17 25.14VN 24480  6.5 2 QE PSG
110103A07900  18 25.84JT  9370  3.0 1  R CSG  SPLAY END OF JT; JOINS V
110103A07900  19 28.35JT  9057  4.0 1  R CRG  SPLAY END
110103A07900  20 29.50FZ 15078  7.0 0  R URG2
110103A07900     30.00    90 0              EOL
33
33 PHOTO S1-03 LINE B
110103B35005  21  0.85JT  5369  3.0 1  R URG  ENDS AT 2
110103B35005  22  1.01JT 14063  2.0 1    PSG
110103B35005  23  1.75FZ 16070  4.0 2  R PRG  ENDS AT 15
110103B35005  24  3.23JT 15374  2.0 1  R URG
110103B35005  25  5.20CN 21575      1    USA  AP DIKE; OFFSET BY NUMER
33 LAT. FAULTS; APOPHYSES SUBPARALLEL
110103B35005  26  6.10JT 34075  5.0 1  R URG
110103B35005  27  7.20JT 35090  2.0 1  R PSG  ENDS AT 15
110103B17015  28  7.60FZ 34075  5.0 2  R URG  ENDS AT 12 & 15
110103B17015  29  9.95FZ 15570  4.5 2  R URG  ENDS AT 12 & 15
110103C35508  30  0.00JT 33369  2.0 2  R PSG
110103C35508  31  1.30JT 23551  1.5 2    PSG  PROJECTED PLANE UP TO SC
110103C35508  32  3.69JT 16584  1.0 1  R PRG
110103C35508  33  4.15CN 21871  9.0 2    --A  10 CM AP DYKE
110103C35508  34  4.25JT  6376 12.0 2  R URG  CROSSCUTS 33; 33 CROSSCU
33  PARALLEL 2CM AP DYKE; 34:10 CM RT. LAT. MOVEMENT
110103C35508  35  5.90CN 20071  9.5 2    --A
110103C35508  36  6.25JT 14428  3.0 0  R PSG1 ENDS AT 34
110103C35508  37  6.83CN 21062  9.0 2    PSA  SIM. TO 33 & 35
110103C35508  38  8.45FZ 14550  7.0 0  R USG0
110103C35508  39  8.74JT 14571  3.0 0  R SSG3
110103C35508  40 10.08JT 15050  8.0 0  R USG1
110103C35508  41 10.42JT 15549  3.0 0  R PSG3 JOINS 40
110103C35508  42 11.05JT 15446  3.0 2  R SSG
110103C35508  43 11.40JT 15446  1.0 2    PSG
33
33 PHOTO S1-02 LINE D
110102D12310  44  0.50JT 16377 11.0 1  R PRG
110102D12310  45  1.65JT 16550  3.0 0    PSG3 SPLAYS TO NE
```

Appendix A

```
110102D12310  46  2.15JT 16680  2.0 1   R PSG  SPLAYS TO NE
110102D12310  47  2.45JT 29052  2.0 0     CSG3
110102D12310  48  3.05JT 27759  1.5 0   R CSG3 PART OF SPLAY; SAME AS 4
110102D12310  49  3.45JT 16340  7.0 2   R PSG
110102D12310  50  4.30JT 16348  3.0 2   R PSG
110102D12310  51  5.10JT 15859  7.0 1   R SSG
110102D12310  52  9.00FZ 14776  4.0 0   R --GO FINELY BROKEN BLOCKY ZON
```

STOP 2

```
33  STOP 2  PHOTO-S1-07  LINE A
110107A34105   1  0.07JT 20257  1.9 1     PSG
110107A34105   2  1.31JT 137 8  1.0 0     PSG0
110107A34105   3  1.67JT 18244  0.6 0     PSG1
110107A34105   4  1.94JT 16246  0.9 0     USG1 FORKS TO W; ENDS AT 11
110107A34105   5  2.17JT 18735  0.7 0     PSG1 ENDS AT 11
110107A34105   6  2.54JT 19377  1.0 0     CSG1 ENDS AT 11
110107A34105   7  2.88JT 19063  0.9 0     PSG1 ENDS AT 11
110107A34105   8  3.18JT 18064  1.5 0     PSG1 ENDS AT 11
110107A34105   9  3.27JT 18076  1.7 0     PSG1 ENDS AT 11
110107A34105  10  4.25FZ 17157  2.1 2   R USG  MOSS; SPANS:3.85-4.50; S
33 IN ZONE 2-10MM
110107A34105  11  5.00FZ 24574 15.7 1 RH USG  FAULT;MOST EW JTS END AT
33 DIVIDES TO NW
110107A34105  12  5.60FZ 18764  2.3 1     PSG  SPANS:5.4-5.8; ENDS AT 1
110107A34105  13  6.18JT 15565  0.8 0     SSG0 ZIGZAG PATTERN
110107A34105  14  7.30JT 15360  1.4 0     PSG1 ENDS AT 11
110107A34105  15  5.81JT 14583  1.3 0     SSG1 ENDS AT 11
110107A34105  16  9.85JT 15778  1.4 0     PSG0
110107A34105  17 10.36JT 17868  1.3 0     PRG1 ENDS AT 11
110107A34105  18 11.16JT 15985  1.5 0     CSG0
110107A34105  19 11.91FZ 17764  2.0 0     PSG1 SPANS:11.8-12.2; ENDS AT
33 SPACING IN ZONE 1-5MM
110107A34105  20 12.32JT 33470  1.7 0     PSG2 ENDS AT 11 & 21
110107A34105  21 12.67JT   378  3.0 0     PSG1 EN ECHELON PAR JT AT 11
110107A34105  22 12.90JT 18379  1.7 0     PSG1 ENDS AT 11
110107A34100  23 13.32JT 18082  3.5 0   R PSG1 MOSS; STR. SPLAYS TO NW
110107A34100  24 13.45JT 24768  0.8 0     PSG2 ENDS AT 23 & 26
110107A34100  25 13.62JT 33162  6.0 1   R PSG  JOINS 23
110107A34100  26 14.14JT 33761  0.7 0     CSG1
110107A34100  27 14.50JT 17976  3.8 1   R USG  MOSS
110107A34100  28 16.50FZ 19063  2.0 0     PSG1 SPANS:16.4-16.6; INTERNA
33  1-2MM
110107A34100  29 18.07JT 31682  1.1 0     PSG0
110107A34100  30 18.28JT 32974  1.4 0     PSG0
110107A34100  31 18.54JT 33058  1.3 1   R SSG  MOSS
110107A34100  32 18.70JT 34885  1.0 0     PSG1
110107A34100  33 20.57JT 16875  1.6 0   H PSG1
110107A34100  34 21.50JT 16782  1.2 0   H USG1
110107A34100  35 22.35JT 17090  1.2 0     PSG0
110107A34100     24.50    90 0                EOL
33
33 PHOTO-S1-07 LINE B
110107B25107  36  0.28JT 26585  8.2 1   H PSG  MOSS
110107B25107  37  1.13JT 18557  4.1 0   R PSG2 MOSS; ENDS AT 36 & 41
110107B25107  38  3.92JT  2753  1.8 0     SSG0
110107B25107  39  6.45FZ  2862  5.0 1   R PSG  MOSS; SPANS:6.2-6.7; END
110107B25107  40  7.42JT 13886  2.0 0   R PSG1 MOSS; ENDS AT 41
110107B25107  41  8.17JT 24865  7.0 2   R PSG  LEFT LAT. SPLAYS AT S EN
110107B25107  42  8.30JT  5355  1.4 0     CRG3 SPLAY FROM 41
110107B25107  43  8.47JT  4066  1.7 0     CRG3 SPLAY FROM 41
```

Appendix A

```
110107825100  44  9.00FZ 27581  2.9 1  R CSG  SPANS:8.95-9.05; JOINS 4
110107825100  45  9.50JT 34485  0.9 0    PSG0
110107825100  46 12.10FZ 27287  1.9 2    PSG  SPANS:12.01-12.05; FORMS
33 FACE AT NE END
110107825100  47 13.55JT 20010  0.7 1    PSG  EXFOLIATION
110107825100  11 16.07FZ 24574 15.7 1 RH USG
110107825100  10 16.30FZ 17157  2.1 2  R USG
110107825100     17.50    90 0                EOL
```

STOP 4

```
33 STOP 4  PHOTO-S1-13  LINE A
110113A25020   1  0.26JT  9851  0.8 1  R SSG
110113A25020   2  0.74JT  7573  8.0 2  R SSG  MOSS
110113A25020   3  1.57JT  3270  2.6 0    CSG1 ENDS AT 2
110113A25020   4  2.60JT 22539  1.5 0    CSG0 EN ECHELON AT SW END
110113A25020   5  3.80JT 21534  1.4 0    PSG1 ENDS AT 7
110113A25020   6  4.12JT 24242  0.7 0    CSG1 ENDS AT 7
110113A25020   7  4.90FZ  9478 10.0 2  R PSG  MOSS; SPANS:4.4-5.4;INTE
33  SPACING 1-10CM
110113A25020   8  5.86JT 10083  3.4 1  R PSG  STR. SPLAYS AT BOTH ENDS
110113A25020   9  6.80FZ  7575  8.3 2    USG  SPANS:6.6-7.0
110113A25020  10  7.25FZ 26377  6.0 1  H USG  SPANS:7.15-7.35;INTERNAL
33 SPACING 3-. M; PARALLEL H-CLOTS
110113A25020   .   7.56JT  8477  4.0 1    PSG
110113A25020  12  7.74JT  8380  3.0 0    PSG3 JOINS 11
110113A25020  13  8.00JT 27486 10.1 1  R CSG
110113A25020  14  9.90JT 23489  2.2 0    CSG3 JOINS 16
110113A25020  15 10.10JT  7672  1.4 0    CSG3
110113A25020  16 10.65JT 25776  9.5 1  Q CSG  DIP REVERSES DIRECTION O
33  FACE TO NW
110113A25020  17 11.50JT 27842  0.8 0    PSG0
110113A25020  18 11.62JT 28345  0.9 0    PSG0
110113A25020  19 12.25JT 28144  0.9 0    PSG0
110113A25020  20 12.90JT 33276  1.6 0    PSG0
110113A25020  21 13.30JT 19068  2.6 0    PSG0 STR. SPLAYS AT W END
110113A25020  22 14.55JT 10244  2.1 1    SSG  EN ECHELON TO N END; STE
110113A25020  23 14.63JT  9444  1.3 0    PSG0
110113A25020  24 15.20JT  5368  1.8 2    PSG  L.E. 1CM SHEAR ZONE; FLA
33 QUARTZ & FELD.
110113A25020     15.70    90 0                EOL
33
33 PHOTO-S1-13 LINE B
110113B16502  25  0.30JT 19731  1.7 0  R CRG0 MOSS
110113B16502  26  0.95FZ 27683  2.8 1    PSG  MOSS; SPANS:0.9-1.0; LEF
33 SPLAY AT SE END
110113B16502  27  0.95JT  2063  1.1 0    PRG0
110113B16502  28  1.54JT  2784  1.0 0    PRG1 ENDS AT 26
110113B16502  29  1.73JT  2082  0.8 0    PSG1 ENDS AT 26
110113B16502  30  2.05JT  2047  1.7 0    CSG2 ENDS AT 26 & 2
110113B16502  31  2.30JT  1948  0.9 0    PSG1 ENDS AT 26
110113B16502  32  2.70JT  3363  1.1 0    USG3 SPLAY FROM 26
110113B16502   3  4.25JT  3270  2.6 0    CSG1
110113B16502  33  4.85JT 17263  1.3 0    CSG0
110113B16502  34  5.03JT   641  0.9 0    PSG2 ENDS AT 33 & 2
110113B16502  35  5.32JT 34425  2.1 0    PSG1 ENDS AT 2
110113B16502  36  5.82JT 22890  1.1 0    PSG1 ENDS AT 35
110113B16502  37  6.54JT 21887  2.9 0    USG1
110113B16502  38  7.43JT 23175  1.3 0    PSG0 S END HAS STR. SPLAYS
110113B16502  39  7.80JT 21331  1.6 0    CSG1 ENDS AT 2
110113B16502  40  8.70JT 17668  1.3 1    CSG
```

Appendix A

```
110113B16502  41  9.61JT 20182  1.0 0    PSG0
110113B16502  42 10.08JT 21088  1.7 1  H PSG  STR. SPLAYS AT W END
110113B16502  43 10.61JT 32783  0.6 1    SSG  MOSS
110113B16502  44 10.69FZ   465  6.0 2  R USG  MOSS; WIDENS TO 60CM TO
110113B16502  45 11.31JT   778  0.7 0    PSG0
110113B16502  46 12.36JT 14890  0.8 0    PSG0
110113B16502  47 12.66JT 18764  1.1 0    SSG0
110113B16502  48 13.40FZ 14664  2.5 1  R USG  SPANS:13.35-13.45
110113B16502  49 14.03FZ  1546  2.3 1  R PSG  SPANS:13.95-14.10
110113B16502  50 14.10CN 15140  4.1 2    PSF  5CM FELSITE DYKE;PROJECT
33 SCAN LINE
110113B16502  51 14.45CN 15140  3.7 2    PSF  1 CM FELSITE DYKE
110113B16502  52 15.41JT 22384  0.9 0    PSG1
110113B16502  53 15.88JT 17666  1.1 0    PSG0
110113B16502  54 16.05JT 17833  0.8 0    PSG0 PROJECTED UP TO SCAN LIN
110113B16502     16.50    90 0              EOL
```

STOP 32

```
110519A04400   1  0.06JT  8251  1.4 1    PSG
110519A04400   2  0.37JT  8348  1.8 2    PSG
110519A04400   3  0.56JT  8474  4.4 2    CSG
110519A04400   4  1.15JT 11768  1.4 0    CSG3
110519A04400   5  1.58JT  8654  6.1 1  H PSG  BRAIDED; IN SPOTS 2 OR 3
33                                          RIGHT LATERAL SPLAYS AT N END
110519A04400   6  1.94JT  8764  2.2 0    PSG0
110519A04400   7  2.08JT  8776  3.4 0  H PSG0
110519A04400   8  2.50FZ  8363  6.9 2  H PSG0  2.35 - 2.65 PARALLEL JO
33                                          GAPS UP TO 2 MM
110519A04400   9  2.86JT  8982  2.3 0  H PSG0  RIGHT LATERAL SPLAYS AT
110519A04400  10  3.45JT 16664  0.6 0    USG2  DIFFUSE MICROJOINTS
110519A04400  11  3.72JT  8484  3.1      H USG  GAP UP TO 1 CM
110519A04400  12  4.01JT  8663  2.3 1  H PSG  RIGHT LATERAL SPLAYS N E
110519A04400  13  4.20JT 21035  0.7       CSG2
110519A04400  14  4.24JT  8474  1.4 0  H PSG1
110519A04400  15  4.54JT  7882  4.3 2  H PSG  DIFFUSE PARALLEL MICROJO
33                                          BRAIDED IN SPOTS
110519A04400  16  4.76JT  7868  1.2 1  H PSG
110519A04400  17  4.95JT  8258  4.0 2    PSG
110519A04400  18  5.67JT  7041  4.7 1    USG
110519A04400  19  6.46JT  8160  3.3 1    PSG
110519A04400  20  6.58JT  7753  3.1 1  H PSG
110519A04400  21  6.94JT 35586  0.8 0    PSG0
110519A04400  22  7.18JT 19866  0.8 0    PSG2
110519A04400  23  7.45JT 19176  0.8 0    PSG2
110519A04400  24  8.05JT 20861  0.9 0    PSG0
110519A04400  25  8.11JT 10577  5.1 0    USG0
110519A04400  26  8.40JT 20158  2.1 1    PSG  DIFFUSE
110519A04400  27  8.61JT 19661  1.4 0    PSG0
110519A04400  28  8.86JT 19165  1.8 1    PSG
110519A04400  29  9.20JT 19843  1.7 1    PSG  DIFFUSE PARALLEL JOINTS
110519A04400  30  9.43JT  9374  3.0 0    PSG3 DIFFUSE MICROJOINTS
110519A04400  31  9.44JT 20163  2.3 0    PSG3
110519A04400  32  9.64JT 20760  1.3 0    PSG2
110519A04400  33  9.71JT 20555  1.3 0    PSG2
110519A04400  34  9.88JT 20572  1.7 0    PSG1
110519A04400  35 10.08JT  7550  6.0 1  H USG  DIFFUSE ZONE 2 - 3 CM
110519A04400  36 10.54JT  8756  0.8 0    PSG0
110519A04400  37 10.80JT  9566  9.2 1 HE USG  LENSOID EPIDOTE IN GAPS
33                                          1 CM
110519A04400  38 11.04JT 20064  1.3 0    PSA1
```

Appendix A

```
110519A04400  39 11.35JT  9363  2.8 1  H PSG
110519A04400  40 11.35JT 20556  0.8 0    PSA1
110519A04400  41 12.06JT  7271  7.0 1  H USG   GAP UP TO 3 MM
110519A04400  42 12.70FZ  6037  3.3 1  H USG   12.55 - 12.85 BRAIDED S
33                                              ZONES WITH FE MATRIX IN PLACES
33                                              COMMINUTED AND LAMINATED.
110519A04400  43 12.97JT 18764  1.2 0    CSG1
110519A04400  44 13.00JT 11558  0.8 0  H PSG0  DIFFUSE LEFT LATERAL
33                                              SPLAYS AT BOTH ENDS.
110519A04400     13.00    90 0                  E.O.L
33
110519B13103  45  0.17JT 18864  1.1 0    PSG0
110519B13103  46  0.61JT 34488  0.7 0    CSG3
110519B13103  47  0.87JT 11944  1.7 1    CSG
110519B13103  48  1.16JT  9863  2.9 2  H PSG  PATCHY FE INFILL
110519B13103  49  1.42JT  9578  0.9 2    PSG
110519B13103  50  1.77JT 27582  0.6 2    PRG
110519B13103  51  2.09JT 10879  3.0 2    PSG  DIP ESTIMATED
110519B13103  52  2.30JT 10375  9.3 2    USG
110519B13103  53  2.57JT 10280  2.5 1    USG
110519B13103  54  3.20JT 16664  0.9 0    PSG1
110519B13103  55  3.21JT  9470  1.8 0 HR CSG0
110519B13103  56  3.56JT 10062  3.3 0  H USG0
110519B13103  57  3.60JT 17070  0.8 1    PSG
110519B13103  58  4.35JT 29085  2.0 2    PSG  DIP ESTIMATED
110519B13103  59  4.58JT 10949  2.0 1    PSG
110519B13103  60  4.89JT 17065  1.8 0    PSG2
110519B13103  61  4.99JT 17571  1.9 0    PSG2
110519B13103  62  5.85JT 17861  1.5 0    PSG0
110519B13103  63  6.20JT 17963  1.1 0    PSG   LEFT LATERAL SPLAY AT N
110519B13103  64  7.17FZ 32366  2.3 0    USG0  7.05 - 7.30 DENSE MICRO
33                                              SPACING 1 - 3 MM BRITTLE
33                                              SHEAR ZONE
110519B13103  65  7.77JT 29081  4.9 2  H PSG
110519B13103  66  8.48JT  8874  6.9 0 HE PSG2
33
110519B13100  67  8.85JT  7078  5.2 1  H USG  GAP UP TO 1 CM.
33                                              BRAIDED SPOTS
110519B13100  68  9.15JT  9580  1.0 0 HE PSG3 DIP VARIES ALONG STRIKE
110519B13100  69  9.55JT  8078  4.1 2  H PSG
110519B13100  70  9.62JT 31378  0.7 0    CSG1
110519B13100  71 10.02JT 33746  0.7 0    PSG2
110519B13100  72 10.05JT  8481  4.1 2 HE USG
110519B13100  73 10.17JT  9366  2.5 1 EH USG  DIFFUSE BRAIDED ZONE 2 -
110519B13100  74 10.55JT  7773  1.8 1  H PSG
110519B13100  75 11.21JT 13489  8.0 2    CSG  DIP ESTIMATED
110519B13100  76 11.95FZ 10083  2.3 1 HE USG  11.80 - 12.10. SUBPARALL
33                                              JOINTS SPACING 2 - 7CM BRAIDED
110519B13100  77 12.35JT 12683  0.8 0    PSG3
110519B13100  78 12.69JT 19967  0.7 0    PSG2
110519B13100  79 12.73JT 12386  3.7 1  H USG
110519B13100   9 12.82    90 0
110519B13100     13.00    90 0                  E.O.L
33
33
110521A26008   1  0.50JT 13583  0.9 0    USG0
110521A26008   2  0.55JT 30481  0.7 1    PSG
110521A26008   3  0.90JT 14852  0.8 0    PSG0
110521A26008   4  2.37JT 12849  0.9 1    PSG
110521A26008   5  2.58JT 11657  0.6 1    PSG
110521A26008   6  2.75JT 14563  1.7 2    USG
110521A26008   7  3.80JT 26585  2.4 1    USG
```

Appendix A

```
110521A26008   8  3.83JT 31783  3.5 0     USG2  LEFT LATERAL SPLAYS AT
33                                                ENDS
110521A26008   9  4.18JT 25490  1.4 0     CSG1
110521A26008  10  4.65JT 22877  0.9 0     PSG0
110521A26008  11  5.95JT 14971  1.4 0     PSG1
110521A26008  12  6.19JT  4060  1.3 0   H PSG3  LEFT LATERAL SPLAY AT S
110521A26008  13  6.70FZ 24175  9.5 0   H PSG1  6.55 - 6.85. BRAIDED JO
33                                                FE CLOTS
110521A26008  14  8.20JT  9575  4.9 0     URG1
110521A26008  15  8.75JT 15623  0.9 0     CSG1
110521A26008  16  8.99JT 20955  0.8 0     PSG0
110521A26008  17  9.30JT 18464  1.2 0     PRG0
110521A26008  18  9.56JT 21351  1.4 0     PSG0  EN ECHELON RIGHT.
33                                                PLANAR SMOOTH SECTIONS
110521A26008  19  9.90JT 29563  0.8 0   H PSG0  DIFFUSE MICROJOINTS. FE
110521A26008     10.00    90 0                  E.O L
33
33
110521B15100  20  0.76JT 26563  0.9 0     PSG1
110521B15100  21  1.21JT 17348  1.0 0     USG3
110521B15100  22  1.60JT 17151  0.8 0     PSG1
110521B15100  23  1.82JT 35075  0.6 0     CSG2
110521B15100  24  2.32JT 32384  3.1 2     URG   DIP AVERAGED
110521B15100  25  3.50JT 15641  0.6 1 EH  PSG   EN ECHELON LEFT
110521B15100  26  4.10JT 16238  1.6 1     USG
110521B15100  27  4.80JT  6563  0.5 0     PSG0
110521B15100  28  5.08JT 33556  1.5 1     SSG
110521B15100  29  5.80FZ 16032  1.9 0     PSG0  5.65 - 5.95 PARALLEL
33                                                DISCONTINUOUS JOINTS
110521B15100  30  6.46JT 16639  1.1 0     USG0  DIFFUSE TRACES
110521B15100  31  6.57JT 13169  1.2 0     USG0  DIFFUSE TRACES
110521B15100  32  7.12JT 13483  2.0 0     USG0  DIFFUSE TRACES. BRAIDED
110521B15100  33  7.52JT 16526  1.4 0     USG0
110521B15100  34  7.90JT  7378  1.2 0 HE  CSG0
110521B15100  35  8.85JT  8373  0.8 0   H USG3
110521B15100  36  9.85JT 11741  0.6 0   H USG1
110521B15100  37 10.00JT 10234  0.8 0     PSG3
110521B15100     10.00    90 0                   E.O.L
```

STOP 33

```
110528A23800   1  1.32JT 33866  1.3 0     CSG1
110528A23800   2  1.50JT 25585  3.2 2 HR  PSG   CRUSH ZONE UP TO 1 CM
110528A23800   3  1.50JT  3472  0.9 0     USG1
110528A23800   4  1.93JT 35066  0.9 0     PSG1
110528A23811   5  2.30JT  1575  1.1 0     CSG1
110528A23811   6  2.53JT 27758  2.3 1     PSG   ENDS AT AN E-W JOINT
110528A23811   7  3.29JT 28362  1.1 1     PSG   ENDS AT AN E-W JOINT
110528A23811   8  4.00JT 14974  1.9 1 HR  USG   LENSOID Fe CRUSH ZONE FI
110528A23811   9  5.40JT 15528  0.6 1     USG   EXFOLATION
110528A23811  10  5.87JT 25573  2.5 2     PSG
110528A23811  11  6.70JT 14224  1.1 1     USG
110528A23811  12  7.29JT 30673  3.3 2 HR  PSG   SPREADS INTO 30 CM FRACT
33                                                ZONE TO E CRUSH ZONE 1 - 5 M
33                                                NO SLIP SENSE SEEN.
110528A23811  13  8.10JT 31482  1.1 0     PSG1
110528A23811  14  8.89JT 30765  2.0 1     USG
110528A23811  15  9.11JT  6647  0.7 1     USG   ENDS AT 16
110528A23811  16  9.87JT 31479  3.1 1     USG   PARALLEL MICROJOINTS; AV
33                                                TRACE LENGTH 30 CM.
110528A23811     11.00    90 0                   E.O.L
```

Appendix A

```
33
33
110527A11500    1  0.00JT 11163   1.2 2  H USG
110527A11500    2  0.45JT 17252   0.6 0    PSG1 PARALLEL SHORT TRACES OV
33                                                  SPACED 1 - 2 CM
110527A11500    3  0.82JT  8958   0.7 0    PSG3
110527A11500    4  0.92FZ  9863   2.0 2  H USG  FAULT. 5 CM BRECCIA BRAI
33                                                  ZONE SLIP SENSE?
110527A11500    5  1.04JT 26465   1.2 0    PSG3
110527A11500    6  1.53JT  8479   2.0 1 HR USG  PATCHY CRUSH ZONES UP TO
33                                                  LONG 5 CM  WIDE.
110527A11500    7  1.67JT  9366   1.9 1 HR PSG  PATCHY CRUSH ZONES UP TO
33                                                  LONG 5 MM WIDE.
110527A11500    8  1.75JT 17973   1.0 0    CSG1
110527A11500    9  2.28JT 27084   0.8 1    PSG
110527A11500   10  2.40JT 15143   0.8 1    USG
110527A11500   11  3.10JT 26489   3.3 1  H CSG
110527A11500   12  3.45JT 15054   1.1 1    PSG
110527A11500   13  3.57FZ 25579   1.8 OHER USG3  3.45 - 3.70. BRAIDED SH
33                                                  ZONES. ESTIMATED DIP.
110527A11500   14  3.57FZ  7677   5.3 1    USG
110527A11500   15  4.05JT  9568   1.0 1HER PSG
110527A11500   16  4.38JT  6788   1.4 1    PSG
110527A11500   17  4.59JT 24572   1.4 1 HR PSG   PATCHY CRUSH ZONES UP T
33                                                  LAMINATED COMMINUTED. SLIP=?
110527A11500   18  4.85JT 14164   1.3 1  H PSG
110527A11500   19  5.35JT 29358   1.2 2 HE PSG
110527A11500   20  5.52JT 12572   0.5 1 HE PSG
110527A11500   21  5.70JT 11586   1.0 2    PSG
110527A11500   22  5.70JT 23572   0.7 1    PSG
110527A11500   23  6.39JT 11682   1.3 2    PSG
110527A11500   24  6.66JT 25280   1.3 2    USG
110527A11500   25  7.30JT 29068   1.2 2    USG
110527A11500   26  8.11JT 11475   2.9 2 HE USG
110527A11500   27  8.48JT 31264   0.8 0    USG2
110527A11500   28  8.54JT 16350   0.6 0    PSG2
110527A11500   29  8.95JT 10976   2.3 1  H USG
110527A11500   30  9.15JT 10578   1.4 0    CSG3
110527A11500   31  9.25JT 25383   1.3 2  H PSG1
110527A11500   32  9.46JT 12272   1.3 1    PSG
110527A11500   33  9.52JT 29666   0.8 0    PSG1
110527A11500   34  9.58JT 26885   2.0 1  H PSG  BRAIDED  DISCONTINUOUS
110527A11500   35  9.73JT  6584   1.6 0    PSG3
110527A11500   36  9.78JT  8685   2.5 1    USG
110527A11500   37 10.13JT  6881   6.1 2    CSG
110527A11500   38 10.27JT  4485   0.9 1    PSG
110527A11500   39 10.90FZ 24480   2.9 1 HE USG  10.60 - 11.20 PARALLEL
33                                                  DIFFUSE MICROJOINT ZONES
33                                                  AVERAGE SPACING 3 CM
110527A11500      11.20    90 0                    E.O.L
```

STOP 34

```
33 STOP 34 PHOTO-S5-30 LINE A
110530A26405    1  0.00JT  9375   6.1 2  R P-G  MOSS; PROBABLY CONTINUES
33 N;FAULT?
110530A26405    2  0.46JT 24580   1.6 2  R SSG
110530A26405    3  2.22FZ 25283   9.2 2  R USG  MOSS; CONTINUES TO N ;
33 SPANS:2.1-2.34
110530A26405    4  2.25JT 14787   2.0 1  R CSG  MOSS; ENDS AT 3
110530A26405    5  3.38JT 26182   7.0 2  R USG  MOSS
```

Appendix A

```
110530A26405   6  4.35FZ  8377   9.1 2  R PRG  MOSS;SPANS:4.1-4.6; S HA
33 MOSS, LEFT LAT. SPLAYS AT SCAN LINE
110530A26405   7  5.45JT  8479   8.1 1  R PSG  MOSS
110530A26405   8  6.51JT 12469   2.6 0    PSG1 MOSS
110530A26405   9  7.03JT 12672   1.9 0  R CSG1 LEFT LAT.HOOK AT S END
110530A26405  10  7.70JT 14178   2.7 0    PSG0 8,9,10 APPEAR TO BE LEFT
33 SPLAYS OF MESOSCOPIC FAULT
110530A26414  11  9.64FZ 25787 23.0 2  R URG  SPANS:9.55-9.72; MAJOR FA
33 SHOULD BE VISIBLE ON AP
110530A26414  12 10.20JT  8759   2.9 0  R USG0
110530A26414  13 11.30JT  8643   7.0 0  R URG1 MOSS; ENDS AT 14
110530A26414  14 11.45JT  6556   6.0 0  R CRG1
110530A26414  15 12.05JT  7271  11.9 1  R URG  MOSS
110530A26414  16 13.40JT 13078   3.8 0  R USG0
110530A26414  17 13.86JT 20015   1.5 0    USG0
110530A26414     13.90    90 0                EOL
33
33 PHOTO-S5-30 LINE B
110530B15500  11  0.72FZ 25787 23.0 2  R URG
110530B15600  18  1.70JT 15786   6.1 0  R SSG2 MOSS; ENDS AT 11 & 6
110530B15600  19  2.75JT 33281   1.1 0    PSG0
110530B15600  20  3.09JT 32832   2.9 0    SSG1 ENDS AT 11
110530B15600  21  3.75FZ 15976 24.5 2  R USG  MOSS;SPANS:3.3-4.2; NARR
33 20CM ZONE TO E & W; ZONE LESS CLEAR DUE W
110530B15600  22  4.60JT 15882   7.9 0    SSG0
110530B15600  23  5.85JT 14679   7.5 1    URG  BRAIDED; EN PASSENT
110530B15600  24  6.23JT 16374   1.0 0  R SSG1 MOSS; LEFT LAT. SPLAYS A
33 ENDS AT 11; CROSS JTS BETWEEN MESOSCOPIC SPLAYS
110530B15600  25  7.42JT 13457   4.2 0  R PRG1 MOSS; E END RT. LAT. SPL
33 AT 11
110530B15600  26  8.36FZ 15785 15.0 2  R PSG  MOSS;SPANS:7.7-9.03
110530B15600  27  9.26JT 16175   3.1 2  R USG  MOSS
110530B15600  28  9.75JT 33585   2.0 0  R CSG1 MOSS; DIP SHIFTS FROM N
33 END; ENDS AT 11
110530B15600  29 11.00JT 15580   4.2 0  R URG0
110530B15600  30 11.55JT 20847   4.0 1  R CSG  MOSS; ENDS AT 29
110530B15600  31 13.13JT 16684   1.2 1    CSG
110530B15600  32 13.13JT 21347   3.0 0  R CSG2 ENDS AT 11 & 33
110530B15600  33 13.95JT 15567   1.3 2  R PRG
110530B15600  34 14.25JT 16774   0.6 1    PSG
110530B15600  35 14.55JT 21677   3.2 1  R URG
110530B15600  36 14.74FZ 16171   0.9 1    PSG  SUBPAR. JTS
110530B15600     15.00    90 0                EOL
```

STOP 36

```
33 STOP 36 PHOTO-S6-14  LINE A
110614A04809   1  0.14JT 23375   1.4 0    USG0 ROCK TYPE: FINE GRAINED
33 (1-2mm) WITH Q PHENOCRYSTS(5-6mm)
110614A04809   2  1.39JT  7282   6.2 1  R USG  SPLAYS AT N END
110614A04809   3  1.55JT 17890   1.9 1    URG  ENDS AT 2
110614A04809   4  2.96JT 22675   0.7 1    URG
110614A04809   5  3.44JT  7779   2.9 0    PRG0 MOSS
110614A04809   6  6.12JT  4360   5.7 0    CRG1
110614A04809   7  7.05JT  6068   2.0 0    URG1
110614A04809   8  7.49JT 22975   5.3 1    URG
110614A04809   9  8.15JT  4588  10.7 2  R URG  MOSS
110614A04809  10  8.79JT  4381   3.2 0    PSG0 SPLAYS AT BOTH ENDS
110614A04809  11  9.32JT 21877   4.0 0    CRG0 EN ECHELON AT N END
110614A04809  12  9.62JT  3479   9.0 0  R URG2 MOSS;SPLAYS AT S END
110614A04809  13 11.20FZ 22067   9.1 1  R CSG  MOSS; SPANS:11.0-11.39;B
```

Appendix A

```
33 WIDENS AT N END; LEFT LAT. SPLAYS AT SCAN LINE
110614A04809  14 12.05JT 22376  1.9 0    PSG0
110614A04809  15 12.60JT 213 8  3.4 1    PSG
110614A22817  16 13.43JT 22775  2.0 1    PSG
110614A22817  17 13.93FZ 22065  6.0 2  R USG  SPANS:13.8-14.05;BRAIDED
110614A22817     14.20    90 0              EOL
33
33 PHOTO-S6-14  LINE B
110614B10505  18  0.23JT 30264  3.0 1    PSG  STR. SPLAYS AT SW END
110614B10505  19  1.34JT 33167  2.9 1    USG  SPLAY FROM 20
110614B10505  20  1.80FZ 31283 11.2 2  R P-G  MOSS;SPANS:1.7-1.9; MAJO
33 FRACTURE; MOST OF TRACE MOSS COVERED
110614B10505  21  2.75JT 31776  8.0 0    PRG1 Q AT W END
110614B10505  22  3.37CN 30480      2    PSA  SPANS:3.3-3.43
110614B10505  23  3.67CN 30480      1    PSA  SPANS:3.65-3.69
110614B10505  24  3.80JT  4184  3.1 0    PRG1 ENDS AT 20
110614B10505  25  3.86JT 14387  1.2 0    PRG1
110614B10505  26  5.04JT 14581  1.9 0    PRG0
110614B10505   6  5.10JT  4042  4.0 0    PRG1 ENDS AT 26; 20CM RT. LAT
33 N END
110614B10505  27  5.90JT 13451  1.7 0    USG1 ENDS AT 6
110614B10505  28  6.58FZ 12662  5.0 0    PSG0 SPANS: 6.18-6.98
110614B10505   8  6.80JT 22975  5.3 1    URG
110614B10505  29  6.98JT 12789  2.7 0  R URG2 ENDS AT 6 & 11
110614B10505   9  8.20JT  4588 10.7 2  R URG
110614B10505  30  8.60FZ 31971  7.5 0    PRG1 NARROWS TOWARD E; SPANS:
110614B10505  31 10.10CN 13852      1    URF  4CM WIDE
110614B10505  32 11.05FZ 31765  6.0 1    PSG  SPANS:10.9-11.2; DISCONT
33 SUBPAR
110614B10505  12 12.00JT  3479  9.0 0  R URG2
110614B10505  33 13.25CN 31031      1      M  PEG. ALONG UPPER SURFACE
33 PEG 5-15CM THICK; Q XTALS UP TO 6CM;12 ENDS AT 33;SPANS:12.75-13.8
110614B10505  34 13.69FZ  9884  7.1 2  R PRG  SPANS:13.6-13.77; SMALL
33 LAT. SPLAYS AT NE END
110614B10505  35 13.87JT  5869  2.6 0  R CSG3 SPLAY FROM 34
110614B10505  36 14.40JT 15281  1.0 0    CSG1 ENDS AT 35
110614B10505  37 15.58FZ 32564  8.1 1  R PRG  SPANS:15.45-15.70 MOSS
110614B10505  38 15.75JT  5377  4.0 1  R PRG  MOSS
110614B10505     16.00    90 0              EOL
33
33 STOP 36 PHOTO-S6-01 LINE A
110601A17000   1  0.42JT 14639  1.2 0  R PSG1
110601A17000   2  0.70JT 14843  1.4 0  R USG1
110601A17000   3  1.25JT 17921  0.9 1    USG
110601A17000   4  1.95JT 24077  1.6 1    USG
110601A17000   5  2.93FZ 33074  8.6 2    U-G  SPANS:2.5-3.35 ; BRAIDED
110601A17000   6  3.27JT  5086  5.2 1  H PSG  1CM FeO HALO EITHER SIDE
110601A17000   7  3.42JT 23379 15.2 0  H PSG0 MOSS; STR. SPLAYS BOTH E
33 SAME HALO AS 6
110601A17000   8  4.98JT 14786  1.0 0    PSG0
110601A17000   9  5.05JT 23689  5.1 1    PSG  MOSS
110601A17000  10  5.14FZ 32387  2.7 0  H PSG1 MOSS; 5CM WIDE FZ;EN ECH
33 LENSOID FeO INFILL
110601A17000  11  5.95JT 32872  2.1 0  R PSG1 ENDS AT 7; STR. SPLAY AT
110601A17000  12  5.95FZ  5681 13.0 1  H PSG  5CM WIDE FZ; EN ECHELON;
33 LENSOID FeO INFILL; FORMS FACE AT NW END OF OUTCROP
110601A17000  13  6.55JT 17363  1.3 0    PSG1 SPLAY END AT SCAN LINE
110601A17000  14  6.89JT 16850  4.8 0    USG2 ENDS AT 7; PHOTO S8-3
110601A17000  15  7.08FZ 24086 12.5 0  H USG1 MOSS; SPANS:6.9-7.25; Fe
33 BOTH SIDES OF FRACTURE; SLIGHT CW BEND AT N END
110601A17000  16  8.10JT 17363  1.2 0    PSG0
110601A17000  17  8.28JT 16969  1.3 0    PSG0
```

Appendix A

```
110601A17000  18  8.50JT 17268  1.1 0    PSG0
110601A17000  19  8.65JT 17167  1.1 0    PSG0
110601A17000  20  8.77JT 16765  3.6 1  R CSG
33
33 LINE A CONTINUES ON PHOTO-S6-00
33 PHOTO-S6-00 LINE A
110600A17000   1  9.20JT 17585  1.1 1    PSG
110600A17000   2  9.66JT 17069  3.2 1  R USG  MOSS; STR. SPLAY AT E EN
110600A17000   3 10.76FZ 16563  2.6 1  H PSG  CLOSE SPACED Fe FILLED
33 DISCONTINUOUS JTS; SPANS: 10.73-10.80
110600A17000   4 10.85FZ  6366  4.5 1 HR USG  12CM OF LEFT LAT. SLIP O
110600A17000   5 11.88JT 16363  2.6 0    PSG0
110600A17000   6 11.90JT  4678  7.8 0  R SSG1 MOSS
110600A17000   7 12.30FZ 16068  3.0 0    CRG0 SPANS: 12.28-12.32; MOSS
110600A17000   8 12.80JT 15450  1.1 0    SRG1 MOSS
110600A17000   9 13.34FZ 16957  8.1 2    PSG  MOSS; SPANS: 13.27-13.40
110600A17000  10 13.90JT 27090  1.5 0    CSG2 ENDS AT 9; S END SPLAYS
33 OBTUSE ANGLE
110600A17000  11 14.58JT 14868  2.0 0    PSG0 RT. LAT. SPLAYS AT SW EN
110600A17000     15.00    90 0                  EOL
33
33 PHOTO-S6-01  LINE B
110601B07900  21  0.41JT  8064  0.9 1    PSG
110601B07900  22  0.46CN  8664  4.0 2    PRF  1CM FELSITE DYKE
110601B07900  23  1.35FZ 29974  4.9 2  R USG  JOINS 5; SPANS:1.1-1.6
110601B07900  24  2.00JT 22082  1.2 2 RH PRG  SLIGHT FeO INFILL
110601B07900  25  3.35JT  4380  1.5 0    PSG0  RT. LAT.SPLAYS AT SCAN
110601B07900  15  3.86FZ 24086 12.5 0  H USG1
110601B07900  12  4.35FZ  5681 13.0 1  H PSG
110601B07900  11  4.90JT 32872  2.1 0  R PSG1
110601B07900   7  5.42JT 23379 15.2 0  H PSG0
110601B07900   6  5.60JT  5086  5.2 1  H PSG
110601B07900  26  6.65JT  4869  3.1 0  R URG0 MOSS
110601B07900  27  7.63JT  5384 13.0 1    USG  MOSS
110601B07900  28  8.40JT  5284  3.2 1  R PSG  MOSS; COVERED BY RUBBLE
33 LINE ; SPLAY FROM 29
110601B07900  29  8.80FZ  6676 10.0 2  R U-G  SPANS:8.4-9.2
110601B07900  30  9.60JT  5777  1.0 2  R PRG
110601B07900  31 10.80JT  8157  1.1 2  R CSG
110601B07900  32 11.67FZ  5775  7.0 2  R PRG  10CM WIDE ZONE; FAULT WI
33 RT. LAT. COMPONENT
110601B07900  33 12.27JT 22888  0.8 0    PSG0
110601B07900     12.50    90 0               EOL
33
33  STOP 36 PHOTO-S6-24  LINE A
110624A02010   1  0.40JT  5885  2.1 1    SSG
110624A02010   2  0.55JT 31860  2.2 0  R URG1 ENDS AT 5
110624A02010   3  0.71JT  6578  1.5 0  R USG1 ENDS AT 2
110624A02010   4  1.20FZ 32863  1.9 0    PSG2 SPANS:1.0-1.4 ; DISCONTI
33 JTS; SPACING 2-10CM
110624A02010   5  2.62FZ 24587 10.0 2  R CRG  SPANS:2.54-2.80 ; MOSS
110624A02010   6  3.05JT  9436  1.4 0  R USG0
110624A02010   7  5.78JT 21984  2.5 0  R URG0 NUMEROUS LEFT LAT. SPLAY
33 SCAN LINE AND N END; MOSS
110624A02010   8  5.92JT 30879  1.9 0  R USG2 MOSS
110624A02010   9  6.52JT 31574  2.3 0  R CSG0 MOSS
110624A02010  10  8.43FZ 25884 10.0 2  R URG  MOSS; SPANS:8.2-8.65
110624A02010  11  8.97JT   090  1.5 0  R CSG0
110624A02010  12  9.28JT  6887  4.1 0  R USG3 SPLAY FROM FRACTURE ZONE
110624A02010  13  9.65JT 18290  5.5 0  R USG1
110624A02010  14 10.45JT 24584  1.8 0  R PSG2
110624A02010  15 10.50JT 30090  4.7 0  R SRG1 MOSS; ENDS AT 13
```

Appendix A

```
110624A02010  16 12.60JT 30369  5.1 0  R USG1
110624A02010  17 13.74JT  3854  1.4 0  R PSG1 LEFT LAT. SPLAYS AT SCAN
110624A02010  18 17.21JT 32046  4.4 0    USG0 MOSS; EN ECHELON
110624A02010     17.70    90 0                EOL
33
33 PHOTO-S6-24 LINE B
110624B13609  19  0.90JT 32268  1.3 0    PSG2
110624B13609  20  1.85JT 10347  1.4 0  R CRG1 MOSS
110624B13609  21  2.50JT  7384  2.0 0  R PRG0 MOSS
110624B13609  22  2.89JT 12284  1.8 0  R CSG1
110624B13609  23  3.15JT 31372  1.2 0  R PRG0 STR. SPLAYS AT W END
110624B13609  24  4.50JT 18889  0.9 0    PSG1
110624B13609  25  5.67JT 23677  3.0 0 RH USG0
110624B13609  10  6.45FZ 25884 10.0 2  R URG
110624B13609  12  6.60JT  6887  4.1 0  R USG3
110624B13609  15  6.80JT 30090  4.7 0  R SRG1
110624B13600  13  7.10JT 18290  5.5 0  R USG1
110624B13600  26  9.10FZ 32282 10.3 1  R PSG  SPANS: 8.9-9.3; ENDS AT
33 SW END COVERED BY MOSS
110624B13600  27  9.66JT 10361  0.6 1  R CRG  MOSS
110624B13600  28 10.26JT 18337  2.3 0    PSG1 ENDS AT 26
110624B13600  29 10.69JT 12290  3.8 0  R CRG2 MOSS; ENDS AT 10
110624B13600  30 10.74JT 35587  4.0 0  R URG1 MOSS
110624B13600  31 12.00JT 27585  3.6 1  R PRG  MOSS; ENDS AT 26
110624B13600     12.00    90 0                EOL
33
33 STOP 36 PHOTO-S6-10 LINE A
110610A33902   1  0.50FZ 12867  4.6 1  R PSG  FZ: 3CM WIDE
110610A33902   2  0.85JT 12755  4.0 2  R PRG
110610A33902   3  1.08JT 12572  1.2 2  R PSG  SPLAY FROM 2
110610A33902   4  1.37JT 14062  1.2 2  R PSG  SPLAY FROM 2
110610A33902   5  1.87JT 13175  2.0 2  R URG
110610A33902   6  2.25JT 11780  3.0 1  R PRG
110610A33902   7  2.90FZ 12668 14.0 2  R CSG  SPANS:2.35-3.45; SPACING
33 IN ZONE
110610A33902   8  3.65JT 35184  1.2 0  R PRG1 ENDS AT 9
110610A33902   9  4.17FZ 12766  3.0 2  R PSG  SPANS:4.07-4.27; MUSCOVI
33 BEARING PEG. IN GRANITE
110610A33902  10  4.98JT 13586  2.0 0    USG0 MUSCOVITE BEARING PEG. I
110610A33902  11  5.16JT 14066  4.0 1  R PSG  MUSCOVITE BEARING PEG. I
110610A33902  12  5.52JT 31889  2.1 0  R PSG0
110610A33902  13  5.69JT 13885  1.2 0  R PSG0
110610A33902  14  6.48JT 14567  2.0 0  O CSG1 INFILL OF GARNET AND MUS
33  PHOTO S8-4 ANDRADITE GARNET & SAMPLE S6-10-14
110610A33902  15  7.13JT 14767  4.0 2  R USG
110610A33902  16  7.37JT  1656  3.0 1  R PSG  MOSS ; ENDS AT 15
110610A33902  17  7.63JT 13576  3.0 1  R SSG
110610A33902  18  9.10FZ 13768  5.0 1  R PSG  SPANS:8.5-9.7
110610A33902  19 10.18JT 31683  5.0 1  R CSG  RT. LAT. SPLAY AT W END
110610A33902  20 11.70JT 14281  2.0 1  R U-G
110610A33902     15.00    90 0                EOL
33
33 PHOTO-S6-10  LINE B
110610B05500  21  2.15FZ 10190  4.5 1  R USG  ENDS AT 18; SPANS:1.75-2
110610B05500  22  5.38JT 20787  1.2 1  R PSG
110610B05500  23  7.40JT 20480  3.0 1  R USG
110610B05500  24  7.60JT 11140  2.1 2  R P-G
110610B05500  25  8.45JT 11854  2.2 0  R PSG2 MOSS; SPLAY AS IS 24;END
110610B05500  26  9.19FZ 20384  3.0 2  R PSG  MOSS;SPANS:9.0-9.37; SPA
33 ZONE:5CM
110610B05500  27 10.82JT 20667  2.4 1    PSG  MOSS
110610B05500  28 12.59FZ 20790  2.1 2  R CSG  MOSS; SPANS:12.40-12.77;
```

Appendix A

```
33  10-20CM
110610B05500     13.45    90 0                EOL


STOP 38

110628A13400   1  0.14JT 20080  1.8 1    PSG
110628A13400   2  0.50JT 15487  4.4 1    PSG
110628A13400   3  0.57JT 15082  3.1 1    PSG  ESTIMATED DIP. JOINS 2 W
33                                             SHORT CROSS JT. WITH SAME
33                                             ORIGIN   AS 2
110628A13400   4  1.32JT 31478  3.9 0    USG1
110628A13400   5  1.40JT 15880  2.9 1    PSG  EN PASSANT LEFT
110628A13400   6  1.50JT 30370  1.6 0    PSG2
110628A13400   7  1.97JT 32735  2.1 0    PSG0 ESTIMATED DIP
110628A13400   8  2.20JT 12490  1.1 0    USG0 VARIABLE DIP plus or min
33                                             FROM VERTICAL
110628A13400   9  2.33JT 33070  2.4 0    PSG3 EN ECHELON LEFT
110628A13400  10  2.54JT 33270  4.0 1    PSG  EN ECHELON LEFT
110628A13400  11  2.92JT 32576  4.0 1    USG  SPLAY FROM 12
110628A13400  12  3.19JT 32371  6.0 2    USG
110628A13400  13  3.35JT  9668  0.9 0    PSG1
110628A13400  14  3.56JT 30265  1.2 0    USG3
110628A13400  15  3.76JT 12788  0.8 0    PSG1
110628A13400  16  4.61JT 34175  1.2 0    CSG3
110628A13400  17  4.72JT 32569  4.1 1    USG
110628A13400  18  4.78JT 26082  5.5 1    USG  NUMEROUS RIGHT LATERAL S
33                                             ALONG E SIDE
110628A13400  19  4.80JT 33462  0.8 0    CSG3
110628A13400  20  5.03JT 33652  0.8 0    CSG1
110628A13400  21  5.60JT 26073  5.0 1    CSG
110628A13400  22  5.70JT 16073  1.7 0    PSG3
110628A13400  23  5.76JT 15881  1.3 0    PSG3
110628A13400  24  5.90JT 26685  2.3 1    USG
33
110628A13419  25  6.08JT 34138  0.7 0    PSG1
110628A13419  26  6.45JT 18888  1.2 0    CSG3
110628A13419  27  7.01JT  2085  5.4 1    USG
110628A13419  28  7.38JT 29885  0.9 0    PSG2
110628A13419  29  8.30JT  25 9  2.5 0    URG1 EXFOLIATION
110628A13419  30  8.73JT 34037  1.2 0    PSG0
110628A13419  31  9.52JT 34873  0.9 0    SSG0 STEPS LEFT
110628A13419     10.00    90 0                 E.O.L
33
33
33
110628B06826  32  0.35JT 22064  1.4 2    PSG  BRAIDED DISCONTINUOUS JO
110628B06826  33  0.53JT 22972  1.0 2    PSG
110628B06826  34  0.73FZ 22581 13.0 2    USG  0.60 - 0.85. Moss filled
33                                             outcrop faces NW & SE parallel
33                                             joints spacing 5 cm with 1 cm
33                                             spaced oblique cross-joints:
33                                             str 102 dip 90. May be left
33                                             lateral tension gashes.
110628B06826  35  1.38JT 21988  1.7 0    PSG3
110628B06826  36  1.59JT  2781  1.3 1    CSG
110628B06826  37  1.74JT  4579  7.0 1    USG
110628B06826  38  1.74JT  7283  1.5 0    PSG2
33
110628B06803  39  2.34JT  7785  1.6 0    PSG1
110628B06803  40  2.42JT  7681  1.3 0    PSG1
110628B06803  41  2.50JT  7281  2.9 0    PSG2
```

Appendix A

```
110628806803  42  2.60JT 25487  1.8 0    PSG1  EN ECHELON LEFT
110628806803  43  2.75JT 21473  1.3 1    CSG
110628806803  44  4.40JT 25090  6.6 2    USG
110628806803  45  4.93JT  3264  0.8 0    PSG0
110628806803  46  5.07JT  8784  2.3 0    USG0
110628806803  47  6.70JT  5452  0.8 0    PSG0  DISCONTINUOUS SUBPARALL
110628806803  48  7.00JT 20090  2.4 0    USG0
110628806803  27  7.62    90 0
110628806803  21  8.16    90 0
110628806803  49  8.84JT 10589  3.7 1    USG
110628806803  50  9.17JT  9086  1.7 0    USG3
110628806803  51  9.95JT  2374  0.8 0    PSG0
110628806803      10.00    90 0                 E.O.L
33
110631A12300   1  0.16JT 16777  2.5 0    USG2
110631A12300   2  0.21JT  8580  1.5 0    PSG0
110631A12300   3  0.23JT 16260  0.6 1    PSG
110631A12300   4  0.30JT  8583  1.7 1    PSG
110631A12300   5  1.17JT 14362  2.3 0    USG1
110631A12300   6  2.05JT 13766  4.0 2    PRG
110631A12300   7  2.23JT 18066  1.7 0    CSG3
110631A12300   8  2.70JT 15885 12.1 1    USG
110631A12300   9  2.80JT  8584  1.7 0    PSG1
110631A12300  10  3.18JT 18880  1.1 0    PSG3
110631A12300  11  3.35JT  8579  3.4 1    PSG
110631A12300  12  3.94JT 19370  3.3 0    USG1
110631A12300  13  4.60JT 34858  4.0 1    CSG
110631A12300  14  4.88JT 25282  1.2 0    PSG1
110631A12300  15  6.06JT 15051  2.0 0    PSG0
110631A12300  16  6.71JT 15761  4.3 0    USG2
110631A12300  17  7.20JT 15351  1.3 0    URG1
110631A12300  18  7.87FZ 12054  7.0 1KHR USG  7.80 - 7.95. ALTERED BRE
33                                           ZONE. STRIKE AND DIP VARIABLE
110631A12300  19  8.26JT 14377  0.9 0    USG2
110631A12300  20  8.48JT 13083  2.9 0    USG1
110631A12300  21  8.65JT  3090  2.0 0    USG2
110631A12300  22 10.14JT 12981  2.7 0    PSG2
110631A12300  23 10.28JT 13084  2.3 0    USG0
110631A12300      10.50    90 0                 E.O.L
33
110631B19519  24  0.10JT 19170  0.9 0    PSG0
110631B19519  25  0.17JT  3178  1.5 1    USG
110631B19519  26  0.63JT 21485  2.0 1    CSG
110631B19519  27  0.75JT 14357  2.6 0  H USG2
110631B19519  28  1.30JT  6958  1.3 0    PSG0
110631B19519  29  1.58JT 23276  2.4 0    SSG0 ESTIMATED DIP
110631B19519  30  2.11JT  3135  1.5 0    USG2
110631B19519  31  2.27JT 16188  1.8 1    USG
110631B19519  32  2.80JT 21488  3.5 0    USG2
110631B19519  33  3.18JT 19486  3.3 0    USG0
110631B19519  34  3.37JT  1579  2.4 0    USG1
110631B19519  35  3.91JT 16075  2.3 1    PSG
110631B19519  36  4.72JT 21559  1.8 0    PRG1
110631B19519  13  5.37    90 0
110631B19519  37  6.81JT 18870  0.9 0    CSG2
110631B19519  38  7.40FZ 20373 12.0 2    USG   7.05 - 7.75. BRAIDED SM
33                                             JOINTS. SPACING 2 - 6 CM
110631B19519  39  7.93JT 14556  1.1 0    USG1
110631B19519  40  8.67JT 19379  4.4 0    CSG2
110631B19519  41  9.02JT 22282  1.6 0    PSG1
110631B19519  42  9.36JT 30286  2.3 0    CSG2
110631B19519  43  9.55JT 22267  1.8 0    PSG0
```

Appendix A

110631B19519	44	9.67JT	21879	1.7	0	CSG3
110631B19519	45	9.70JT	12184	0.9	0	PSG0
110631B19519	46	9.87JT	21884	3.5	1	PSG
110631B19519	47	10.02JT	9376	1.4	1	USG
110631B19519		10.50	90	0		E.O.L

STOP 39

110633A12404	1	0.57JT	16044	3.1	1	SSG
110633A12404	2	0.66JT	27081	3.0	1	PSG
110633A12404	3	0.93JT	28580	2.2	0	PSG3
110633A12404	4	0.94JT	373	1.1	0	USG3
110633A12404	5	2.40JT	14061	2.5	2	USG
110633A12404	6	2.72JT	15069	1.8	2	USG
110633A12404	7	2.75JT	14548	2.4	1	USG
110633A12404	8	3.22JT	7785	0.7	0	CSG1
110633A12404	9	3.36JT	34377	0.6	0	PSG0
110633A12404	10	3.40JT	24784	1.8	0	CSG1
110633A12404	11	3.94JT	34464	1.1	0	USG1
110633A12404	12	4.47JT	14063	1.0	0	USG0
110633A12404	13	4.60JT	23783	3.2	0	USG2
110633A12404	14	4.83JT	13050	0.7	0	PSG3
110633A12404	15	5.20FZ	15669	17.1	2	USG FAULT BRECCIA ZONE 10 CM
33						FRAGMENTS. NO SLICKS SEEN.
33						EXTENDS W OFF PHOTO
110633A12404	16	5.38JT	18057	2.1	0	USG3
110633A12404	17	6.02JT	14670	1.5	0	CSG0
110633A12404	18	6.13JT	18469	0.8	0	PSG0
110633A12404	19	6.17JT	13374	1.2	0	CSG1
110633A12404	20	6.66JT	8079	0.7	0	PSG2
110633A12404	21	6.83JT	16670	6.3	0	CSG3
110633A12404	22	7.00JT	10390	1.6	0	USG0
110633A12404	23	7.09JT	18183	2.0	0	USG3
110633A12404	24	7.30JT	18767	1.4	0	CSG0
110633A12404	25	7.50JT	18472	2.1	0	USG1
110633A12404	26	7.57JT	11466	0.8	0	PSG0 ESTIMATED DIP
110633A12404	27	8.11JT	18779	2.9	0	CSG1
110633A12404	28	8.11JT	27982	0.8	0	PSG0
110633A12404	29	8.25JT	35066	1.1	0	PSG3
110633A12404	30	8.70JT	18356	2.4	0	USG0
110633A12404	31	9.00JT	18859	3.0	0	PSG1 DIFFUSE EN ECHELON RIGHT
110633A12404	32	9.73JT	18378	0.8	0	PSG0
110633A12404		10.00	90	0		E.O.L
33						
110633B21600	33	0.55JT	33078	1.3	1	PSG
110633B21600	34	0.85JT	22232	1.6	0	PSG1
110633B21600	35	0.95JT	17633	1.9	1	USG
110633B21600	36	1.30JT	22450	1.3	0	PSG1
110633B21600	37	1.52JT	24580	1.5	0	PSG0
110633B21600	38	1.79JT	24290	1.3	1	USG VARIABLE DIP Plus or Min
33						FROM VERTICAL
110633B21600	39	2.07JT	22544	0.8	0	PSG1
110633B21600	13	2.33	90	0		
110633B21600	11	2.77	90	0		
110633B21611	10	2.84	90	0		
110633B21611	40	3.07JT	24568	1.6	0	PSG1
110633B21611	41	3.30JT	12342	0.9	0	CSG0
110633B21611	42	3.62JT	24078	1.9	0	PSG2
110633B21611	43	4.17JT	20645	0.7	0	PSG1
110633B21611	44	4.28JT	23563	1.9	0	PSG2
110633B21611	45	4.33JT	22746	1.3	0	PSG3

Appendix A

```
110633821611  46  4.62JT 19383  0.8 1    PSG
110633821611  47  5.20JT 15275  4.0 0    USG2
110633821611  15  5.55    90 0
110633821611  21  5.82    90 0
110633821611  48  6.27JT 19368  1.9 1    CSG
110633821611  49  6.64JT 17488  2.8 0    CSG3
110633821611  50  7.22JT 16339  1.8 0    USG0
110633821611  51  7.94JT 15467  1.0 0    PSG1
110633821611  52  8.04JT 19462  3.2 1    CSG
110633821611  53  8.16JT 18358  1.5 0    CSG0
110633821611  54  8.70JT 22452  1.9 1  H CSG  DIFFUSE DISCONTINUOUS MI
110633821611  55  9.08JT  1469  1.4 1    PSG
110633821611  56  9.33JT 21361  1.9 0    PSG1
110633821611  57  9.42JT 21061  1.8 0    PSG1
110633821611  58  9.58JT 21165  1.7 0    PSG1
110633821611  59  9.64JT 35672  2.3 2    PSG
110633821611  60  9.81JT 21258  2.5 0    PSG1  PARALLEL SHORT JOINTS S
33                                              1 CM. MAKE UP 3 CM ZONE.
110633821611  61 10.00JT 21860  2.3 0    USG1
110633821611     10.00    90 0                    E.O.L
```

Appendix B Regional Water Chemistry Data

Surface Waters

Sample ID	Mg mg/l	Na mg/l	K mg/l	Ca mg/l	SO4 mg/l	Alk mg/l	pH	Cl mg/l
RP2	0.2	5.3	0.12	0.4	2.6	0.0		8.4
WH3040	0.7	5.5	0.29	1.8	2.4	3.5		10.2
RP3040	1.6	40.8	0.52	4.6	5.4	0.0		74.6
P07	1.4	50.1	1.19	6.8			5.86	
P11	1.8	86.8	2	8.5			5.73	
P13	0.5	3.71	0.27	1.3			5.5	
P14A	0.5	4.08	0.28	1.8			5.6	
P14B	0.6	5.86	0.36	1.4			5.18	
P25	0.5	3.12	0.39	1.2			5.52	
P33	0.5	4.1	0.3	1.1			5.57	
P34	0.5	4.08	0.32	1.7			5.7	
P37	0.3	2.8	0.3	0.7			4.56	
P40	0.5	4.2	0.3	1.3			4.72	
P42	0.6	3.9	0.4	1.3			5.63	
P44	0.5	3.4	0.4	1			4.43	
P50	0.6	3.8	0.4	1.4			5.1	
P62	0.4	2.8	0.3	1			4.45	
P64	0.5	8.2	0.3	1.4			4.75	
P85	0.4	7.3	0.3	1.3			4.7	
P136	0.5	4.4	0.3	1.3			5.1	
P137	0.4	3.6	0.3	1.1			4.7	
P173	0.8	9.2	0.31	1.5			5.77	
P174	0.4	3	0.4	0.7			5.13	
P174-1	0.55	5.1	0.12	0.51				
P174-2	0.57	4.73	0.11	0.68				
P174-3	0.56	4.76	0.11	0.58				
P174-4	0.58	4.76	0.11	0.73				
P174-M	0.61	5.08	0.11	0.85				
P175	2	173.6	0.95	11.1			6	
P176	0.6	9.4	0.4	1.7			5.5	
P176-1	0.53	9.05	0.28	1.07				
P177	0.5	5.6	0.4	1.1			4.9	
P177-1	0.59	6.84	0.2	0.71				
P178	0.8	31.9	0.5	2.7			5.14	
P181	0.7	13.1	0.5	1.8			4.4	
P183A	0.4	2.97	0.22	0.8				
P183B	0.4	3	0.4	0.9			3.94	
P184A	0.3	2.5	0.3	0.8			5	
P184B	0.5	3.6	0.3	1.1			5.31	
P186	0.5	3.3	0.4	1.2			4.7	
P213	0.4	3.1	0.3	1			5	
WHALE	0.3	2.3	0.2	0.8			7.8	

Appendix B

S326-1	0.72	7.56	0.11	0.43				
S326-A	0.43	4.23	0.05	0.29				
S326-B	0.52	5.41	0.08	0.24				
S327-1	0.57	4.74	0.11	0.75				
RP3040	1.6	40.8	0.52	4.6				
WH3040	0.7	5.5	0.29	1.8				
RP2	0.2	5.3	0.12	0.4				
H2	0.9	4.5	0.6	6.7				
GP6512	1.1	11.4	0.42	2.2	2.4	3.7		21.2
GP2030	1.1	12	0.42	2.2	2.4	5.0		21.4
GP2	0.6	7.6	0.28	1	2.6	1.1		13
DP8565	3.1	163.2	1.05	15.2	12.7	2.8		278
DP2	0.5	38.9	0.5	1.8	4	<1.0		62.8
BP2	0.4	4.7	0.27	0.9	2.6	1.3		7.6
BP1-1	1.92	15.18	0.54	8.79				
BP1515	1.1	10.1	0.37	3.2	2.4			19.6
PPLAKE	1.1	5.3	0.2	0.9	2.4	3.9	4.64	0.5
GPLAKE	1.4	14.5	0.4	3	2.6	7.8	6.04	1.3

Appendix B

Groundwaters

Sample ID	Mg mg/l	Na mg/l	K mg/l	Ca mg/l	SO4 mg/l	Alk mg/l	pH	Cl mg/l
CB003	3.7	23.1	0.9	71.9	11	146.22	7.52	72.3
CB007	2.8	9.9	0.5	39.2	8	127.32	7.65	18.4
CB010	9.2	71.5	1.3	35.9	6.6	14.79	5.7	192
CB014	4.9	19.4	0.6	27.6	13.8	100.63	6.92	26.8
CB017	2.1	8.5	0.7	26.9	5.6	86.66	7.35	12.3
CB020	3.6	82.4	1.3	7.6	16.6	2.26	4.82	81
CB024	2.5	118.7	1.9	11.9	7.5	275.19	9.05	55.8
CB028	6.1	21.8	1.4	20.7	12	50.52	6.16	48
CB031	4.4	11.7	0.8	10.5	11.2	22.18	6.05	25
CB034	4.5	15.3	1.7	47.7	5.2	145.81	7.63	34
CB038	0.1	123.9	0.2	0.6	9.9	277.2	9.94	19.6
CB041	2.8	11	0.7	42.3	6.5	6.16	5.27	23
CB044	8.3	18.3	1.1	17.7	13.8	17.25	5.71	49.3
CB047	3.4	8.8	0.7	24.7	14.7	33.27	7.15	14.9
CB050	4.7	8.3	2.3	9.1	15	0.8	4.5	18.6
CB053	5	35.3	1.2	46.1	12	42.71	6.89	69
CB058	15.9	51.4	3.6	41.7	126.5	4.11	4.88	111.5
CB062	2.9	13.7	0.7	29	15	38.2	6.59	14.4
CB066	1.4	7.7	3.5	12.1	7	17.25	5.78	12.4
CB069	9.3	32.4	3.1	17.6	12	3.29	5.11	97.5
CB072	3.8	23.9	3.7	10.7	12.3	2.46	4.44	44
CB076	4.7	10.1	1.4	38	14.7	58.73	7.24	13.1
CB079	5.2	8.4	1.1	15.2	15.6	25.05	5.85	12.9
CB082	4.9	10.3	1.2	31.4	9.8	48.06	7.21	20
CB087	10.9	12.1	1	53.2	5.5	47.64	7.53	73
CB091	0.2	88.3	0.5	1.6	5.7	96.93	9.8	11.7
CB094	0.1	100.1	0.4	1.3		115.83	9.12	10.1
CB097	3.9	9.1	1.4	21.2	4	55.86	6.98	11
CB101	6.5	31.2	0.9	36.1	26	83.79	7.04	68.7
CB105	3.5	10.8	1.6	27.6	16.6	87.9	7.2	17.6
CB109	4	19.9	0.9	8.6	4.2	22.18	5.31	34
CB112	3.6	13.1	1	11.5	4.2	41.07	6.15	26.6
CB116	2.5	58.3	1.2	20.7		204.55	9.05	34.8
CB120	2.5	21.7	1.2	32	7.8	137.6	7.83	10.8
CB123	0.9	7.5	0.5	3	4.2	10.68	4.8	10.4
CB127	7.9	15.8	1.6	68.9	39.3	94.47	6.51	78
CB131	5.4	9.3	0.7	45		168.4	7.71	13.2
CB134	4.2	14	2.1	28.4	9.4	111.72	6.64	19.8
CB138	0.7	44.7	0.8	2.3	7.2	108.43	6.24	12.2
CB142	3.5	7.3	0.9	29.5	3.6	103.09	7.65	8
CB145	4.6	32.1	1.1	15.5	8.7	34.91	6.08	71.3
CB149	2.9	30.1	1.1	39	22	108.84	7.49	43.7
CB153	3.1	20	1.2	26.5	5.6	52.78	6.28	41.1

Appendix B

CB157	2.6	7	0.7	25	11.8	77.12	6.4	9.4
H2851	0.8	4.6	0.7	3.4	2.4	11.96	5.04	7.4
H2852	0.6	3.9	0.7	2.9			4.92	6.2
H2853	0.6	3.8	0.7	2.6			5.26	6.2
H2854	0.6	3.9	0.7	2.6	2.6	3.99	5.23	8.8
H2855	0.5	3.2	0.6	2.5			5.23	5.2
H2856A	0.5	3.6	0.7	2.6			4.75	5.2
H2856C	0.6	3.8	0.7	2.5			4.78	5.2
H285B4	1.5	8.2	0.9	18.4	4.2	50.97	7	17.8
H285B5	1.6	8.3	1	18.8	2.6	61	6.1	14.4
H285B6	1.4	8.1	1	17.9	2	59.1	6.03	13.4
H3852	3.7	8.3	0.7	32.5	5.2	127.51		8.2
H3854	3.7	8.4	0.6	32.7	3.8	128.1		7.8
H41	1	4.9	0.5	5.1	3.6	14.2		8.2
H46	1	4.9	0.5	5.2	3.6	13.1		8.4
H418	1	4.8	0.5	5.2	3.6	14		8
H424	1.2	5.3	0.9	9.3	4.2	30.4		9.6
BP1	3.7	7.2	0.5	41.2	2.4	130.3	8.08	18
BP2	3.4	6.7	0.5	38.9	2.4	119.4	8.43	18.6
BP3	3.7	7	0.5	41.5	2.4	129.72	8.6	18.6
BP4	3.1	6	0.4	36.1		113.53	8.48	16.8
BP5	3.3	6.5	0.4	37.9	4.4	120.24	7.83	14.2
H213.4	0.8	4	0.5	7.5				
GPGW	2.9	16.2	1	11.8	1.2	46.3	6.66	1.5
PP1	2.7	7	0.2	43.2	4.1	123.4	7.21	0.4
PP2	3	40.2	3.3	46.4	73.1	138.9	7.44	0.7
PP3	2.6	9.1	0.5	41.5	9.4	123.4	7.2	0.4
NS-1	0.72	50.7	0.41	15.8	5.48	195.2		34.6
NS-2	2.4	12.7	1.05	8.4	4.69	12.2		23
NS-3	0.6	53.8	0.34	10.6	8.6	97.6		32.3
NS-4	2.65	17.7	0.46	42.9	3.9	152.5		7.7
NS-5	2.8	60.5	1.63	33	10	134		65.7
NS-6	3.4	29.1	1.32	33.1	3.33	79.3		63.7
NS-7	4.5	40.9	5.51	53.7	15.8	152.5		57.8
NS-8	13.8	2493	6.51	101.8	45.5	61		4797

Appendix C Analytical Results of Pond Sediment Samples

Gull Pond Surface Lake Sediment Analysis

sample #	x loc	y loc	Cu ppm	Pb ppm	Zn ppm	Mn ppm	Fe %	Mo ppm	Cd ppm	U ppm	LOI %
1001	100	200	14	19	92	544	1.27	8	.9	24.5	34.0
1002	100	300	15	20	81	499	3.20	11	.5	20.8	36.4
1003	100	400	14	17	82	1800	5.10	11	.6	29.6	36.4
1004	100	500	15	21	94	818	2.79	11	.6	21.3	32.2
1005	100	600	14	17	101	817	3.25	11	.6	20.3	34.8
1006	100	700	26	20	88	553	2.07	11	.8	102.0	12.0
1007	200	100	14	31	45	10760	4.62	13	.2	21.0	18.8
1008	200	200	13	17	86	695	1.58	8	.8	23.3	34.0
1009	200	300	15	17	102	5420	5.99	12	.7	20.4	35.4
1011	200	400	15	17	92	941	4.19	13	.6	19.9	34.2
1012	200	500	10	16	77	159	1.10	6	.7	19.2	28.8
1013	200	600	15	19	92	404	1.14	8	1.0	25.7	32.2
1014	300	500	12	13	74	374	1.49	6	.3	23.1	25.6
1015	400	500	21	18	87	503	1.89	8	.5	50.3	12.0
1016	400	600	35	23	177	435	1.69	11	1.5	85.8	31.6
1017	400	900	7	16	72	28600	5.54	20	.6	25.2	12.4
1018	500	500	18	20	127	6100	6.29	16	.9	21.1	33.6
1019	500	600	18	36	140	25100	7.11	11	1.0	18.1	29.8
1021	500	800	7	19	50	9940	4.32	7	<.1	18.3	17.2
1022	500	900	33	14	104	358	.96	11	1.0	65.3	28.6
1023	500	1000	17	23	98	904	1.63	7	.9	21.8	30.8
1024	600	500	17	27	70	660	2.25	7	.6	19.1	41.6
1025	600	600	16	21	87	3790	3.27	9	.8	18.9	38.6
1026	600	1100	16	20	104	486	3.08	11	.6	19.6	33.2
1027	650	1150	25	19	70	463	1.85	9	.2	40.6	3.2
1028	685	800	16	21	121	10270	6.39	10	.9	17.5	35.0
2001	100	650	14	18	93	475	2.19	10	<.1	15.4	37.1
2002	100	700	24	16	110	274	.55	6	1.1	37.0	33.5
2003	150	550	15	14	116	2210	5.19	13	.8	18.0	37.8
2004	150	650	16	20	117	2540	2.41	11	.9	48.1	33.2
2005	150	700	28	13	185	248	.72	6	1.4	62.7	32.6
2006	150	750	21	16	154	548	.77	6	1.1	42.4	34.3
2007	200	800	16	16	138	390	.55	4	.9	26.9	36.5
2008	250	550	15	14	107	281	.79	6	1.0	27.0	35.8
2009	250	750	17	17	139	179	.50	4	1.4	27.0	40.0
2011	300	600	52	18	139	253	1.05	12	1.6	159.0	27.8
2012	350	600	32	17	81	401	1.86	18	.4	71.0	12.7
2013	350	650	31	22	88	501	2.05	14	.3	60.1	7.6
2014	400	550	39	12	139	339	1.50	10	1.2	87.0	34.2
2015	400	650	19	15	149	623	.87	5	1.3	35.4	38.5
2016	450	550	21	26	153	3350	4.86	16	1.1	44.5	30.2

Appendix C

2017	450	600	14	18	108	685	3.16	13	.7	14.6	37.4
2018	450	650	20	15	118	339	1.21	7	1.1	38.9	36.1
2019	500	410	18	22	102	981	3.05	30	.5	18.8	34.8
2021	500	700	21	20	78	593	1.72	21	.2	52.7	2.8
2022	500	450	15	15	134	8800	6.83	14	.8	16.9	36.5
2023	550	550	16	15	134	3440	6.01	11	.7	16.5	38.0
2024	550	650	15	17	107	523	2.39	11	.6	14.9	37.7
2025	550	950	15	18	125	611	1.70	3	.7	16.7	19.2
2026	600	400	18	18	106	435	3.05	13	.9	21.3	40.0
2027	600	600	15	14	103	3480	6.05	11	.6	15.1	41.6
2028	600	900	16	16	141	4400	5.57	11	.9	16.0	37.1
2029	600	1000	15	15	127	3420	5.36	11	.8	16.0	39.3
2031	650	550	15	18	74	789	2.68	10	.6	16.0	44.2
2032	650	650	15	15	81	1500	4.79	10	.6	16.0	42.9
2033	650	750	21	54	138	2780	5.00	11	.8	17.1	39.6
2034	650	850	16	15	67	605	2.08	7	.5	15.5	43.6
2035	650	950	17	15	102	567	3.61	10	.6	16.8	38.2
2036	700	600	15	16	101	686	5.30	11	.6	15.3	39.1
2037	700	700	15	15	115	972	5.77	18	.5	14.9	36.9
2038	700	800	16	16	139	5020	5.21	10	.9	14.0	39.1
2039	700	900	16	17	138	3730	5.14	11	.9	15.0	38.0
2041	700	1000	15	17	102	525	3.73	12	.6	13.4	38.4

Appendix C

Nut Brook Pond Surface Lake Sediment Analysis

sample #	x loc	y loc	Cu ppm	Pb ppm	Zn ppm	Mn ppm	Fe %	Mo ppm	Cd ppm	U ppm	LOI %
1054	25	100	9	33	20	536	1.46	5	.2	39.8	25.6
1055	25	125	13	30	17	65	.38	6	.4	34.8	27.2
1056	50	50	15	46	16	206	.45	10	.4	79.9	32.8
1057	50	75	11	45	27	377	.83	9	.4	76.9	30.4
1058	50	100	10	27	15	145	.63	6	.3	31.9	35.4
1059	50	125	12	23	18	120	.63	4	.2	39.6	34.6
1061	50	150	10	23	4	35	.35	3	<.1	30.8	22.8
1062	50	175	17	34	3	34	.27	3	<.1	46.9	19.8
1063	75	50	16	53	23	372	.66	12	.6	126.0	40.6
1064	75	75	17	44	124	296	1.54	12	1.5	126.0	15.0
1065	75	100	19	41	15	76	.60	7	.3	96.5	26.4
1066	100	50	10	43	35	116	1.21	10	.4	250.0	34.2
1067	100	75	15	53	16	217	.62	9	.5	144.0	30.2
1068	100	100	13	27	5	79	.43	6	.2	51.5	24.4
1069	125	50	15	60	72	272	1.14	13	1.0	233.0	34.8
1071	125	75	21	40	13	104	.56	6	.3	63.9	27.6

Appendix C

Pennys Pond Surface Lake Sediment Analysis

Sample #	X loc	Y loc	Cu ppm	Pb ppm	Zn ppm	Mn ppm	Fe %	Mo ppm	Cd ppm	U ppm	LOI %
25	125	175	4	12	7	20	.60	3	<.1	18.8	13.0
26	75	175	5	15	6	38	.70	4	<.1	31.5	12.1
27	75	125	4	10	5	14	.51	4	<.1	19.1	15.3
28	125	50	8	14	6	18	.30	3	<.1	17.1	22.5
29	100	50	5	12	4	13	.17	3	<.1	17.5	16.5
31	100	75	4	16	7	37	.50	4	<.1	17.5	16.0
34	100	100	5	20	8	<2	1.55	5	<.1	19.5	18.5
35	75	100	4	13	5	29	.49	3	<.1	16.4	17.2
36	50	75	5	11	5	48	.28	4	<.1	22.3	25.0
38	100	125	4	13	7	84	1.13	5	<.1	17.6	15.4
39	50	125	4	16	8	75	.81	4	<.1	22.1	16.2
41	100	150	4	12	4	10	.53	3	<.1	15.9	11.2
42	75	150	4	24	14	76	.85	4	<.1	69.1	11.6
43	50	150	4	15	10	194	.80	5	<.1	28.3	15.1
45	100	175	9	23	19	22	.52	4	<.1	106.0	14.5
46	50	175	5	16	11	102	.58	4	<.1	41.5	16.8
47	150	200	11	26	29	74	1.87	5	<.1	142.0	17.4
48	125	200	9	19	13	33	.70	3	<.1	71.6	13.9
49	100	200	9	34	33	70	1.30	7	<.1	309.0	16.3
50	75	200	3	12	5	109	2.50	5	<.1	17.0	12.3
51	150	225	29	47	15	19	.20	10	<.1	94.7	37.1
52	125	225	4	16	9	89	1.10	6	<.1	25.1	12.4
54	100	225	3	13	5	94	1.00	5	<.1	19.2	12.2
55	75	225	3	15	13	30	.20	7	<.1	31.6	16.9
56	125	250	3	16	5	19	.60	4	<.1	27.5	1.1
57	100	250	4	17	5	23	.70	4	<.1	31.4	11.8
58	75	250	6	18	6	53	.40	4	<.1	30.8	16.3
59	100	275	7	15	4	13	.50	4	<.1	16.5	16.9

Appendix C

Rocky Pond Lake Sediment Analysis

sample #	x loc	y loc	Cu ppm	Pb ppm	Zn ppm	Mn ppm	Fe %	Mo ppm	Cd ppm	U ppm	LOI %
1041	100	500	15	22	83	448	1.32	10	.6	16.0	18.6
1042	200	100	8	15	33	8920	7.46	10	<.1	17.1	15.2
1043	200	200	12	12	23	1260	3.84	6	<.1	7.1	28.6
1044	200	400	15	14	38	467	1.75	7	.4	13.9	34.6
1045	200	500	12	11	44	980	2.28	8	.4	11.6	32.4
1046	200	600	15	18	71	355	1.07	6	.6	11.2	32.0
1047	300	100	11	11	38	1510	1.92	5	.3	8.1	31.8
1048	300	200	8	10	32	943	4.44	6	<.1	15.7	11.2
1049	300	300	24	29	72	449	3.03	3	<.1	41.1	10.8
1051	300	400	14	17	54	920	2.77	9	.4	23.8	34.8
1052	300	500	14	16	48	740	2.33	8	.4	20.5	35.2
1053	400	100	11	22	23	2880	4.18	9	<.1	69.0	16.8
2042	150	150	9	8	36	2390	11.72	14	<.1	6.2	23.5
2043	150	450	12	18	42	7090	4.18	8	.3	8.5	29.7
2044	200	150	11	14	35	6740	4.14	5	.2	7.7	32.8
2045	200	450	13	15	45	527	1.78	5	.2	12.5	37.6
2046	250	100	9	14	39	13350	7.80	10	<.1	9.6	23.6
2047	250	150	11	13	30	2680	9.40	7	<.1	6.5	29.3
2048	250	200	9	9	59	50600	8.43	68	.5	8.1	20.1
2049	250	300	9	27	98	27100	6.27	10	.3	42.2	17.6
2051	250	350	13	11	53	678	2.37	7	.3	9.2	36.9
2052	250	400	14	12	34	584	1.51	5	.2	11.4	39.9
2053	250	450	12	11	50	850	2.30	9	.3	9.6	35.5
2054	250	500	12	9	44	945	2.66	12	.3	14.8	36.7
2055	250	550	11	10	30	539	1.29	4	.2	8.7	36.1
2056	300	150	9	11	38	5090	11.20	11	<.1	6.2	23.8
2057	300	350	13	12	40	945	3.19	9	.2	10.6	37.8
2058	300	450	14	12	31	508	1.09	4	.2	10.0	40.3
2059	350	100	10	12	30	399	4.68	4	<.1	7.8	16.9
2061	350	150	10	12	35	1670	1.87	4	.2	6.2	34.7
2062	350	250	14	16	92	1320	2.38	7	.6	10.0	36.0
2063	350	300	13	14	69	1210	2.37	8	.4	9.5	37.7
2064	350	350	14	11	61	926	3.07	8	.2	9.8	35.7
2065	350	400	12	10	42	995	2.54	9	.2	11.3	36.1
2066	350	450	12	10	40	862	2.24	7	.2	10.9	36.7
2067	350	500	12	10	50	734	2.49	14	.2	9.9	35.8

Appendix D Analytical Results of Lake Sediment Cores

Nut Brook Pond Lake Sediment Analysis
Core DPA (75 75)

#	depth (m)	Cu ppm	Pb ppm	Zn ppm	Mn ppm	Fe %	Cd ppm	Mo ppm	U ppm	LOI %
2242	0.05	17	29	52	513	1.66	0.3	na	na	35.3
2243	0.10	13	32	48	284	2.45	0.2	24	691	36.3
2244	0.15	16	44	40	172	3.55	0.4	49	1110	36.9
2245	0.20	17	47	43	182	3.36	0.3	52	1060	37.1
2246	0.25	17	49	49	167	3.07	0.5	47	na	35.9
2247	0.30	18	50	51	195	3.45	0.5	46	na	41.2
2248	0.35	20	38	57	182	4.39	0.6	69	3080	42.4
2249	0.40	23	46	116	276	5.98	1.2	63	1620	31.9
2251	0.45	29	25	159	423	7.38	1.3	46	985	27.1
2252	0.50	37	43	216	382	8.21	1.7	na	na	27.4

na - no analysis, insufficient sample

Nut Brook Pond Lake Sediment Analysis
Core DPB (50 100)

#	depth (m)	Cu ppm	Pb ppm	Zn ppm	Mn ppm	Fe %	Cd ppm	Mo ppm	U ppm	LOI %
2253	0.05	13	39	50	679	2.70	0.2	8	79.3	na
2254	0.10	11	28	23	252	1.08	0.1	6	62.0	na
2255	0.15	10	31	23	204	0.89	0.1	6	56.8	33.1
2256	0.20	11	32	25	215	0.77	0.2	7	58.7	39
2257	0.25	13	37	28	259	0.59	0.2	8	66.0	41.4
2258	0.30	13	39	28	246	0.55	0.3	9	na	43.4
2259	0.35	14	38	30	279	0.56	0.3	8	68.2	45.3
2261	0.40	15	35	29	251	0.50	0.3	9	72.3	46.5
2262	0.45	14	36	26	217	0.54	0.3	8	62.8	39.9
2263	0.50	16	36	26	208	0.50	0.4	na	74.4	na
2264	0.55	8	19	14	115	0.37	0.1	7	164.0	35.6
2265	0.60	15	40	24	235	0.66	0.2	7	76.2	35.6
2266	0.65	16	43	25	180	0.73	0.2	7	78.1	33.6
2267	0.70	17	36	29	175	0.76	0.2	7	na	31.1
2268	0.75	16	30	52	214	1.01	0.4	9	na	34.3
2269	0.80	18	33	55	191	0.81	0.4	9	na	32.0
2271	0.85	20	35	92	688	1.00	0.8	9	87.9	na
2272	0.90	31	30	162	179	1.08	1.4	11	155.0	28.9
2273	0.95	23	22	74	235	0.88	0.8	11	106.0	41.9
2274	1.00	21	20	60	234	0.93	0.7	12	91.9	na
2275	1.05	20	27	71	237	1.11	0.7	11	na	34.0
2276	1.10	25	28	140	221	1.14	1.2	11	na	31.9
2277	1.15	29	30	148	179	1.12	1.1	17	na	28.4
2278	1.20	29	37	179	118	1.32	1.0	21	na	23.1
2279	1.25	38	37	276	109	1.66	1.6	16	188.0	22.0
2281	1.30	39	35	259	95	3.79	0.8	26	na	23.4
2282	1.35	44	19	124	128	3.01	0.4	26	221.0	na
2283	1.40	37	19	176	126	2.56	0.8	27	223.0	32.3
2284	1.45	44	17	119	119	2.24	0.9	41	270.0	32.9
2285	1.50	46	21	87	106	2.12	1.1	44	303.0	31.4

na - no analysis, insufficient sample

Nut Brook Pond Lake Sediment Analysis
Core DPC (125 50)

#	depth (m)	Cu ppm	Pb ppm	Zn ppm	Mn ppm	Fe %	Cd ppm	Mo ppm	U ppm	LOI %
2286	0.05	11	42	54	411	1.32	0.3	7	181	34.0
2287	0.10	12	44	61	357	1.17	0.2	8	242	34.2
2288	0.15	16	57	63	248	0.84	0.3	8	228	33.7
2289	0.20	18	57	88	252	0.99	0.8	9	363	36.8
2291	0.25	18	49	126	309	1.15	1.3	12	351	42.4
2292	0.30	20	37	136	384	1.17	1.0	16	278	46.5
2293	0.35	22	35	116	393	1.46	1.0	24	458	49.6
2294	0.40	22	49	118	371	1.42	1.0	22	471	41.9
2295	0.45	27	52	211	390	1.53	1.3	28	369	41.8
2296	0.50	27	45	241	312	1.67	1.2	29	341	38.4
2297	0.55	31	43	255	360	2.71	1.7	37	459	na
2298	0.60	39	36	300	208	3.20	2.0	44	858	na
2299	0.65	39	36	169	212	2.92	1.0	30	1220	31.7

na - no analysis, insufficient sample

Gull Pond Lake Sediment Analysis
Core GPA (150 350)

#	depth (m)	Cu ppm	Pb ppm	Zn ppm	Mn ppm	Fe %	Cd ppm	Mo ppm	U ppm	LOI %
2085	0.1	17	12	39	279	1.17	0.5	7	24.0	42.4
2086	0.2	15	8	51	250	1.35	0.4	9	23.6	39.4
2087	0.3	16	11	56	261	1.50	0.5	9	24.8	40.6
2088	0.4	18	12	43	246	1.28	0.5	9	24.9	na
2089	0.5	18	13	64	241	1.20	0.5	9	31.1	42.6
2091	0.6	19	14	60	257	1.21	0.6	8	31.9	39.7
2092	0.7	16	9	56	211	1.04	0.6	9	24.7	36.7
2093	0.8	16	8	72	205	1.00	0.6	8	33.6	36.0
2094	0.9	19	12	93	213	1.04	0.7	7	40.3	39.3
2095	1.0	20	12	85	227	1.03	0.6	7	47.0	38.4
2096	1.1	19	10	81	227	1.23	0.6	8	43.3	37.3
2097	1.2	22	12	100	235	1.46	0.6	8	41.1	40.1
2098	1.3	26	13	94	226	1.03	0.7	7	48.5	40.6
2099	1.4	29	14	117	241	1.10	0.7	8	58.7	39.1
2101	1.5	35	14	133	230	1.24	0.6	10	81.4	36.5
2102	1.6	30	13	111	221	1.20	0.8	9	71.3	37.3
2103	1.7	42	14	115	224	1.27	0.9	10	96.8	36.1
2104	1.8	42	12	86	193	1.08	0.9	12	116.0	32.7
2105	1.9	32	9	73	192	1.22	0.7	21	77.1	27.3
2106	2.0	34	9	72	210	1.23	0.6	26	58.6	24.9
2107	2.1	14	6	34	297	1.39	0.1	1	3.2	0.4
2108	2.2	14	6	34	292	1.29	0.1	2	1.9	0.4
2109	2.3	19	11	46	366	1.49	0.1	17	14.4	1.0
2111	2.4	25	16	60	400	1.99	0.3	32	54.8	7.2
2112	2.5	48	27	74	498	2.22	0.3	27	48.4	8.6

na - no analysis, insufficient sample

Gull Pond Lake Sediment Analysis
Core GPB (100 700)

#	depth (m)	Cu ppm	Pb ppm	Zn ppm	Mn ppm	Fe %	Cd ppm	Mo ppm	U ppm	LOI %
2113	0.1	18	11	119	130	0.60	1.2	4	40.2	31.8
2114	0.2	37	13	167	136	0.61	1.5	6	84.4	31.0
2115	0.3	45	11	85	152	0.71	1.0	11	85.3	na
2116	0.4	37	12	78	186	0.78	0.6	18	73.7	22.7
2117	0.5	29	20	60	369	2.36	0.1	35	47.9	3.8

na - no analysis, insufficient sample

Gull Pond Lake Sediment Analysis
Core GPC (600 600)

#	depth (m)	Cu ppm	Pb ppm	Zn ppm	Mn ppm	Fe %	Cd ppm	Mo ppm	U ppm	LOI %
2118	0.1	22	14	177	1310	3.43	0.9	19	34.9	38.6
2119	0.2	21	12	277	1060	2.96	0.9	16	34.8	37.0
2121	0.3	19	10	191	992	3.03	1.0	17	39.2	30.7
2122	0.4	23	12	237	1270	2.80	1.1	16	43.8	37.2
2123	0.5	24	13	311	1360	2.70	1.1	16	45.6	36.6
2124	0.6	24	13	283	1070	2.35	1.1	15	40.8	37.8
2125	0.7	26	12	315	1050	2.71	1.1	17	46.3	na
2126	0.8	29	13	331	1390	2.34	1.1	14	51.9	39.8
2127	0.9	32	14	249	1400	3.30	1.1	18	61.1	38.8
2128	1.0	38	15	405	1520	3.19	1.2	21	75.1	37.0
2129	1.1	19	25	352	5940	6.28	1.0	12	23.9	39.8
2131	1.2	22	28	327	9450	6.50	1.0	13	32.7	40.0
2132	1.3	25	15	286	2390	4.67	0.9	14	43.1	39.6
2133	1.4	25	14	266	1640	3.54	0.9	16	44.1	37.8
2134	1.5	36	13	187	927	2.15	0.9	20	71.9	31.4
2135	1.6	37	16	108	632	2.02	0.6	32	76.2	20.5
2136	1.7	46	27	108	666	2.55	0.3	28	51.6	8.4
2137	1.8	27	19	75	609	1.95	0.2	37	65.4	4.8

na - no analysis, insufficient sample

Gull Pond Lake Sediment Analysis
Core GPD (650 850)

#	depth (m)	Cu ppm	Pb ppm	Zn ppm	Mn ppm	Fe %	Cd ppm	Mo ppm	U ppm	LOI %
2138	0.1	20	12	270	293	0.96	0.7	6	33.9	41.2
2139	0.2	24	11	259	303	0.94	0.7	6	36.2	na
2141	0.3	27	19	254	273	0.82	0.8	5	47.6	41.7
2142	0.4	24	13	157	294	0.83	0.8	5	47.1	42.3
2143	0.5	31	13	237	298	0.84	0.8	5	58.5	41.1
2144	0.6	40	14	195	273	0.87	0.8	6	77.1	40.0
2145	0.7	46	13	235	249	0.83	0.9	9	105.0	38.0
2146	0.8	38	9	201	214	0.73	0.7	12	70.4	31.5
2147	0.9	31	9	167	217	1.06	0.7	20	73.3	27.6
2148	1.0	43	12	144	245	1.29	0.6	28	84.9	25.3
2149	1.1	30	12	206	274	1.01	0.7	12	51.7	38.1
2151	1.2	37	14	144	299	1.14	0.6	23	71.1	28.3
2152	1.3	42	25	107	498	2.17	0.4	23	40.9	10.8
2153	1.4	28	15	76	406	1.71	0.3	33	59.5	13.1
2154	1.5	29	15	111	407	1.87	0.3	34	54.1	11.2

na - no analysis, insufficient sample

Gull Pond Lake Sediment Analysis
Core GPE (425 600)

#	depth (m)	Cu ppm	Pb ppm	Zn ppm	Mn ppm	Fe %	Cd ppm	Mo ppm	U ppm	LOI %
2155	0.1	19	12	298	457	1.09	1.3	8	30.8	na
2156	0.2	18	11	286	434	1.12	1.1	7	30.8	na
2157	0.3	18	11	258	469	1.14	1.1	8	31.2	36.4
2158	0.4	19	12	269	448	1.10	1.1	8	32.6	36.3
2159	0.5	18	9	238	398	0.91	1.1	6	33.2	35.5
2161	0.6	17	8	282	404	1.03	1.0	6	40.7	33.4
2162	0.7	35	10	307	387	0.91	1.1	5	41.3	34.4
2163	0.8	52	9	349	428	1.05	1.1	5	48.1	33.8
2164	0.9	23	10	310	448	0.99	1.1	5	43.4	35.3
2165	1.0	27	10	347	489	1.23	1.2	5	50.2	35.5
2166	1.1	25	15	333	542	1.39	1.1	8	36.5	36.9
2167	1.2	29	12	349	634	1.77	1.1	10	53.8	37.8
2168	1.3	32	12	376	593	1.63	1.2	10	60.4	35.4
2169	1.4	35	12	346	2920	1.47	1.3	13	69.3	33.9
2171	1.5	225	11	313	2690	1.77	1.4	15	87.5	32.9
2172	1.6	90	12	312	10940	1.58	1.5	23	108.0	32.7
2173	1.7	57	10	220	1730	1.53	1.2	16	119.0	31.9
2174	1.8	42	8	231	973	1.05	1.0	17	78.6	29.4
2175	1.9	35	8	145	619	0.97	0.7	17	63.6	24.0
2176	2.0	37	10	98	560	1.12	0.6	26	63.8	22.4
2177	2.1	38	20	143	585	2.22	0.4	31	83.9	13.2
2178	2.2	33	19	98	484	1.96	0.2	29	51.8	5.4

Rocky Pond Lake Sediment Analysis
Core RPA (250 500)

#	depth (m)	Cu ppm	Pb ppm	Zn ppm	Mn ppm	Fe %	Cd ppm	Mo ppm	U ppm	LOI %
2179	0.1	15	10	71	714	1.56	0.5	10	8.7	34.5
2181	0.2	15	10	80	697	1.62	0.4	10	9.2	35.9
2182	0.3	16	11	93	695	1.79	0.5	11	11.6	35.2
2183	0.4	17	9	94	633	1.60	0.6	10	12.4	35.0
2184	0.5	18	11	87	522	1.54	0.5	10	15.5	34.6
2185	0.6	20	11	85	579	1.43	0.5	11	17.3	33.1
2186	0.7	21	12	82	544	1.52	0.6	13	na	33.2
2187	0.8	23	10	97	490	1.70	0.7	18	26.8	34.5
2188	0.9	23	11	107	420	2.28	0.6	32	26.0	33.6
2189	1.0	22	10	96	386	2.19	0.5	43	26.6	35.3
2191	1.1	22	11	94	401	2.12	0.7	44	25.9	36.3
2192	1.2	25	12	246	369	2.44	4.6	40	47.0	35.2
2193	1.3	27	13	103	395	1.89	1.3	23	211.0	32.2
2194	1.4	34	14	129	397	1.70	1.2	19	317.0	31.0
2195	1.5	44	20	134	381	1.63	1.1	16	449.0	31.1
2196	1.6	66	26	156	355	1.48	2.8	20	449.0	na

na - no analysis, insufficient sample

Rocky Pond Lake Sediment Analysis
Core RPB (400 100)

#	depth (m)	Cu ppm	Pb ppm	Zn ppm	Mn ppm	Fe %	Cd ppm	Mo ppm	U ppm	LOI %
2197	0.2	10	28	169	9410	4.91	0.5	8	29.6	23.8
2198	0.3	6	15	120	5350	3.21	0.3	8	44.7	17.8
2199	0.4	12	17	169	7030	3.72	0.4	14	45.9	18.8
2201	0.5	35	21	208	7490	5.74	0.5	20	54.5	24.8
2202	0.6	48	25	206	2600	6.31	0.1	16	37.4	25.0

Rocky Pond Lake Sediment Analysis
Core RPC (300 400)

#	depth (m)	Cu ppm	Pb ppm	Zn ppm	Mn ppm	Fe %	Cd ppm	Mo ppm	U ppm	LOI %
2203	0.1	16	19	59	569	1.66	0.3	6	16.1	40.0
2204	0.2	15	11	44	488	0.97	0.2	5	8.3	41.4
2205	0.3	14	9	29	411	0.75	0.2	5	7.8	40.6
2206	0.4	16	12	45	382	1.11	0.2	6	12.6	41.0
2207	0.5	13	12	63	312	1.15	0.2	6	18.1	36.9
2208	0.6	14	11	63	311	0.93	0.2	5	13.0	39.6
2209	0.7	16	10	89	283	0.79	0.2	5	10.5	40.6
2211	0.8	16	9	182	282	0.70	0.2	5	8.5	41.1
2212	0.9	17	10	205	281	0.81	0.2	5	12.6	41.6
2213	1.0	17	11	94	285	0.78	0.2	5	10.5	41.5
2214	1.1	16	11	38	303	1.04	0.2	5	10.7	40.5
2215	1.2	16	10	41	360	0.87	0.3	5	9.0	40.5
2216	1.3	16	12	45	361	0.90	0.3	5	10.5	40.9
2217	1.4	19	12	54	392	0.95	0.3	6	14.3	41.4
2218	1.5	22	12	42	421	0.98	0.3	6	15.9	42.9
2219	1.6	21	12	51	408	1.10	0.3	6	18.0	41.3
2221	1.7	23	12	49	366	1.09	0.3	6	18.5	40.2
2222	1.8	24	12	46	318	1.08	0.3	6	21.9	37.1
2223	1.9	23	10	49	325	1.17	0.3	7	27.4	35.7
2224	2.0	22	11	57	329	1.05	0.4	7	29.3	36.6
2225	2.1	16	18	224	537	1.66	0.4	7	19.6	36.9
2226	2.2	20	16	206	450	1.58	0.4	7	25.0	36.8
2227	2.3	18	12	215	384	1.16	0.3	6	24.6	36.1
2228	2.4	23	12	275	418	1.18	0.4	6	26.7	38.2
2229	2.5	26	13	301	485	1.21	0.4	6	34.6	38.8
2231	2.6	36	17	177	1070	1.26	0.5	6	38.6	43.1
2232	2.7	42	16	188	751	1.06	0.5	6	46.8	40.6
2233	2.8	51	17	110	507	0.76	0.5	6	48.3	35.0
2234	2.9	78	25	207	454	0.92	0.5	7	56.6	33.0
2235	3.0	72	31	155	366	1.88	0.4	14	60.9	27.9

Appendix E Sample Calculation

Calculation of time required to produce observed uranium concentrations in lake sediment from groundwater under present day conditions.

U = mass of uranium in 1 m^3 of lake sediment
U_s = concentration of uranium in lake sediment
U_{gw} = concentration of uranium in groundwater
ρ_s = bulk density of sediment
Q = seepage flux
t = time

The amount of uranium (U) in 1 m^3 of lake sediment having a concentration of U_s is;

$$U = \rho_s * U_s;$$

which is equal to groundwater with a uranium concentration of U_{gw} seeping through 1 m^3 of lake sediment at a rate of Q over a period of time t.

$$U = U_{gw} * Q * t$$

Therefore the time required to accumulate a given amount of uranium in 1 m^3 of lake sediment at a given seepage flux is,

$$t = \frac{\rho_s * U_s}{U_{gw} * Q}$$

Given;

Q = 0.00113 m^3/day
U_s = 100 (g/1*10^6g)
U_{gw} = 0.090 (g/m^3)
ρ_s = 1.8*10^6 g/m^3 (assumed)

then;

$$t = \frac{1.8*10^6 \text{ g/m}^3 * 100 \text{ g}/1*10^6\text{g} * 1 \text{ m}^3}{0.090 \text{ g/m}^3 * 0.00113 \text{ m}^3\text{/day}}$$

= 1769911 days

= 4849 years